Master of Science Thesis

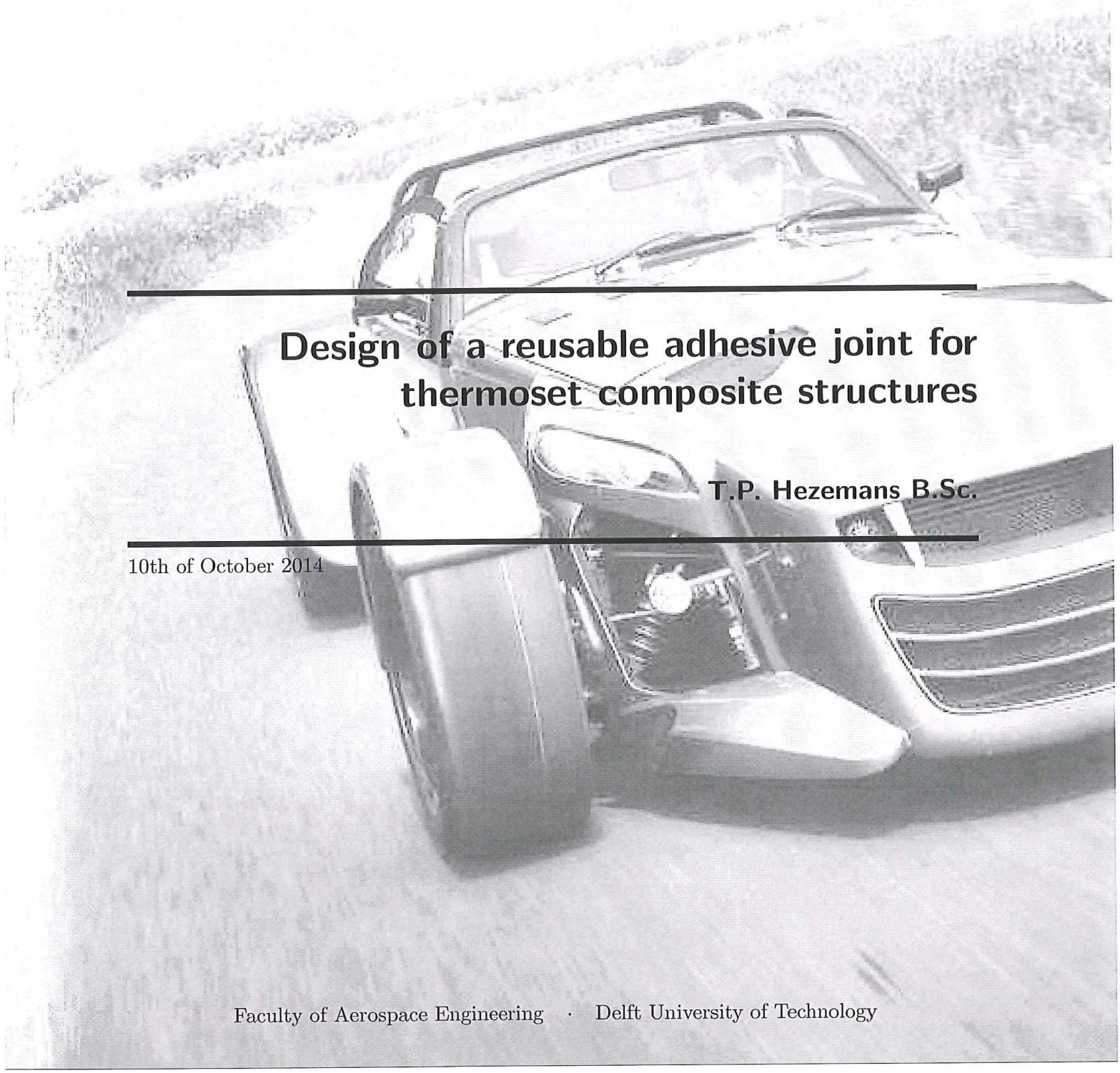

Design of a reusable adhesive joint for thermoset composite structures

T.P. Hezemans B.Sc.

10th of October 2014

Faculty of Aerospace Engineering · Delft University of Technology

Design of a reusable adhesive joint for thermoset composite structures

Master of Science Thesis

For obtaining the degree of Master of Science in Aerospace Engineering
at Delft University of Technology

T.P. Hezemans B.Sc.

10th of October 2014

Faculty of Aerospace Engineering · Delft University of Technology

Delft University Of Technology
Department Of
Structural Integrity

The undersigned hereby certify that they have read and recommend to the Faculty of Aerospace Engineering for acceptance a thesis entitled **"Design of a reusable adhesive joint for thermoset composite structures"** by **T.P. Hezemans B.Sc.** in partial fulfillment of the requirements for the degree of **Master of Science**.

Dated: 10th of October 2014

Head of department:

Prof.dr.ir. R. Benedictus

Supervisor:

ir. J. Sinke

Reader:

Dr. C. Kassapoglou

Abstract

The V-Cart project was a collaboration between Donkervoort Automobielen B.V. and Delft technical university, with a common goal to design a composite chassis for the next generation of cars. This research originates from the need of a reusable adhesive bond for connecting large structural composite parts. Unfortunately, the collaboration ended during the research. This thesis focuses on the design of the reusable bond itself, with application in a small sportscar chassis in mind.

First steps in the project were investigating which adhesive joining methods for thermoset composites are available, and how these can be made reusable. Using a thermoplastic polymer adhesive, the bond can be weakened by heating the adhesive. Typical thermoset adhesive require physical removal, which likely damages the substrates. Consumer demands were investigated and translated into technical demands. Several connection concepts were developed. Using a trade-off analysis, resistance welding was deemed most promising.

Tests were performed obtaining material properties. Polymer adhesives experience glass transition at lower temperatures than the recommended application temperature, potentially enabling manufacturing at lower temperatures. It must be ensured the structural composite parts do not suffer from damage during the assembly process. For a typical carbon epoxy, damage is not initiated at temperatures below 300°C for short exposure times.

One of the initial tests performed was the ASTM D 5868 single lap shear test. It is a standard joint test, exposing the bond to multiple load types. Production method has a large effect on bond strength. Thermoplastics show bad adhesion to carbon epoxy due to similar surface tension values. An extensive pretreatment of the substrate is required for desired results, including sanding, degreasing, drying and UV treatment. Pre-impregnating the mesh with adhesive before assembly reduces the number of voids present to a minimum.

The bond satisfies the strength requirement conceived for the V-Cart chassis. A mean ultimate shear strength of $3.33MPa$ was found at RT for a mesh pre-impregnated with a polyamide adhesive, with bondline thickness of $0.20mm$. At high temperatures practically all strength is lost, easing disassembly. Disassembly and reassembly (without additional pretreatment of the substrate) did not influence strength values negatively. It remains uncertain how many times this process can be repeated without strength degradation. Performance at elevated

temperatures is strongly dependent on adhesive used, the thermoplastic adhesives tested offered insufficient strength at 60°C. For the V-Cart application another adhesive should be selected with better thermal resistance.

Failure of the bond happens mostly by resin-mesh debonding. Testing of similar samples without a mesh yielded higher strength values. The effect of the mesh in the connection could potentially be reduced by selecting a coarser mesh, this remains for future research.

The connection allows for easy scaling, meaning incorporating the joint for different applications becomes possible. A power of $35\frac{kW}{m^2}$ was used for manufacturing, application temperatures of the adhesive were reached within 30 seconds for a 12.5 by 192mm area. Assembling larger areas requires a proportional increase in power input. For resistance welding, some changes in geometry might be required to reduce the gap between the joint and electrical connectors to a minimum. Furthermore, a sealant should be applied to reduce water absorption and the corresponding polymer strength degradation.

It is recommended to get a better understanding of the life time performance of the connection in order to ensure a safe joint in the chassis. By using a coarser mesh, the resin-mesh interface is reduced, potentially offering improved strength levels. It is most important to select a polymer that keeps its strength values within the desired temperature window, however but disassembly should not be compromised.

Acknowledgements

This report is a condensed presentation of the work on my thesis assignment. Fascinated in lightweight engineering and composites I started this master. With my interest in cars, being able to work on a project for Donkervoort Automobielen B.V. was very inspiring.

I would like to thank my supervisor Jos Sinke for his help, especially because the collaboration started only halfway through the project. The discussions and open views on problems really helped me to improve my research. I would also like to thank the rest of the committee member, Rinze Benedictus and Christos Kassapoglou. Finally, this project would not have been possible without the patient support of the DASML staff. Other people who have contributed are Mark Bakker, Philippe Willems and Huajie Shi.

I really enjoyed the period with the other students from my room at the TU Delft. The discussions about technical problems provided a lot of insights, but I also loved the lunches with broodjes Leo.

Support also came from many people in my personal life: Anke, my parents, my roommates and other close friends where most important and often surprised me with out-of-the-box thinking.

Delft, The Netherlands
10th of October 2014

T.P. Hezemans B.Sc.

Contents

List of Figures

List of Tables

Nomenclature

Latin Symbols

A	Area	$[m^2]$
d_{wire}	Wire diameter	$[m]$
F	Force	$[N]$
F_{max}	Maximum force	$[N]$
f	Frequency	$[\frac{-}{s}]$
$j^\star$	Black-body radiant exitance	$\frac{[J]}{[m^2]}$
T_{appl}	Application temperature	$[\circ C]$ or $[K]$
T_{deg}	Degradation temperature	$[\circ C]$ or $[K]$
$T_{g,onset}$	Glass transition temperature onset	$[\circ C]$ or $[K]$
T_g	Glass transition temperature	$[\circ C]$ or $[K]$
T_{max}	Maximum temperature	$[\circ C]$ or $[K]$
T_{min}	Minimum temperature	$[\circ C]$ or $[K]$
T	Temperature	$[\circ C]$ or $[K]$
x	Axis in the longitudinal direction of the car	-
y	Axis in the lateral direction of the car	-
z	Axis in the height direction of the car	-

Greek Symbols

α	Coefficient of thermal expansion	$[\frac{\mu strain}{K}]$

δ	Skin depth	$[m]$
Δ_{wire}	Space between wires in mesh	$[mm]$
γ_{LV}	Surface tension of fluid with vapour	$[\frac{N}{m}]$
γ_{SL}	Surface tension of solid with liquid	$[\frac{N}{m}]$
γ_{SV}	Surface tension of solid with vapour	$[\frac{N}{m}]$
μ	Magnetic permeability	$[\frac{H}{m}]$
σ	Stefan-Boltzmann constant	$\frac{[W]}{[m^2 \cdot K^4]}$
σ	Electrical conductivity	$[\frac{S}{m}]$
σ_{ILSS}	Interlaminar shear strength	$[MPa]$
σ_{OHTu}	Ultimate open hole tensile strength	$[MPa]$
σ	Stress	$[MPa]$
τ_{12}^{m}	In-plane shear stress	$[MPa]$

Abbreviations

CFRP	Carbon Fibre Reinforced Plastic
DIC	Digital Image Correlation
DSC	Differential Scanning Calorimetry
EVA	Ethylene-Vinyl Acetate
FBD	Functional Breakdown Diagram
FEA	Finite Element Analysis
FEM	Finite Element Modeling
FRP	Fibre Reinforced Plastic
ILSS	InterLaminar Shear Strength
PUR	PolyURethane
RH	Relative Humidity
RT	Room Temperature (20°C)
TGA	ThermoGravimetric Analysis
TP	Thermoplastic
TS	Thermoset
UD	Uni-Directional
V-Cart	Versatile CARbon fibre reinforced Thermoplastic platform

Chapter 1

Project introduction

1.1 Donkervoort Automobielen B.V.

Donkervoort is a Dutch sports car brand founded in 1978 by Joop Donkervoort in Tienhoven. All cars are hand-built and focus on the motto 'No Compromise'; a minimal design with no electronic aids such as ABS, ESP or power steering, focuses on high performance.

The S7 was the first model produced by Donkervoort. It was based on the Lotus Seven, using Ford components for the engine and rear suspension. A steel space-frame formed the basis of the car providing low weight with high torsional stiffness. Only five years after the launch of the S7, Donkervoort started production of the S8; a similar car to the S7, but developed from scratch by Donkervoort.

Figure 1.1: Donkervoort S7 [16]

Over the years, the company has gone through some big changes. For example, Donkervoort now uses Audi engines for their cars. The growth of the company also meant the need for a better facility. Since 2000, it is established in Lelystad. The location provides enough room for the showroom, development and production.

1.1.1 Recent developments and future

In 2007, the start of production of the Donkervoort D8 GT was a new step for the company. It was the first hard-top car produced by Donkervoort, and the first to compete in races. In terms of design, carbon fibre reinforced plastic (CFRP) was introduced as material for shear panels, increasing the torsional stiffness of the spaceframe chassis. It was also used for body panels to reduce weight. This development introduced new challenges but showed a large potential for performance enhancement.

1.1.2 V-Cart project

To explore the possibilities of applying composites in a car chassis the V-Cart project (Versatile CARbon fibre reinforced Thermoplastic platform) was started. This national R&D project is a collaboration between Donkervoort and TU Delft, with a common goal to design a composite car chassis.

Objectives are an increased torsional stiffness of the chassis without adding weight[58]. This allows handling characteristics to be better determined by suspension only. Production costs have a maximum of 7500 euro's. For a small company as Donkervoort, the investment required for tooling might be problematic.

Four students have graduated for the V-Cart project. Jasper Terdu made a preliminary design of the chassis[58], figure 1.2. Further research included thermal heat management of composite panels by Joris van Gestel[27], load analysis and design of suspension mounting points by Arnoud Haffmans[29] and testing methods for the resin system choice by Ruben IJperlaan[35].

Uncertainty for the new design is the joining method between the composite panels. Adhesives deliver best performance for composites[40][63], however are notorious for being difficult to disassemble. Donkervoort demands a removable connection; this is obligatory for repair and maintenance. Furthermore a one-piece chassis would require high insurance costs; composite repairs are time consuming and complex, irreparable damage would render it totaled. The concept of a releasable adhesive connection which allows for easy replacement of a composite part seems a perfect solution.

This research focuses on the development of a reusable adhesive connection. The V-Cart project serves as context, but is not the main goal of this research.

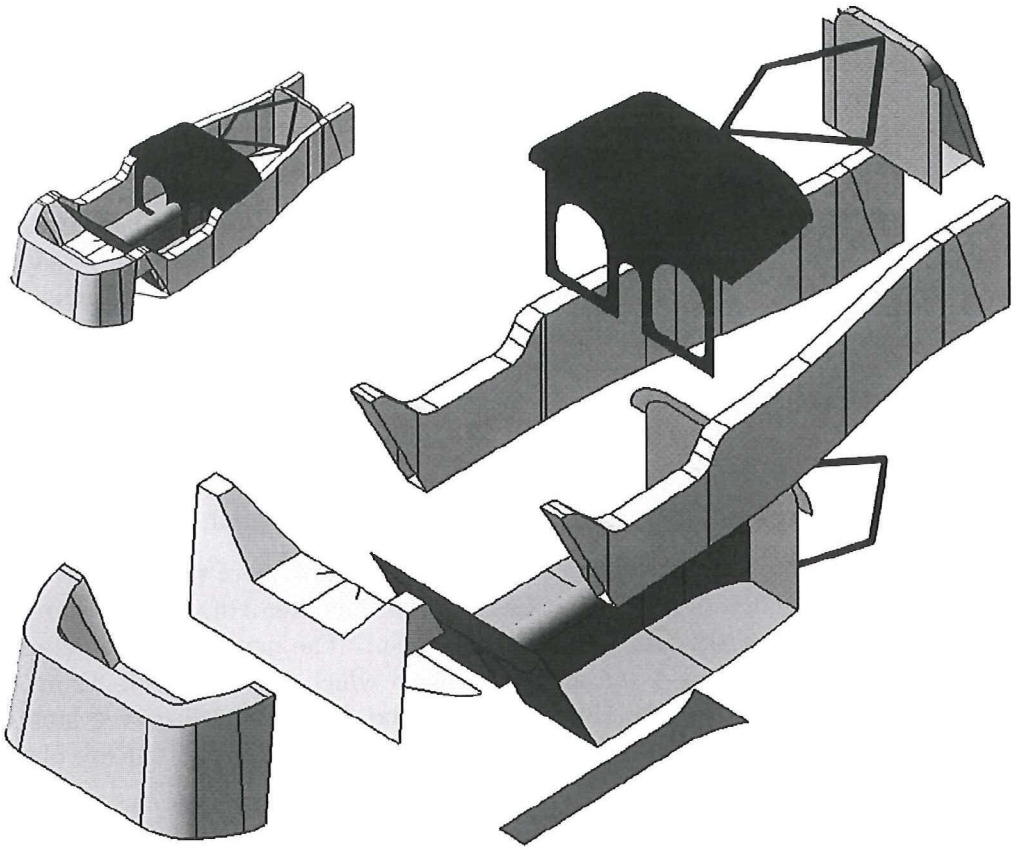

Colour code	Component
	Chassis beams
	Bulkheads and floor panel
	Rear suspension bracket
	Rear impact structure
	Scuttle and dashboard
	Front suspension bulkhead
	Transmission tunnel panel
	Engine bay frame

Figure 1.2: Exploded view of preliminary V-Cart design[58]

1.2 Thesis objective

The mission need statement for this thesis is as follows:

Design a reusable adhesive joining method suitable for connecting composite parts as in the Donkervoort V-Cart chassis.

The project objective statement defines the project objective and constraints, based on the mission need statement:

Develop a reusable adhesive joining method for joining composite materials, and perform manufacturing tests, quality assessment and destructive testing to assess its properties and suitability, within a time frame of 9 months.

1.3 Thesis approach

The thesis work can be divided into four parts, in which the design & materials requirements, the concept designs, the detailed design and the final design are covered.

The design & materials requirements starts with a functional analysis of the adhesive joint in chapter 2. This identifies all functions the joint has to fulfill. Chapter 3 discusses requirements of the joint, both from a consumer and technical standpoint. The next chapter 4 defines the materials and sizes of the joint, and the environment to which it is exposed. From these chapters a list of demands for the adhesive system can be distilled. Adhesive systems are discussed in chapter 5, and several candidates are selected. Material properties are obtained in chapter 6.

In the conceptual design part several concepts and associated manufacturing methods are explored in chapter 7. Selecting the best candidate is done in chapter 8. A first set of samples is made with several adhesives and tested in chapter 9, and some improvements are discussed.

In the detailed design part all improvements are taken into account. Samples are made and tested in chapter 10. Different samples are tested to determine different properties of the connection method.

The final design part discusses how this connection can be applied in the V-Cart chassis in chapter 11. Chapter 12 & 13 discuss conclusions and recommendations of this research respectively.

Part I

Material & Design Requirements

Chapter 2

Functional Analysis

To discover what functions a reuseable adhesive connection has to fulfill, a functional analysis is made. This is used to develop a list of requirements. The overview can be represented graphically in a functional breakdown diagram (FBD), figure 2.1.

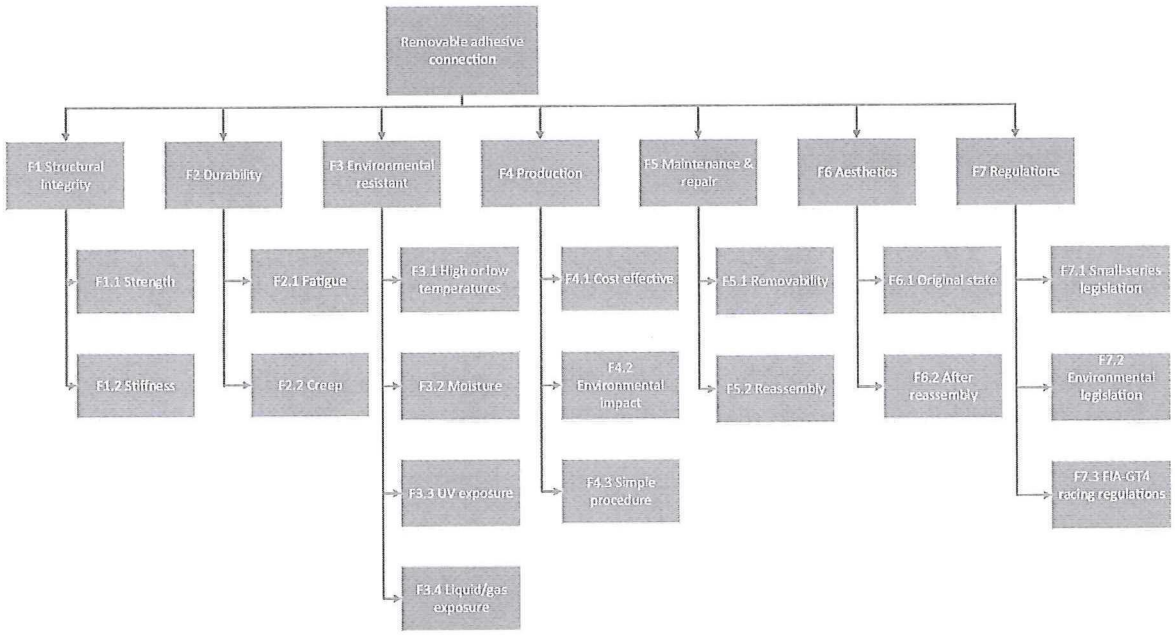

Figure 2.1: Functional breakdown diagram of a removable adhesive joint

Functions F1 to F4 apply for any structural connection. Especially F5 but also some other functions are specifically for a *reusable* adhesive connection. F6 and F7 are only involved for the V-Cart chassis and Donkervoort. The functions are discussed briefly.

F1 Structural integrity The main function of the joint is to provide structural integrity. This includes enough strength to prevent failure, but also enough torsional stiffness for desired

handling characteristics.

F2 Durability The joint should remain intact during its life, and may not fail after prolonged use. This is affected mostly by fatigue and creep.

F3 Environmental resistant Aside from mechanical loading, the joint's environment has a strong impact on durability as well. For a car chassis, environmental influences include high and low temperatures, high moisture conditions, exposure to UV radiation, and exposure to liquid and gasses from the engine bay compartment.

F4 Production Selling the final product for a competitive price is always of concern. Production of the joint should therefore be considered during the whole design process. One must take into account cost effectiveness, which applies to materials, tooling, and the manufacturing process. It also means avoiding environmentally polluting production methods. A high component count or process step count should be avoided. Note that a high production cost can be justified if the reusable connection saves on e.g. maintenance costs. Finally, the joining method should be realistic for the facility in Lelystad.

F5 Maintenance & repair Being able to remove the connection is the killer requirement of the adhesive joint. This should be an easy process. Equally important is the ability to re-use the components with similar strength & stiffness values. If the adherents cannot be re-assembled after the bond is broken, or mechanical properties are strongly reduced, the ability to remove the bond is of no value.

F6 Aesthetics The V-Cart car chassis (and thus the removable adhesive joint) is a luxury product. Aesthetics are important, regardless of the number of times it has been reassembled.

F8 Regulations Finally, the V-Cart chassis should satisfy several regulations to become road legal. Specific regulations are required for GT4 racing.

Chapter 3

Design Requirements

For the design to result in an effective concept, a list of requirements must be clearly defined. The consumer (Donkervoort Automobielen BV) has a list of requirements (section 3.1), but there is also a list which result from the functional analysis as discussed in chapter 2 (presented in section 3.2). Finally, in section 3.3, a classification of the requirements is made according to their importance.

3.1 Consumer demands

The list of requirements from Donkervoort Automobielen BV are based on the previous V-Cart chassis projects performed by Terdu[58] and Haffmans[29], as well as on meetings with Joop Donkervoort and Jordi Wiersma.

- *CFRP structural parts* - Donkervoort selected this material for its good material properties and appearance. The car is a luxury product, and a CFRP exterior creates a sense of high performance to the buyer, increasing the perceived value. The substrate material has consequences for the joining methods available.
- *Chassis torsional stiffness of* $20.000\frac{Nm}{deg}$ - This goal should improve the car's handling. A torsional stiff chassis allows handling characteristics of the car to be better controlled by the spring dampers. It is a combination of the stiffness of the composite components and the joints connecting them.
- *Cost per chassis* €*7.500* - Based on a production of 50 cars per year, the total costs of the chassis should not exceeds €7.500, unless offering added value. This is already a higher value than the original €5.000[58].
- *Chassis weight of 85kg* - The current steel space frame chassis weighs 85kg. The aim of the V-Cart project is to increase torsional stiffness while keeping weight identical.
- *Safety* - Despite the high performance nature of the car, it should still be safe in the event of a crash. Part of this is achieved by crash cones in the structure. For the joint, this means it must remain intact during a crash, requiring a strong connection.

A composite structure is also chosen by Donkervoort to increase passenger safety[58], this must not be negated by a weak joint.

- *'A-class' surface finish* - The buyer expects a good surface finish of an expensive product. This applies to the CFRP structures but also the joint. The connection should be smooth with no adhesive residue visible.
- *Unique joining method* - The buyer expects an unique product. This can be a result of exceptional performance characteristics, but also of manufacturing methods and structural design. A reusable adhesive joint is unique and forms a selling point to the consumer, something Donkervoort tries to achieve.
- *Fit for modular design* - Donkervoort requests a modular design for the chassis. Rescaling of the product should be possible, allowing the use of the same techniques for other cars, saving costs on design and tooling.
- *25 year life* - The car is designed for a service life of 25 years. This is relatively long for a car; most Donkervoort owners drive it only occasionally, hence the long life. This does not mean the life of every component should be longer than this; maintenance is allowed. Maintenance intervals should be clearly defined to prevent premature failure.

3.2 Technical requirements

Technical requirements follow from the functions a joint should have, as defined in chapter 2. For each major function, the requirements are discussed below.

- *F1. Structural integrity* - The strength values required to keep the joint intact are derived from the forces acting on the mounting points (section 4.4). In the removable joint a shear strength of $2.0MPa$ is needed. Designing for torsional stiffness criterion is much more complex; thin bondline thicknesses are preferred but stiffness is largely determined by the adhesive selected.
- *F2. Durability* - The connection should be able to withstand the loads (mentioned in F1) for 25 years (safe-life). Alternatively, it can be designed such that occasional maintenance is required (damage tolerant design). Crack detection is difficult in the complex connection (section 4.2), therefore a safe-life joint is expected to be the best solution (section 11.4).
- *F3. Environmental resistant* - Durability of the connection should be guaranteed under various environmental conditions. These depend strongly on the geographic location of the car, but also on seasonal changes and include hot/wet & cold/dry conditions.
- *F4. Production* - The frame should be able to be produced for €7.500, at a rate of only 50 cars per year. Production should be possible for low quantities, while maintaining high quality. Also, it should be producible in the facility in Lelystad. Finally, environmental impact should be minimized.
- *F5. Maintenance & repair* - Maintenance is periodically required to replace worn out or damaged parts. Therefore, the joint should be reusable, without damaging the structural parts. This maintenance interval should be at an acceptable level for the user. Regardless, release and removal should be performed in a short amount of time to keep the costumer satisfied, preferably a week. Another method to ease repairs is to make certain parts more easily accessible.

- *F6. Aesthetics* - The car is a luxury product, good aesthetics of the connection are a must. This means an 'A-class' surface finish, smooth joining surface and no adhesive residue, both in the original state and after repairs.
- *F7. Regulations* - The vehicle should be deemed road legal for use on the roads. This requires satisfying demands for a small series production, and European demands on emission. If a race version of the car is to be built and used in GT4 races, additional regulations of the FIA should be satisfied.

3.3 Classification of requirements

This section divides the requirements listed above in three categories, according to importance. This is useful when compromises are needed because satisfying all requirements is impossible. 'Killer requirements' are vital and should be met at all cost. 'Driving requirements' should be considered but are less important. Finally 'other requirements' are least important but desirable nonetheless.

3.3.1 Killer requirements

- CFRP structural parts
- Average shear strength larger than $2MPa$
- Satisfy road-legal regulations
- No failure before scheduled maintenance
- Replacement process possible within a week

3.3.2 Driving requirements

- Production cost of €7.500 per chassis
- Fit for maintenance and repair
- Fit for modular design
- 'A-class' surface finish
- Chassis weight of 85kg
- Satisfy FIA regulations

3.3.3 Other requirements

- Minimize environmental impact
- Production of 50 cars per year
- Unique joining method

Chapter 4

V-Cart joint

This chapter explores properties of the V-Cart chassis, in particular those required to design an adhesive bond. Geometry and operating environment are discussed, culminating to a set of demands for the adhesive joint.

4.1 Reference Frame

To correctly describe forces and directions on the car, a frame of reference is required. To avoid problems within the project, the frame as chosen by Haffmans is used[29] (figure 4.1).

4.2 Joint Shape

The shape and geometry of a connection determine the connection methods applicable. This research focuses on the joint between the front bulkhead and chassis beams, which has already been optimized for joining using adhesives.

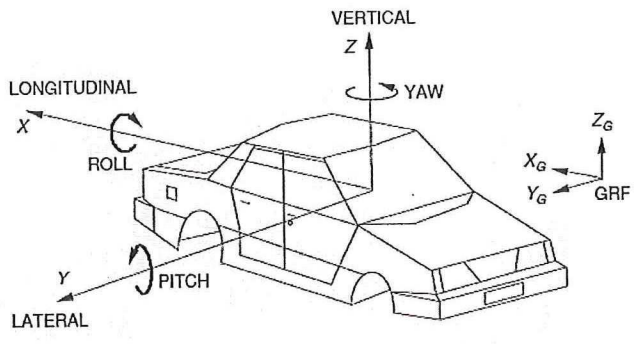

Figure 4.1: Reference frame of the car[29]

The original concept was developed by Terdu[58]. Both the bulkhead and beams consist of sandwich panels with CFRP epoxy facings. Researcher Mark Bakker modified the original geometry to make it suitable for joining using adhesives (figure 4.2). Also, Bakker designed the geometry to be compatible with the Donkervoort GTO, the latest car from Donkervoort Automobielen B.V. Dimensions of the mounting points correspond with the GTO, and there is enough space for all the packaging (radiator, intercooler etc.).

Fibre reinforced plastics (FRP) perform best when loaded in the in-plane direction of the fibres. Integrating the suspension mounting structure into the bulkhead thus seems an efficient use of material. This requires the bulkhead to be larger in y-direction than the chassis beams. Holes in the bulkhead structure create an interface between the composite parts. Dimensions of the holes and thickness of the material (table 4.1) determine the available area for adhesion, and can be modified slightly.

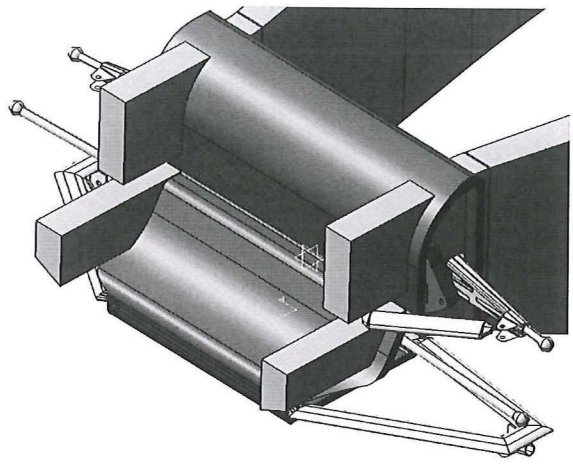

Figure 4.2: Front bulkhead as designed by Mark Bakker

Hole dimension	Length [mm]
Width (y-direction)	50
Depth (x-direction)	30
Height upper hole (z-direction)	200
Height lower hole (z-direction)	150

Table 4.1: Hole dimensions in the front bulkhead

The intersection of the two panels creates a large adhesive area. The flat surface of the panels makes it difficult for two parallel surfaces around the same part of the beam to be adhered, partly as a result of tolerances. This is shown schematically in figure 4.3, which shows a frontal view of one half of the bulkhead. The image on the left contains no adhesive, the white lines illustrate the gap between the adherents. The image on the right shows which of these areas are difficult to adhere both; same colours become problematic.

Depending on the adhesive strength, not all areas are needed to achieve desired strength values of the chassis. This will come back later on in the report, as well as measures to be able to adhere all surfaces.

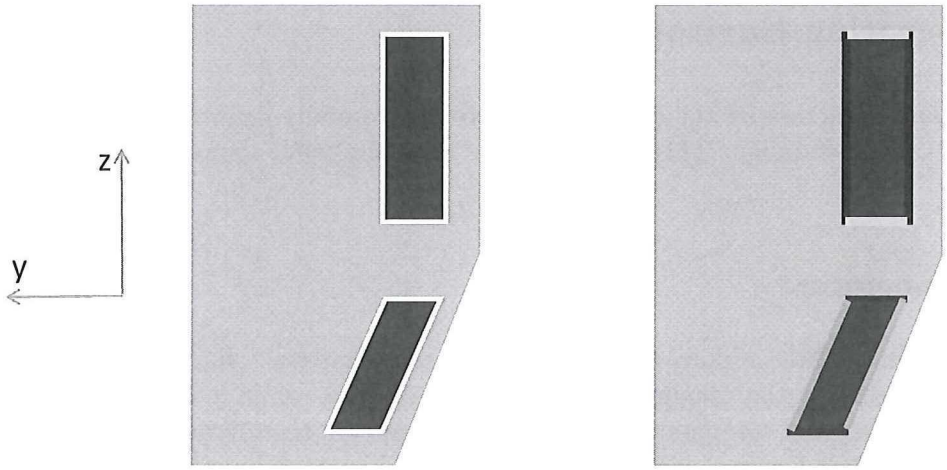

Figure 4.3: Frontal view of one half of the bulkhead. The left image shows the gap between adherents, the right images shows which interfaces are complicated to adhere both. Same colours become problematic

4.3 Joint Interface

The adherent's interface material depends on the manufacturing process. For both the bulkhead and chassis beams, it is easiest to first build the sandwich panel shape without holes. Holes can be milled subsequently. Note that milling is a complex process; local temperatures should not exceed the resin's glass transition, and high out of plane milling pressures can cause damage to the underlying structure. It is impossible to achieve perfectly square corners by milling, these will always have the radius of the milling tool. A square corners can be approximated by a two-stage milling process. First the hole is milled using a mill with large radius, then a mill with small radius is used to finish the corners.

The resulting structure leaves the core material exposed at the joint interface, resulting in core-core and core-CFRP adherents. Alternatively, the core material can be covered with CFRP. This extra manufacturing step can provide several advantages. First of all, the 'closed' surface prevents moisture ingress into the sandwich structure. More importantly, larger bond strength values are expected. The joint will likely fail cohesively for a weak foam core material. For the V-Cart the effect is partially compensated by the strong core material required to take up surface pressure. The size of the effect thus depends on the combination of adherent and adhesive material. In order to be conservative, it is assumed the core is covered with CFRP for the V-Cart application.

The core material must be able to deal with large contact pressure (as a result of forces from the suspension). Maximum vertical forces add up to $12kN$ on one side of the chassis[29]. This results in a compressive strength of $2.0MPa$ (equation (4.1)). It is a conservative result, as it assumes the load is taken up by contact pressure only.

$$\sigma = \frac{F}{A} = \frac{12000}{4 \cdot 30 \cdot 50} = 2.0[MPa] \tag{4.1}$$

4.4 Operating Environment

Operating conditions restrict the choice of adhesives, a carefully defined operating window is essential for safe joint design. This section defines these limits for temperature, humidity and stress.

4.4.1 Temperature

Polymers become brittle at low, and soft at high temperatures. Participation in races in Abu Dhabi is used for the maximum temperature scenario, while a winter in Scandinavia illustrates the minimum temperature scenario. Average air temperatures drop to -15°C in winter in Finland[33]. Engine heat can increase this temperature, but this takes time. Failure must be ruled out under these cold conditions.

Maximum air temperatures in Abu Dhabi are reported at 45°C[32]. Joint temperature is elevated upon this level by engine heat, conducted through the chassis beams. Engine bay temperatures reach 100°C[57]. However simulations performed by Van Gestel showed the temperature of the inner CFRP facing was only 46°C, 40 centimeters from the heat source[27]. This is a result of the low thermal conductivity of the material.

The car will heat up under direct sunlight, especially for a dark paint. Outer surface temperature can be approximated by the Stefan-Boltzmann law, equation (4.2). Here $j^\star$ is the radiant exitance (in $\frac{W}{m^2}$), σ is the Stefan-Boltzmann constant ($5.67E^{-8}\frac{W}{m^2\ cdotK^4}$) and T is the absolute temperature in $[K]$. Highest measured daily mean solar radiation in Abu Dhabi is $730W/m^2$[36].

$$j^\star = \sigma \cdot T^4 \tag{4.2}$$

$$730 = 5.67E^{-8} \cdot T^4 \tag{4.3}$$

$$T = 337K = 63°C \tag{4.4}$$

This simple estimation is conservative for a number of reasons; (1) it assumes the car is a black body (absorbing all radiation, regardless of the angle of incidence), (2) it only takes into account cooling from the outer panel, and (3) the joint will likely be in the shade of the bodywork. Therefore, maximum service temperature T_{max} is taken at 60°. It is unlikely higher temperatures are reached.

4.4.2 Moisture absorption

Polymers absorb moisture when exposed to a humid environment. This process is called plasticization, decreasing T_g and mechanical properties. Furthermore, moisture absorption leads to degradation of the fibre matrix interface, creating poor stress transfer efficiency[30]. This section explores the influences moisture has on the adhesive bond.

Static & fatigue strength of adhesive bonds are highest when testing at room temperature (RT) and low relative humidity (RH)[20][5]. Hot/wet conditions result in the largest performance decrease[47]. As will be discussed in chapter 5, one of the adhesives used for testing is based on a polyamide polymer. Properties of polymers (and especially polyamide) are strongly influenced by moisture uptake[30]. The size of the change depends on the saturation percentage. Comparing dry specimens to completely saturated, T_g has been reported to drop from 50°C to -13°C (with corresponding drop in strength). Yield strain of the polymer also increases dramatically, from 10% for the dry polymer, to larger than 50% for humid conditions[51].

Moisture saturation of the polymer is a time dependent process. Moisture is taken up more quickly for environments with higher relative humidity. The process is accelerated under higher temperatures[67]. In a standard environment (23°C & 50% relative humidity (RH)) PA6 absorbs about 3 weight-% of water. This increases to 9% when immersed in water[51].

Moisture uptake is reversible; material dries by placing it in a standard environment[67] or by heating it[65]. At the same time, the changes in T_g and mechanical properties shift back to their original values. Similar to the moisture uptake process, drying is time dependent. Note that even in standard atmosphere there is some moisture saturation. Values will thus never reach those of the original dry polymer.

In the life of the car, the joint will experience various moisture levels from the environment. These range from 50% humidity in dry weather conditions, to moisture immersion during showers or cleaning. Moisture content of the adhesive will vary accordingly. Absorbed moisture is mostly lost during dry conditions, however this process takes time. During this time, the adhesive exhibits worse mechanical properties. Therefore, in order to develop a safe design, the adhesive should have enough strength in wet conditions, or a method to seal the it from moisture is required (section (11.3). Note that, if the adhesive has been wetted before assembly, detrimental mechanical properties can be expected regardless of the sealing method.

4.4.3 Mechanical Loading

The V-Cart chassis is a completely new design. In order to select a suitable adhesive, stresses in the adhesive layer should be known. Using FEA methods is the most time-efficient method for this situation.

Determining the stresses in the adhesive layer requires knowledge of the external forces acting on the chassis. Haffmans defined six ultimate load cases for the car[29]. Using an Adams model, the forces acting on the wheel and on the suspension mounting points were determined. These forces were used as input in Bakker's ABAQUS model. Simulating the flexible nature of adhesive in FEM is complex; as a simplification a rigid connection between the adherents is assumed (simulating an adhesive with infinite stiffness). This is not realistic and will give larger stress values than reality; the flexibility of the adhesive will distribute loads over a larger area, minimizing peak loads. The results can be seen as a worst-case scenario; if an adhesive satisfies these values, failure is ruled out.

Results can be seen in table 4.2. Shear 1 and 2 indicate shear stresses in different directions. Maximum values were never at the same location and thus did not amplify each other. The

average value represents the largest stress value present over a larger area. All values had to be determined manually from a figure, it is therefore not a 'real' average value. Only four of the six load cases of Haffmans were used; the other two featured much lower forces and would not require larger strength values.

		Pressure [MPa]	Shear 1 [MPa]	Shear 2 [MPa]
Static	Max	0.8	1.0	0.7
	Average	0.2	-	-
Braking	Max	1.25	1.48	1.06
	Average	0.5	0.3	0.4
Bump	Max	3.2	4.6	3.2
	Average	-0.5	0.8	0.5
Cornering	Max	4.7	3.6	2.0
	Average	2.0	1.0	0.5

Table 4.2: Loads in adhesive layer determined by ABAQUS simulations using Bakker's V-Cart model

The table shows shear stresses remain relatively low, as a result of the large bonding area. The largest stress peak measured was $4.6MPa$. This was deemed unrealistic for two reasons; (1) a flexible adhesive would distribute stresses over a larger area, reducing the stress peak, and (2) it seemed to be a result of edge effect in the model. Average stress values are therefore more realistic. These do not exceed $1.0MPa$. Taking into account an additional safety factor, it would seem an average adhesive shear strength of $2.0MPa$ is required. Note that this does assume the complete area is used for adhesion.

Satisfying the strength requirement does not necessarily satisfy the chassis' torsional stiffness requirement. This depends on the bonded area, but also stiffness properties of the polymer and bondline thickness. The research focuses on developing a reusable adhesive bond; the chassis' stiffness properties go beyond its scope. The strength criterion is used to judge suitability of the adhesive, but note this might not satisfy stiffness properties.

Aside from these six load cases, there are some more extreme forces experienced during crashes. In those situations the most important thing is the safety of the driver. This can be assured by crash cones, dissipating energy. Integrity of the chassis becomes very important, but this is mostly around the passenger area. The adhesive joint of the front bulkhead is less important for safety of the passenger, and therefore does not require an extra load case.

4.5 Alternative geometries

Developing a car chassis made entirely from composite parts - with an re-useable adhesive connection method - is a new and complicated process. Currently most supercar manufacturers use a CFRP 'tub' which houses the passengers, and attach aluminium truss structures to connect the other components. There are a few cases where the complete chassis is made from CFRP, but in all cases the connection is made using bolts. This probably has to do with certification and safety of the joint. Several examples are discussed in appendix A.

For the V-Cart design, a different design without adhesives can achieve similar goals for Donkervoort. For example, a slight change in design enables the parts to be bolted together. Although inherently less efficient than adhesives in load transfer for composites materials, a bolted connection has better environmental resistance. Furthermore, it allows for an infinite number of disassembly - assembly cycles. Although it is expected this re-assembly process is only require one to three times in the car's life, using bolts becomes more cost effective if it is required more often.

Alternatively, a design using a 'passenger tub' and aluminium truss structure can be applied. Unlike the sports cars covered in the appendix, the Donkervoort has a front mounted engine. As a result, the passenger section is located more rearward in the car. The passenger tub can be made from CFRP, with an aluminium truss structure bolted to the front to connect the front suspension and engine. This also eliminates degradation of the CFRP panels as a result of engine heat, a problem Donkervoort had with the first D8 GT-models.

A completely different solution could be to build the complete chassis from the mounting points of the front suspension to the rear suspension from composites, and adhering these together with a non-removable thermosetting adhesive. At the front and back of the chassis replaceable crash cones can be placed. This way, the thermosetting chassis is unlikely to experience damage from small crashes, while offering the advantages of thermosetting adhesives. Any small damages to the structure could be repaired.

Another solution (which remains closer to the current design) would be to build structural sandwich panels without adhering them directly. At the joints, thin laminates (overlapping both panels) keep them together, using the reusable adhesive connection. The advantage here is that the laminates allow the joint to be removed by loading in peel.

Many designs are possible for achieving the same goal. What is the most suitable solution depends on the priorities of the consumer, cost, tooling required etc. This research will focus completely on the design as specified in this chapter, with the dove-tail joint. However note that other designs might be possible and just as successful.

Chapter 5

Adhesives

Adhesives are a suitable way of joining composite parts. It allows for bonding materials over a large area, with uniform stress distribution along the joint width. Adhesion is a complex process, and properties of the joint depend strongly on the manufacturing process and the combination of adherent & adhesive materials. This chapter discusses adhesives on an atomic level, and mentions aspects to consider during assembly. Finally, some adhesives are selected.

5.1 Introduction to adhesives

Adhesives are materials that bond items together. They can be used next to other joining methods such as soldering, riveting, bolting, welding etc. Two materials that are bonded together by an adhesive form an adhesive bonded joint. Most adhesives used for structural applications are synthetic polymers.

Polymers are long chains of monomers linked to each other. The length and thus weight of the molecules determine structural properties. Softening temperature and tensile strength both increase with molecular weight, but this is not a proportional process[6]. Certain monomers can bond at three or more places. This allows branches to form, or networks between chains (cross-links).

Thermoset polymers feature a strong network between polymer branches. As a result, they cannot be remoulded after curing. Thermoplastic polymers do not form networks. This makes them remouldable at high temperatures, regaining strength after cool down. This property can be exploited for the reusable bond; elevated temperatures make the adhesive very weak, easing disassembly of the structure.

5.2 Polymer properties

Mechanical properties of polymer depend strongly on temperature[12][13]. Unlike metals and ceramics, these changes occur much closer to room temperature (RT). The effect of

temperature and amount of cross-linking on Young's modulus is illustrated in figure 5.1. The polymer experiences T_g at about -100°C, however the trend of the figure is similar for other polymers. A sharp decrease occurs at the glass transition T_g, the amount depending on the degree of cross-linking. The lack of cross-links makes thermoplastic adhesives more prone to creep.

A thermoplastic adhesive can be heated to the point were most strength is lost. This is impossible for thermoset polymers. This poses a problem for structural thermoplastic adhesives; high temperatures weaken the bond, possibly causing premature failure. The transition is often described with the glass transition temperature T_g and becomes an important design parameter. Note that the transitions occur over a temperature range as a result of polymer chains having different lengths. A decrease in strength can be noted at temperatures below T_g[52]. It is also a function of thermal history; lower heating rates result in a lower glass transition temperature[11][44]. For structural applications, it must be ensured these changes occur at temperatures outside the operating regime.

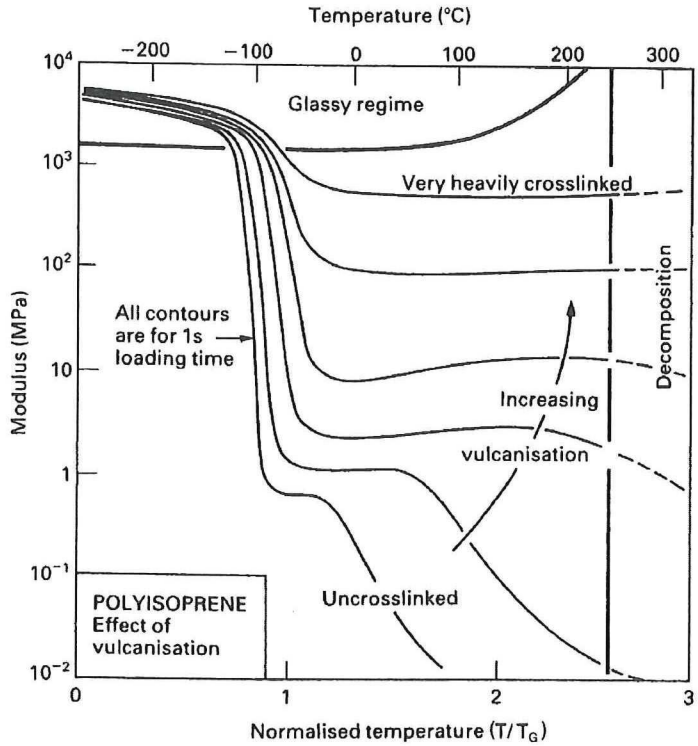

Figure 5.1: Influence of degree of cross-linking on the Young's modulus for polyisoprene[6]

5.3 Adhesion theories

There is no universal theory that explains the concept of adhesion. Several theories exist next to each other to explain certain observations.

Adhesion and cohesion Bond strength consists of two parts; adhesion and cohesion. Cohesive forces exist between molecules of the same material, and must be sufficient to keep the materials together. Properties are determined by the material. Adhesive forces keep two different materials together at the joint interface, and are also influenced by the manufacturing process. Failure of a bonded joint can therefore be adhesive, cohesive, or a combination of the two.

Adsorption theory The adsorption theory states that adhesion between two different materials is a result of close contact between the surfaces. The ability of a liquid to maintain contact with a solid surface is called wetting. Proper wetting will ensure a good contact with the substrate surface, and thus a strong bond[48]. The surface of a substrate is, on a microscopic scale, quite rough with valleys and crevices. A liquid exhibits good wetting if it maintains contact with the substrate despite the unevenness. This provides more surface area for van der Waals forces to develop, and avoids stress concentrations due to trapped air pockets.

Wetting can be expressed as a difference in surface tensions of the materials, expressed in the Young equation (equation (5.1))[66].

$$\gamma_{LV} cos\theta = \gamma_{SV} - \gamma_{SL} \tag{5.1}$$

Where γ_{LV} is the surface tension of the fluid with the vapour, γ_{SV} the surface tension between the solid and the vapour, γ_{SL} the surface tension between the solid and the liquid, and θ the contact angle of the liquid with the solid. Surface tension of the substrate must be higher than that of the adhesive to achieve good wetting. Metals, glasses and ceramics have high surface tension values because of the strong chemical bonds. Polymeric substrates on the other hand have low surface energies and are consequently harder to wet. A pretreatment can increase the surface energy.

Mechanical theory During the adhesion process, the adhesive flows over the substrates surface. If proper wetting is achieved, holes and cavities in the substrate are filled with adhesive. This interlocking provides mechanical grip, improving adhesion. There is a limit on this effect; at a certain point a rougher surface results in incomplete wetting[48].

Diffusion theory The diffusion theory describes the penetration of adhesive molecules in the substrate, creating better adhesion. Across the interface, the molecules mingle with each other, creating mechanical strength. This happens after wetting. It only occurs for polymers with similar chains, which are mutually soluble.

Weak boundary layer theory Failure of a joint occurs at the weakest link. According to the weak boundary layer theory, when a failure of a joint seems to be at the interface, it is usually the result of adhesive failure of a weak boundary layer. They can form during all steps in the life of a joint.

5.4 Surface pretreatment

The structural chassis parts are made from CFRP epoxy facings, which typically has a surface tension of $40\frac{dyn}{cm}$[3][19]. This is a typical value for a plastic, and much lower than other material as glass ($250 - 500\frac{dyn}{cm}$) and stainless steel ($700 - 1100\frac{dyn}{cm}$)[42]. To achieve good wetting and adhesion, a pretreatment is recommended. This also ensures better reproducibility which is important for research applications.

Mechanical methods The most simple pretreatment is mechanical; sanding of the substrate. In addition to the larger surface area, contaminants are removed. For composites, this can be achieved using a peel ply (amongst others). The cloth does not bond to the laminate leaving a roughened surface suitable for bonding. Other mechanical methods include grit blasting, but this could initiate surface damage.

Chemical methods Another common method is cleaning/degreasing of the substrate. This removes dirt, contaminants, and release agent, preventing failure by a weak boundary layer. Other, more complex chemical methods include etching, conversion coating and anodizing.

Physical methods Physical methods are mainly developed as pretreatment for polymers. The following treatments are available in the DASML lab at the aerospace faculty.

Corona treatment uses a corona discharge plasma generated by a high voltage between two electrodes. Material is fed through the corona. It is an effective method but also results in surface damage and is difficult to reproduce.

During flame treatment, the substrate is slowly transported over an open flame. The heat treatment oxidizes the surface. It is cheap and fast process, but is difficult to reproduce.

Exposing the substrate to UV/ozone cleans and activates the material at the same time. The method is simple to use and has reproducible results. The emitted wavelengths are important variables. The $184.9nm$ wavelength is absorbed by oxygen, generating atomic oxygen and eventually ozone. Ozone has very strong oxidation power, removing contaminants. The $253.7nm$ wavelength is absorbed by most hydrocarbons[61], resulting in their dissociation. These atoms react with atomic oxygen to form molecules as CO_2, H_2O and N^2. The combination of UV and ozone cleans the substrate several orders faster than UV or ozone separately[61].

Primers and promoters Finally, primers and promoters can be used. A primer is a strongly diluted adhesive, which conserves the properties of the pretreatment and improves wetting of the surface. An adhesion promoter is a chemical that adheres to the surface through chemisorption and covalent bonding, improving adhesion of the subsequently applied adhesive. It should therefore have an affinity with both the adhesive and substrate.

5.5 Adhesive selection

Based on the specification from chapter 4, adhesives were selected after contact with several manufacturers. The research focuses abilities and properties of a reusable bond, not necessarily on selecting an adhesive best suitable for the V-Cart chassis. Nevertheless, several thermoplastic adhesives were selected which should all satisfy the properties mentioned in chapter 4. Manufacturers were asked for a thermoplastic adhesive with shear strength of $2.0MPa$, in a temperature regime from -15°C to 60°C. The proposed adhesives can be seen below.

Heating of thermoplastic adhesives has a strong influence of mechanical properties, making them easy to remove at high temperatures. A thermoset and elastomer adhesive adhesive were selected as well; if these connections can be reused, there is no reason not to use these. Datasheets can be found in appendix B.

Thermoset adhesive Hexion Epikote 04908 with Epikure 04908 were selected as a thermoset adhesive. The epoxy-based adhesive has low viscosity, long pot life, and typical mechanical properties for an epoxy. It was selected due to the good availability in the aerospace faculty.

Elastomer adhesive Sabatack 780 was selected as a elastomer adhesive. It is an MS-polymer based adhesive currently used by Donkervoort. If the new reusable connection performs worse than Sabatack 780, there is no need for Donkervoort to change their manufacturing method.

Thermoplastic adhesives 3M Scotch-Weld 3731 and 3789, and Henkel Technomelt Q 9268 H were selected as thermoplastic adhesive. All three should offer sufficient shear strength and thermal stability. They feature different chemical bases; 3M 3731 is polyolefine based, 3M 3789 polyamide based, and Henkel EVA-copolymer based. Several other manufacturers were contacted as well but deemed their thermoplastic adhesives unsuitable for CFRP adherents.

Chapter 6

Material Properties

This chapter discussed several tests performed to retrieve relevant material properties, which cannot all be found in manufacturer's datasheets. As discussed in the previous chapters, the adhesive needs to hold its strength up to 60°C. Furthermore, thermoplastic adhesive has an application temperature of 180°C, which the substrate must be able to withstand. If higher or lower temperatures are possible, this could offer many advantages.

6.1 CFRP thermal stability

6.1.1 In-plane shear strength test

During assembly, damage to the structural parts must be avoided. Several tests are performed to determine if CFRP epoxy can sustain temperatures of the adhesive at application (180°C or higher), see table 6.1. All three test methods were performed, but both the open-hole tensile strength test and the ILSS produced unreliable results (see appendix C). Therefore, the in-plane shear strength test is discussed here. Tests are performed at RT, but the specimens have undergone a heat treatment simulating the adhesive application. Note that conclusions can only be drawn for this specific carbon-resin combination.

Test specimen The rectangular test specimens consist of five plies of woven carbon, all laid in the ±45°direction (table 6.2). Loading is in the 0°direction. Failure is thus largely resin determined. Five groups of six specimens were made. Each group received a different heat

Test	Type
ASTM D5766	Open-hole tensile strength
ISO 14130	ILSS by short beam method
ASTM D3518	In-plane shear strength

Table 6.1: List of test methods for determining CFRP thermal stability

treatment, aiming to represent the temperature excursion experienced during manufacturing in increasing intensities (table 6.3).

Item	Details
Fibres	Carbon [0°/90°] TenCate CD 0286 050 030
Lay-up	$[\pm 45]_5$
Resin	RIM 235
Hardener	RIM 237H
Release agent	2 layers Marbocote 227CEE
Degassing pressure	3mBar
Infusion pressure	56mBar
Curing pressure	491mBar
Curing	20 hours @ RT + 5 hours @ 80°C
Cutting	Sepitom with diamond cutting blade
Specimen size	200x25 mm

Table 6.2: Manufacturing of in-plane shear strength test specimen

Group	Temperature (°C)	Duration (min)	Testing temperature (°C)
1	-	-	RT
2	90	15	RT
3	200	15	RT
4	200	30	RT
5	-	-	200

Table 6.3: Heat treatment of in-plane shear specimens

Test procedure The tensile test is performed in accordance to ASTM D3518. Strain rate is constant at $1\frac{mm}{min}$, the test is stopped when the maximum force is reached. Maximum in-plane shear strength can be calculated using equation (6.1). Here τ_{12}^m is the maximum in-plane shear stress and F_{max} is the maximum force at 5% strain or lower.

$$\tau_{12}^m = \frac{F_{max}}{2 \cdot A} \tag{6.1}$$

Test results & discussion The test results are plotted in figure 6.1, original data can be found in table K.3 & K.4. The error bars show the minimum and maximum values within the group.

The effect of the heat treatment does not result into statistical difference between the test groups; average values lie close to each other, and fall within the error bars. The heat treatment can be considered a post-cure cycle, and seems to have little effect on the epoxy. The results from group 5 show the epoxy is very weak at 200°C. Loading of the composite should thus be avoided during assembly.

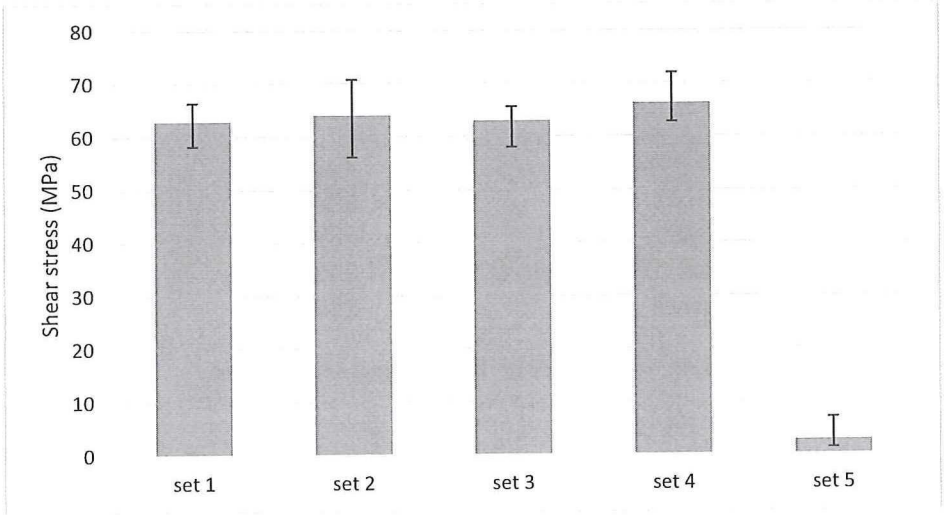

Figure 6.1: In-plane shear strength results

6.1.2 Thermogravimetric analysis

The in-plane shear strength test illustrated how a short-term exposure to high temperature has little effect on properties of the resin. However, while at this high temperature, the resin becomes very weak. In order to obtain a better quantitative answer to short term thermal stability of the resin, a ThermoGravimetric Analysis (TGA) is performed. Mass is accurately measured while a sample is slowly heated. A decrease in mass indicates degradation of the polymer, and thus damage to the sample.

A Perkin Elmer Pyris Diamond TG/DTA was used for TGA measurements, heating the sample from 25°C to 595°C at a rate of $10\frac{^oC}{min}$. Air was used as an environment, to mimic the real-life conditions. Using a sharp blade and sanding paper, the material was made to fit in a pan with a diameter of 5mm. Weight measured was between 5 and 10mg.

As a guideline, thermal degradation temperature (T_{deg}) occurs when the weight of the sample is only 95% of the original. Initiation can also be deduced from a sharp peak in the energy flow rate curve. Degradation of CFRP epoxy starts at about 315°C. The original graph can be found in appendix K.3. Short term exposure to temperatures lower than 200°C during manufacturing should thus be no problem for this fibre-resin combination. Properties are typical for an epoxy, it can thus be expected the same applies for other CFRP-epoxy material.

6.2 Adhesive thermal stability

6.2.1 Thermogravimetric analyses

Application temperature of the thermoplastic adhesives is (T_{appl}) lies between 170 and 190°C. Degradation is expected to occur at higher temperature. A large difference between T_{appl} & T_{deg} is beneficial, allowing for larger temperature gradients within the adhesive during manufacturing and possibly faster heat up times. TGA is performed for all adhesives under identical conditions as for the CFRP epoxy samples.

Test results & discussion The results are summarized in table 6.4, the original graphs can be found in appendix K.3. All thermoplastic adhesives are able to withstand higher temperatures before degradation. This is especially true for 3M 3789.

Adhesives	T_{deg} (°C)
3M 3731	300
3M 3789	380
Henkel Technomelt Q 9268 H	280
Sabatack 780	225

Table 6.4: Test results of TGA testing of adhesives

6.2.2 Differential scanning calorimetric analyses

Application of the adhesive at lower temperature than the prescribed T_{appl} can have many advantages. Damage is less likely to initiate and the process is safer for workers. Differential Scanning Calorimetric (DSC) tests are performed allowing us to determine the T_g of the material. This an indicative value for the minimum assembly temperature, furthermore it shows at what temperature strength is definitive lost.

Test procedure A Perkin Elmer Sapphire DSC was used for DSC measurements. The specimens were heated from 20°C to 180°C and back twice, at a rate of $20\frac{^oC}{min}$ for 3M 3789 and 3M 3731, and $10\frac{^oC}{min}$ for Henkel Technomelt. Unfortunately the Henkel test was performed under different circumstances, but it should not results in a large deviation. An nitrogen environment was used. Samples were cut from a $0.20mm$ thick adhesive film (section 10.3). Three circles were stacked together for the measurement.

Test results & discussion When an adhesive goes through the glass transition T_g, the amount of energy required to heat the material decreases. T_g can thus be defined as the average temperature between the slope changes in the energy curve. The results are shown in table 6.5, the original figures and more details on how the values were determined can be found in appendix K.4.

All adhesives' T_g values lie higher than 60°C. However, structural changes begin at a lower temperature than T_g; the glass transition onset $T_{g,onset}$. It is thus not guaranteed that the adhesives keep their strength at 60°C.

All T_g are lower than 180°C. The decrease in viscosity at T_g could be sufficient to enable wetting of the substrate, allowing for assembly at lower temperatures. This requires experimental verification. Together with the TGA results, which showed the adhesives can sustain

Adhesives	T_g (°C)
3M 3731	110
3M 3789	140
Henkel Technomelt Q 9268 H	80

Table 6.5: Test results of DSC testing of adhesives

higher temperatures than their T_{appl} before degradation, it seems the possible manufacturing temperature window is much larger than anticipated.

The DSC curves show the adhesives are not thermally stable in the 20-180°C interval. For thermally stable polymers the energy curves would perfectly overlap, which is not the case. The adhesives are a mixture of materials, resulting in complex DSC curves.

Part II

Conceptual Design

Chapter 7

Manufacturing Methods

Unlike mechanical joining methods, the strength of an adhesive bond depends largely on the manufacturing methods and conditions. Many methods are available, depending on the polymeric nature of the adhesive. This chapter covers some common assembly and removal methods for both thermoplastic and thermoset adhesives.

7.1 Applying thermoplastic adhesive

Thermoplastic adhesives have a low viscosity during application[2], and are typically applied with a glue gun. The quick cool down of the polymer makes bonding large areas complex. Furthermore, it gives little control over the adhesive thickness, and is thus not a feasible option for the V-Cart chassis. Some concepts are conceived to allow the application of thermoplastic adhesive.

Solid adhesive If the adhesive can be manufactured into a film, it can be cut to size and applied between adherents. A heating method is required to activate the adhesive and achieve adhesion.

Internal channels By drilling holes from the outer surface of the adherent to the joining interface, warm adhesive can be pushed through these holes. With the other substrate present at the desired spacing, the crevice fills up with adhesive. This requires an extra manufacturing step, resulting in stress concentrations. Keeping the adhesive warm throughout the channels can also be problematic for large adherent thicknesses. Lastly, all air must be pressed out from the interface.

Integrated thermoplastic layer The step of applying adhesive can be eliminated by integrating a thermoplastic layer in the thermoset composite. By co-curing a thermoplastic prepreg on the outer surface of the epoxy prepreg composite, polymer chains entangle creating

a strong bond. Conventional thermoplastic welding methods are now possible, with equal or superior bond strength compared to thermoset adhesives[34].

This method also has its limitations. An additional step is required during manufacturing, and production is limited to using prepregs. It is also unclear how such connection performs during fatigue loading.

7.2 Thermoplastic adhesion methods

There are many methods for joining thermoplastic composites. V-Cart chassis parts are manufactured using a thermoset resin, but a thermoplastic film or integrated layer (as described in the previous section) should enable these joining methods.

7.2.1 Ultrasonic welding

Principle Ultrasonic welding uses friction to heat up the polymer material. The bonding surfaces contain energy directors; small triangular resin protrusions that can be highly strained. The areas are pressed together, and low amplitude high frequency (20-40kHz) vibrations are applied[50]. The cyclic strain of the polymer causes intermolecular friction, melting the protrusions. It is a very fast, low cost process, well suited for automation. However, controlling the quality of the weld is difficult, and only spot welds are possible. Tooling costs for clamping the adherents can also be high.

7.2.2 Resistance welding

Principle Resistance welding is an electromagnetic welding technique. A direct current is sent through a heating element (often a metal mesh) located at the interface. Electrical resistance causes the element to heat up, together with the surrounding material. The material consolidates when current is shut off. Current leakage is a problem when welding CFRP adherents. Unless the surface consists of woven fabric, the current can run through the composite product, dissipating the heating energy[23]. Alternatively, the mesh can be coated with TiO2, or a GFRP layer[64].

Using this method for thermoset adherents, an thermoplastic adhesive layer should be applied to (at least) one adherent beforehand. Alternatively, the mesh could be infused with adhesive.

Clamping distance The clamping distance (the distance between the edge of the specimen and the electrical connector (figure 7.1)) influences the temperature distribution at the welding interface[24]. The exposed mesh can only dissipate heat by convection and radiation, while mesh at the interface transfer heat by conduction. As a result, the exposed mesh heats up more quickly, causing a sharp temperature gradient at the edge of the connection. This can result in local overheating and burning of the edge material, not to mention burning of the mesh itself. For the experiments performed in this research, burning of the mesh did not occur for clamping distances below $1mm$.

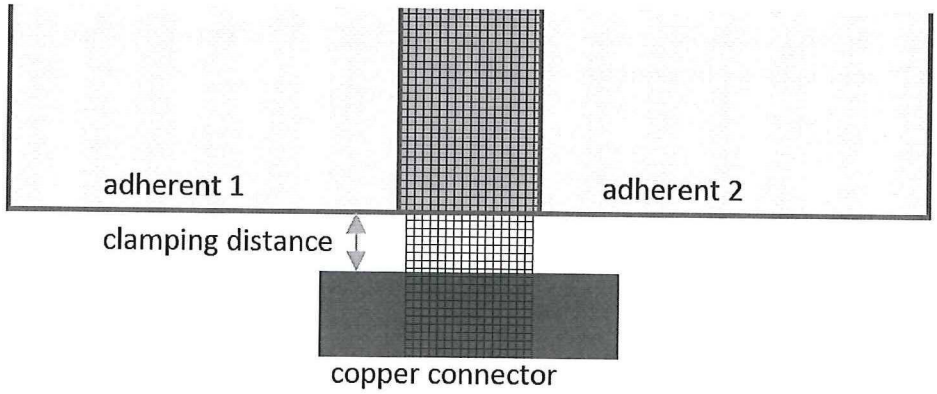

Figure 7.1: Schematic representation of clamping distance for resistance welding

Residual stress As a result of differences in coefficient of thermal expansion of the mesh and adhesive material, residual stresses originate in the adhesive layer. Coefficient of thermal expansion $\alpha \approx 15\frac{\mu strain}{K}$ for stainless steel but $\alpha \approx 140\frac{\mu strain}{K}$ for polyamides (polyamide is taken as an example because it is one of the adhesive used in this research, it is a typical value for a polymer). Viscosity of the adhesive becomes very low during heating. During cool down, the polymer solidifies and residual tensile stresses are generated; it shrinks more than the mesh. Steel experiences compressive stresses but this is not problematic. Adhesive stresses in the polymer are calculated in equations (7.1) to (7.2). Note that the outcome is strongly dependent on the values of T, α and Young's modulus of the polymer.

As a simple estimation, a residual tensile stress of $0.40MPa$ can be expected from the assembly cycle. Tensile strength of the adhesive lies at $14.5MPa$; it will thus not induce failure, but lowers the external load required to initiate failure slightly.

$$\epsilon = \Delta\alpha \cdot \Delta T = (180 - 20) \cdot (140 - 15) = 20E^{-3} \tag{7.1}$$

$$\sigma = E_{polyamide} \cdot \epsilon = 20E^{6} \cdot 20E^{-3} = 0.40MPa \tag{7.2}$$

The large difference in thermal expansion also has advantages. Adhesion of the thermoplastic adhesive to stainless steel is generally not very good. The adhesive shrinks around the steel mesh, providing mechanically grip. Although these tensile stresses are detrimental for crack growth in the adhesive, it does provide a good connection between resin and mesh.

7.2.3 Induction welding

Principle Induction welding uses induction to heat the polymer. An alternating magnetic field induces Eddy currents in a susceptor at the joint interface[17]. The susceptor should be a conductive material such as metal, of woven conducting fibres. The heating consistency of carbon fibres is generally worse than that of a metal mesh[4].

The alternating magnetic field induces Eddy currents in the material, causing heat up. Current density decreases with material depth, especially for high frequencies. The skin depth δ

is defined as the depth below the surface of the material where the current density has fallen to 1/e (≈ 0.37), and is given by equation (7.3)[21].

$$\delta = \frac{1}{k} = \sqrt{\frac{1}{\pi f \mu \sigma}} \tag{7.3}$$

Here f is the frequency of the alternating current generating the magnetic field, μ is the magnetic permeability of the material and σ is the electrical conductivity of the material.

Induction welding can also be performed using magnetic hysteresis. This is possible when small magnetic particles are present in a material. No closed loops exist, therefore no Eddy currents are induced. The magnetic field aligns the magnetic dipoles. Because the material keeps an amount of magnetization even with no magnetic field present, it costs a lot of energy to change the alignment in another direction. The particles heat up, and thus the surrounding material as well. This process occurs at much higher frequencies than the Eddy current principle[59].

Residual stress Similar to resistance welding, the adhesive will expand and shrink during the production process. It can be assumed similar stress levels are achieved as those found in the section 7.2.2. However, if no mesh is present in the adhesive layer, and the joint geometry allows the adherents to move closer to each other (for example a single lap joint of two panels), residual tensile stresses are slightly reduced by the adherents moving closer to each other. It thus depends on final geometry and presence of a mesh, but values larger than $0.40MPa$ will not be achieved.

7.2.4 Other heating methods

Thermoplastic welding techniques are different in operation, but are based on the same principle. A heat source warms the thermoplastic adhesive, allowing the material to adhere to the substrate. Any method able to heat the adhesive could thus in theory be suitable as a manufacturing method.

A thin, heat producing layer could be attached to the substrate's surface. Several experiments were conducted with such layers, designed for injection moulding systems[37][38]. Similar to resistance welding, it is an electromagnetic technique, were current is sent through a material to generate heat.

In his study, Jansen used a heating element consisting of three layers; an thermally insulation layer of polyimide, a heat producing layer of carbon filled resin, and a protective coating of polyimide. Heating proved to be much quicker than conventional injection moulding systems. However, variations in thickness of the layers, caused local power density fluctuations of up to 30%.

In order for the joint to be strong, good adhesion needs to be achieved between the heat producing layer and the adhesive, but also between and the heat producing layer and the composite part. This is not necessarily a quality of the design by Jansen. All layers contribute to the strength and stiffness of the connection.

7.2.5 Comparison of welding methods

Thermoplastic welding methods are different in execution. This section takes a look at the differences in properties of the connection resulting from the welding method.

Visual inspection and microscopy analyses show some differences corresponding with the welding techniques. Resistance welding introduces the least amount of porosity in the material[62] (see figure 7.2). Ultrasonic welding shows some porosity on the outer surface. This is thought to be the result of surface heating from the sonotrode, probably in combination with stiff clamping. Induction welding samples show most porosity. Bulk heating of the material gave rise to melting and reconsolidation of the material, reducing material thickness.

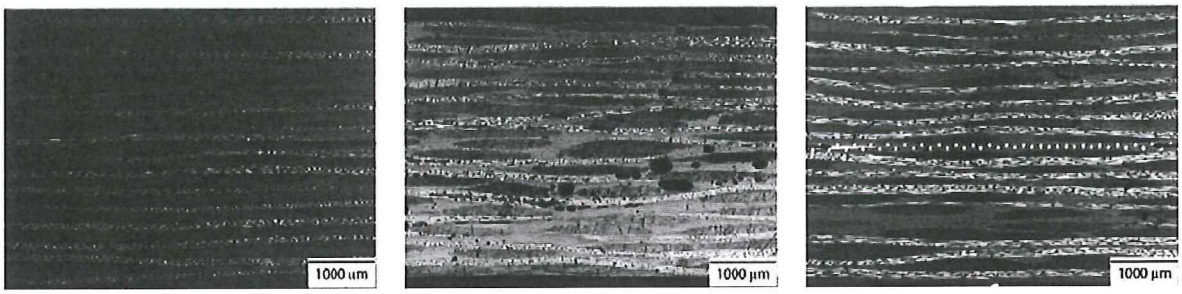

Figure 7.2: Cross-sections of ultrasonic welding (left), induction welding (middle) and resistance welding (right)[62]

Static testing performed by Villegas et. al. showed the presence of voids had little influence on strength[62]. In single lap shear testing, ultrasonic and induction welded specimens showed similar average strength values, while resistance welded specimens' strength values lied 15% lower. This is thought to be a result of poorly welded areas at the edges of the overlap (the area exposed to largest stresses). Heat transfer from the mesh to the adherent is more effective at the edges, resulting in lower temperatures of the adhesive[62]. Another possible cause for lower strength is the presence of the mesh at the interface, which has lower adhesion to the polymer. The other welding techniques showed absence of non-bonded areas and had a very uniform appearance.

Fatigue testing of the lap shear specimens showed a similar outcome regardless of the manufacturing technique. Residual strength remained between 85 and 100% of original static strength after 10^6 cycles, indicating little to no damage was initiated during fatigue testing. The fracture surfaces were similar to those obtained from static testing.

7.3 Thermoset resin

Assuming the bond of a thermoset adhesive can be released, there is no reason not to select it. Using a thermoset adhesive provides several advantages w.r.t. thermoplastic adhesive, seen in chapter 5. It typically consists of two components; a resin and a hardener, forming a viscous paste when mixed. To control the bondline thickness glass beads can be added to the mixture, often in a mass percentage between 4 and 7%. It is than smeared on the adherent, and pressed together with the other adherent. Curing ofter takes about 24-48 hours at RT, under a prescribed pressure. The process can be sped up at higher temperatures, but this may introduce residual stresses.

7.4 Removal methods

The following section explores methods to break the adhesive connection, for both thermoplastic and thermoset adhesives. This is required for disassembly and maintenance of the chassis. For the bond to be reusable, the process must prevent damage to the substrate, and re-assembly must be possible afterwards.

7.4.1 Physical

The most simple method of removing the bond is physical removal. It consists of forcing a sharp object through the adhesive layer, e.g. a knife or wire. This is commonly used in the automotive industry for removal of the windscreen, and the only realistic way of breaking an thermoset adhesive bond.

A more sophisticated method than a knife to physically remove the bond is using a oscillating saw. The hard blade material oscillates at a frequency between 11000 and 18500/minute with a small amplitude, allowing for easy cutting. The blade should be thinner and longer than the bond layer, and tooling should not be hindered by the geometry.

Physical removal methods are simple and cost effective, but labour-intensive. To prevent damage to other parts it is important the connection has enough room for access, which is difficult for thin bondlines. Furthermore, Donkervoort already indicated breaking of an adhesive bond using a knife always resulted in one of the parts being damaged. A less precarious removal method is preferred.

7.4.2 Temperature

Heating Heating reduces strength of thermoplastic polymers. Assuming two workers are working on the front bulkhead, both exerting a pulling force of $200N$, shear strength must be lower than equation (7.4) for easy removal. Loading the adhesive is only possible by shear when sliding the bulkhead over the chassis beams due to the geometric constraints.

$$\sigma = \frac{F}{A} = \frac{2 \cdot 200}{108000} = 0.0037MPa = 3.7kPa \tag{7.4}$$

The temperature where this value is reached differs per adhesive. A local heating method is required, which can be done with the same welding method used to assemble the construction (induction or resistance welding), reducing cost and production time.

For this calculation it is assumed all adhesive is heated uniformly. This should not be a problem for one large rectangular bonding area, but for the latest V-Cart design this becomes problematic. For resistance welding, it is possible to connect each bonding area to a power source, and heat the complete area at once. However, it is a tedious process, and requires careful timing to control the adhesive temperature.

The same is true for induction welding. The heating effect is concentrated around the coil. Theoretically many coils could be used to cover a larger area, but the geometry complicates heating of the inner surfaces. A solution would be to remove the bond in parts; disconnecting

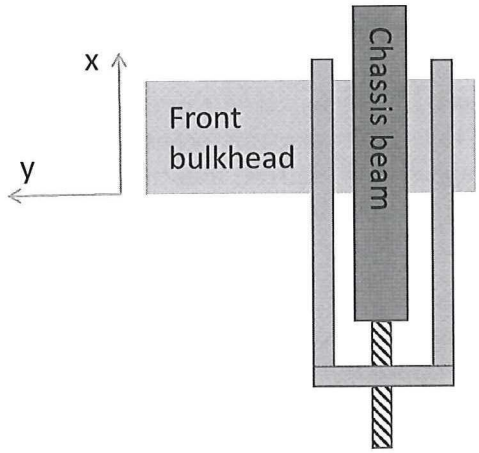

Figure 7.3: Top view of a device used to assist in releasing the adhesive bond. The blue structure hooks around the bulkhead, pulling slowly backwards by turning the screw at the bottom of the image

one area before the other. This would be a solution for the V-Cart chassis, but assuming the rest of the chassis is still intact, this is not possible due to geometric constraints.

Cooling Polymers become very brittle at low temperatures, resulting in fracture at small failure strains. Cooling of the joint could be performed using liquid nitrogen. Unfortunately the CFRP goes through the same structural changes; making sure only the adhesive breaks is thus problematic.

7.4.3 Chemical

Chemicals can be applied to dissolve the adhesive bond. The nature of the chemical depends on the polymer base of the adhesive. It is a suitable process, requiring little access space. However, it should be ensured the chemicals do not damage the composite chassis panels. Furthermore, the effectiveness remains questionable depending on the adhesive used.

7.4.4 Assistance during disassembly process

Disassembly of the front bulkhead is a difficult process, because the only loading scenario possible is shear. It is possible that, despite the measures taken, the adhesive is still too strong for removal by hand. This is tested experimentally in chapter 10. If it proves too strong, several devices can be used to ease disassembly.

One method is too increase the exerted force on the bulkhead, which is limited by the people working. A device with a similar working principle as a crank puller (used for removing the crank from a bike) can be applied to exert a large force in a controlled manner. A top view is shown in figure 7.3. Turning the bolt at the front of the chassis slowly increases the distance, pulling the bulkhead from the chassis beams. The front of the chassis is designed to cope with large surface pressures, this should therefore not be a problem.

7.4.5 Alternative loading scenario's

Adhesive is strongest when loaded in shear. It is therefore recommended to use a different load type when disconnecting the adherents; this requires less force for the same adhesive, or the adhesive needs less weakening to still be able to remove it. Note that making the adhesive as weak as possible is preferred because it prevents damage (e.g. delamination) of the substrate.

The geometric constraints in the V-Cart geometry limit the load case for disassembly to shear. Ideally a peel load case is applied during removal. The crack front propagates requiring relatively little force. This is the opposite to the shear load case, where the complete bonding area is broken almost instantaneously. If this re-usable joining method is applied elsewhere, it should ideally be designed to enable loading in peel. Of course, peel loading should be prevented during normal use of the product.

Chapter 8

Concept Selection

Donkervoort can only afford to develop one concept in more detail, taking the concept that is most promising. This is done using a trade-off analysis. Note that although the reusable joint is universally applicable, the selection process is performed for the Donkervoort car chassis. Other applications might prefer other manufacturing methods.

A House of Quality analysis is performed to rank the importance of the technical requirements, based on the consumer requirements the design aims to satisfy. The obtained weight factors are subsequently used in a trade-off analysis to determine the most suitable concept.

8.1 Consumer & technical requirements

The car is designed for a market need, therefore it is important to consider the consumer requirements during the designing process. For our case, Donkervoort Automobielen B.V. is the consumer. A set of requirements with weight factors is made based on dialogue with Donkervoort[58] and left unchanged (table 8.1).

Consumer requirements	Weight factor
High performance	10.0
Unique product	9.0
Feeling of safety	8.5
Beautiful product	8.0
High quality	7.0
Low cost insurance	7.0
Easy maintenance	6.0
Relative low cost	6.0

Table 8.1: Consumer requirements with weight factors

A list of technical requirements is made, which should help satisfy the consumer requirements. These are based on those presented in chapter 3 and can be seen in table 8.2. For some

requirements more precise numbers are known (section 3.2), the table shows more subjective requirements. This is done because for the concepts, it is impossible to say what strength & stiffness values are achieved without experimental research.

Technical requirements
High stiffness & strength efficiency
Increased safety
Low part count
Low part complexity
Fit for automated production
Fit for maintenance
Fit for modular design
Easy access to components
'A-class' surface finish

Table 8.2: Technical requirements

8.2 House of Quality

Finding a solution that satisfies all requirements is impossible, it is always a compromise. To judge which technical requirements are most important to satisfy the consumer needs, the house of quality tool is used. It presents a relationship between the consumer needs ('Whats') and technical requirements ('Hows').

Figure 8.1 depicts the analysis performed. The 'Whats' are presented on the left hand side, the 'Hows' on top. A matrix emerges, symbols are used to indicate the relationships. These can be strong, moderate, weak, or absent. Typically 9 points are given for a strong relationship, 3 for a moderate relationship, 1 for a weak relationship and 0 for no relationship, these scores are therefore used here as well. The triangular matrix on top describes the relationship between the technical requirements. An elaboration on how these ratings are chosen can be found in appendix D.1. Note that despite efforts to remain objective, the method is inherently subjective, especially when performed by one person.

Several calculations are performed. First, the weight factors of the 'Whats' are expressed as a percentage, as can be seen in the 'relative weight' column. The weight of the 'Hows' is calculated by multiplying each relationship score (begin 9, 3, 1 or 0) with the relative weight of the 'Whats'. These are listed in the row at the bottom. The relative weight is deduced from these scores by expressing them as a percentage of the total.

The relative weight factor represents the importance of each technical requirement (table 8.3). This factor is based on the correlation with consumer requirements; a highly ranked technical requirement is thus likely to satisfy one or more aspects important to the customer. Donkervoort views the modular design property as an essential part of their strategy, therefore its relative weight was raised by five points. This value is based on dialogue with Donkervoort from previous research[58][29], therefore no changes are made. Section 8.3 shows this favours resistance welding and bonding using thermoset adhesive.

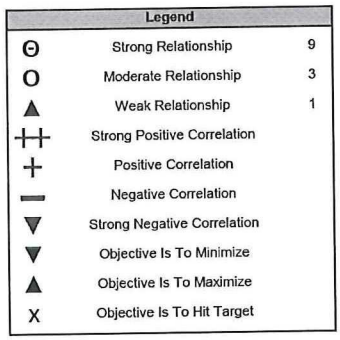

Relative Weight	Weight / Importance	Demanded Quality (a.k.a. "Customer Requirements" or "Whats") / Quality Characteristics (a.k.a. "Functional Requirements" or "Hows")	1 Stiffness & strength	2 Increased safety	3 Low part count	4 Low part complexity	5 Fit for automated production	6 Fit for maintenance	7 Fir for modular design	8 Access to components	9 Aesthetics
		Direction of Improvement: Minimize (▼), Maximize (▲), or Target (x)									
16,3	10,0	High performance	Θ	O							
14,6	9,0	Unique product	Θ	O	▲		▲				Θ
13,8	8,5	Feeling of safety	▲	Θ		▲		▲			
13,0	8,0	Beautiful product			O	O	▲				Θ
11,4	7,0	High quality	▲	O			O				▲
11,4	7,0	Low-cost insurance			O	O	O	Θ	O	O	
9,8	6,0	Easy maintenance			O	Θ		Θ		Θ	
9,8	6,0	Relative low cost			Θ	Θ	▲	▲	O	Θ	
		Weight / Importance	303,3	251,2	204,9	262,6	105,7	213,8	63,4	209,8	260,2
		Relative Weight	16,2	13,4	10,9	14,0	5,6	11,4	3,4	11,2	13,9

Figure 8.1: House of Quality for Donkervoort chassis joint

Technical requirements	Grade
High stiffness & strength efficiency	16.2
Low part complexity	14.0
'A-class' surface finish	13.9
Increased safety	13.4
Fit for maintenance	11.4
Easy access to components	11.2
Low part count	10.9
Fit for automated production	5.6
Fit for modular design	3.4/8.4

Table 8.3: Consumer requirements with weight factors

8.3 Trade-off analysis

Using the results of the HoQ, the concepts are judged to find the most promising solution. A trade-off analysis is presented in table 8.4. The concepts are compared on a relative scale. The ultrasonic welding method is chosen as the baseline and given 0 points. The other concepts are compared to the baseline and given a score varying from -3 to $+3$ in each category (where -3 is much worse, and $+3$ is much better than the benchmark concept. The last column shows the weighted average of the scores, divided by 10. Note that for each concept, the method for disassembly is the same as assembly to save cost and time. For the ultrasonic & thermoset concept, a physical removal method has to be used, as was discussed in chapter 7. Also note that although the trade-off analysis seems an objective process, the scores given to the concepts in each category are still intrinsically subjective. The same is true for the determined weight factors. Still, much effort was put into the ratings to make it as objective as possible.

Judging from table 8.4, using resistance or induction welding with a mesh seem most promising. Resistance welding is easy to apply and suitable for different dimensions, and does not have any real weaknesses. Using an integrated heating layer is a complex and expensive process, and therefore not suitable for small series production of Donkervoort. Also, strength values are expected to be low due to the many thin bonding layers. Induction welding seems more promising when a mesh is used; the manufacturing process of the adhesive layer is much simpler. Using a thermoset adhesive scores low because maintenance becomes impractical. Ultrasonic welding has the same disadvantages, but is still faced with the weaknesses of a thermoplastic adhesive and incomplete bonding area. A more elaborate description of the scores is presented in D.2.

Resistance welding and induction welding using a mesh are both very suitable for the process. Both were at my disposal in the lab, however the induction welding setup recently broke down. Because the difference between the techniques is very small, but there is a time constraint on this research, the resistance welding setup will be used for testing.

	High stiffness & strength efficiency	Low part complexity	'A-class' surface finish	Increased safety	Fit for maintenance	Easy access to components	Low part count	Fit for automated production	Fit for modular design	
Weight factors	16.2	14.0	13.9	13.4	11.4	11.2	10.9	5.6	8.4	Total
Ultrasonic	0	0	0	0	0	0	0	0	0	0
Resistance - mesh	2	0	-1	2	3	0	-1	-1	2	7.98
Resistance - integrated heating layer	0	-3	0	1	3	0	-3	-3	3	-1.87
Induction - mesh	2	0	0	2	2	0	-1	1	0	7.67
Induction - hysteresis	2	-2	0	2	2	0	-1	1	0	4.87
Thermoset epoxy	3	-1	0	3	-3	0	-1	-3	3	3.81

Table 8.4: Trade-off analysis

Chapter 9

Concept tests

In this chapter the first samples are manufactured (using the resistance welding assembly method) and tested. These preliminary tests serve an exploratory purpose, to see what strength values can be expected by adhering TS composites with a TP adhesive. This is not a common adhesion method, it is unknown what strength values can be expected. At the same time, a relatively simple test can show several improvements that could be incorporated in the final design.

9.1 Proposed test

A shear strength test is performed to determine adhesive strength. This is a common test for an adhesive joint, and will be performed using lap shear specimen.

Originally adhesive was applied using a glue gun. This is an adequate method for the test's purpose. However, it proved difficult to achieve a reproducible bondline thickness due to the rapid solidification of the adhesive. This makes comparison unfounded; a thicker bondline results in larger eccentricities in the joint, resulting in larger peel stresses and failure at lower load levels. A more detailed overview of the test with glue gun can be read in section E.

The tests did show that the elastomer adhesive (currently used by Donkervoort) had by far the lowest strength values. Although this was expected, it cannot be seen as a suitable adhesive for the V-Cart application. Average shear strength values was only $0.74MPa$, requiring a immense increase in bonding area to reach desired strength values of the chassis.

To overcome differences in bondline thickness, resistance welding is used to manufacture samples. It allows the adhesive to be heated as a whole, controlling the solidification. This could also be done using induction welding, but the setup was not available at the moment of testing. To reduce bending moments in the test samples, the test is performed with double lap shear samples.

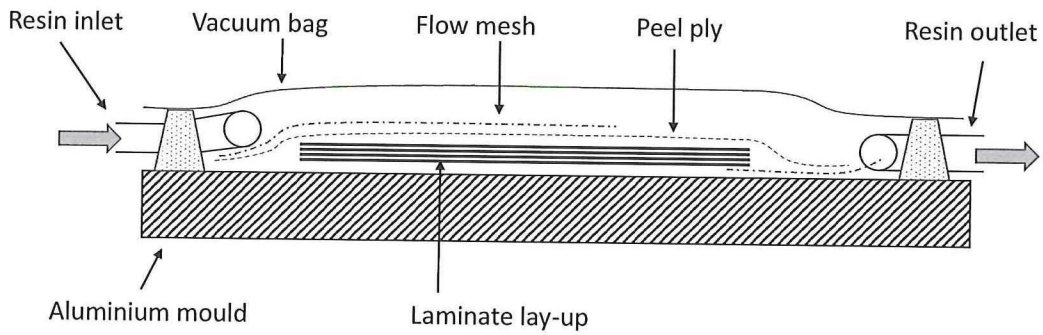

Figure 9.1: Schematic representation of the vacuum infusion process

9.2 Manufacturing of samples

Manufacturing of CFRP Two panels of different thicknesses were manufactured using vacuum infusion. A schematic representation of the infusion process can be seen in figure 9.1. A double lap joint consists of two large panels (panel A), and two smaller thinner panels to keep them together (panel B) (figure 9.2). Panel A is twice as thick as panel B to prevent an adherent stiffness imbalance; this would result in larger stress peaks at the edges of the overlap. An overview of the manufacturing conditions are presented in table 9.1.

Item	Details
Fibres	Carbon [0°/90°] TenCate CD 0286 050 030
Lay-up panel A	$[0/90, \pm 45, 0/90]_2$
Lay-up panel B	$[0/90, \pm 45, 0/90]$
Resin	Bakelite EPR 04908
Hardener	Bakelite EPH 04908
Release agent	2 layers Marbocote 227CEE
Degassing pressure	3mBar
Infusion pressure	49mBar
Curing pressure	504mBar
Curing	16.5 hours @ RT + 5 hours @ 80°C
Cutting	Belt saw and Sepitom with diamond cutting blade
Specimen size panel A	150x100mm
Specimen size panel B	50x100 mm
Pretreatment	Sanding P240, PF-SR wipes, drying (1 hour @ 50°C)

Table 9.1: Manufacturing of double lap joint adherent material

Manufacturing of thermoplastic adhesive A thin thermoplastic film was made by pressing solid blocks of adhesive in a hot press between foils of teflon. Under a constant force of $10kN$, temperature was increased to 190°C, held for two minutes, and allowed to cool down. An aluminium frame of $0.20mm$ thickness was placed at the edge of the press, to prevent spillage and control the thickness of the adhesive film.

Assembly with thermoplastic adhesive The double lap joint was manufactured in the resistance welding setup. CFRP material was stacked with an adhesive foil and mesh in between, figure 9.3. The mesh diameter $d_{wire} = 0.04mm$ with a spacing between the wires $\Delta_{wire} = 0.08mm$. A wooden mould with kapton film held the material in place. The width of the connection caused a relatively low electrical resistance, limiting the power input density to $50kW/m^2$. Temperatures (which were measured using two thermocouples) were monitored and power was cut when 180°C was reached. A constant pressure of $0.017MPa$ was applied, also during consolidation. The process was twice to form a complete joint.

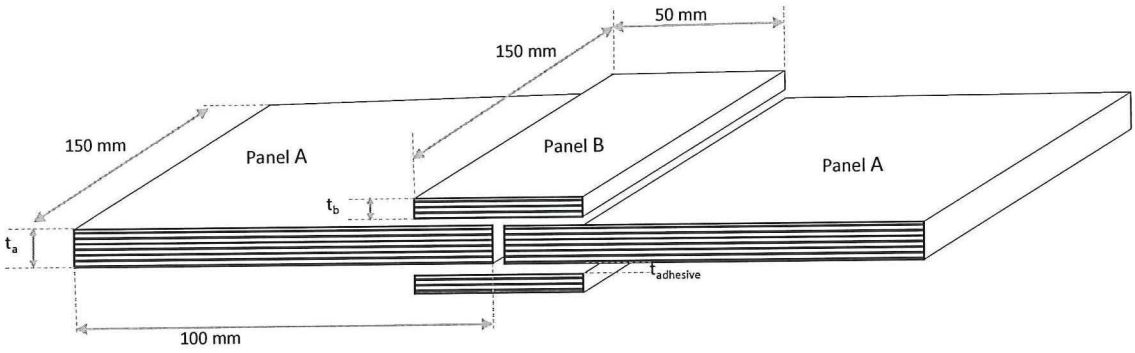

Figure 9.2: Schematic representation of the double lap joint lay-up

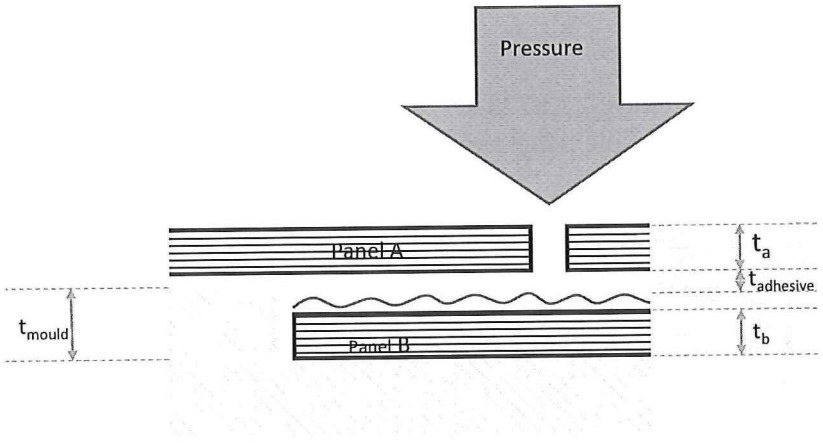

Figure 9.3: Schematic representation of the resistance welding setup

Assembly with thermoset adhesive For comparison, a similar joint was manufactured using a thermoset Scotchweld 9323 B/A epoxy. The resin and hardener were mixed first, after which glass beads with a diameter between 0.20 and 0.30 mm were added to ensure uniform bondline thickness. Assembly was done on an aluminium mould with teflon foil to prevent adhesion to the mould. Curing took place at RT for 48 hours, at a pressure of 860mBar.

Creating test specimens Test specimens were cut from the wide double lap joint manually using a silicon carbide cutting blade. The diamond cutting blade has higher hardness, resulting in a smoother cutting surface than the silicon carbide blade. However, cutting thermoplastic adhesive is not possible as they become attached to the blade. Test samples were

Adhesive	Test temperature (°C)	DIC	Number of test specimens
Henkel	RT	yes	6
	60	no	5
3M 3731	RT	yes	4
	60	no	5
3M 3789	RT	yes	5
	60	no	5
Epoxy	RT	yes	6
	60	no	6
Total number of specimens			42

Table 9.2: Test matrix for double lap shear

cut to 200x25mm. A slight scatter in sample dimensions existed as a result of manual cutting; all samples were measured using a digital caliper for accurate dimensions. Paper tabs were adhered to the samples with cyanoacrylate to prevent slipping of the samples in the test bench. A speckle pattern was applied on one side, enabling Digital Image Correlation (DIC).

9.3 Test protocol

The test is performed according to ASTM D3528[7] in a 250kN Zwick test bench. Table 9.2 shows the test matrix. One sample failed before the test, hence only four samples of 3M 3731 manufactured at RT could be tested. Several panels were slightly wider, allowing six to be cut from the material. Strain rate was constant at 1.27mm/min, the test stopped when the maximum force was reached. For the tests at 60°C, samples were placed in the temperature chamber 15 minutes before testing.

If the aim of the test is *just* discovering strength values of adhering TS composites with TP adhesive, one adhesive would have sufficed. At the time of testing there was still a collaboration with Donkervoort. The company was interested in applying the connection method in the future V-Cart, but also in smaller applications in the current car if this proved advantageous. Therefore several adhesives were tested, to be able to make a comparison. This is of lesser importance now.

9.4 Results

An overview of the results can be seen in table 9.3. A complete list of results can be found in appendix K.6.

Decent strength values are obtained, typical for thermoplastic adhesives. Values are still notably lower than manufacturer's specifications (table 9.4, values were not specified by Henkel), but this can be explained by differences in test method and material. At 60°C, thermoplastic adhesives show a large degradation in strength. Based on the DSC data (section 6.2.2) the

	Test temperature [°C]	Average shear strength [MPa]	Standard deviation [MPa]
Henkel	RT	2.89	0.32
	60	0.20	0.036
3M 3731	RT	2.10	0.082
	60	0.32	0.23
3M 3789	RT	3.33	0.45
	60	0.64	0.073
Epoxy	RT	18.43	2.2
	60	20.64	0.34

Table 9.3: Strength values of double lap joints

difference in strength was not expected to be this large. A $2.0MPa$ shear strength was considered to be a requirement for the V-Cart chassis, which is never satisfied at 60°C. Failure modes are discussed in section 9.5.1.

Adhesive	Average shear strength [MPa]	Test details
3M 3731	3.3	Lap shear at RT with douglas fir adherents
3M 3789	4.3	Lap shear at RT with douglas fir adherents
Epoxy	30	Lap shear at RT with 1.66mm thick aluminium adherents

Table 9.4: Shear strength values as specified by manufacturer[2][1]

9.5 Discussion and quality assessment

Using one of these adhesives for application in the V-Cart chassis seems impossible. Shear strength values are not high enough at 60°C. Some improvements can be made, but selecting another, more temperature resistant adhesive seems more founded. Still, the research focuses on the reusable bond, and some interesting conclusions can be drawn.

9.5.1 Failure modes

Every specimen was inspected, and the failure mode noted. If it was a combination of several modes, the percentage of each was noted. The cumulative percentage of every test group can be seen in figure 9.4, a more detailed result can be seen in table K.7.

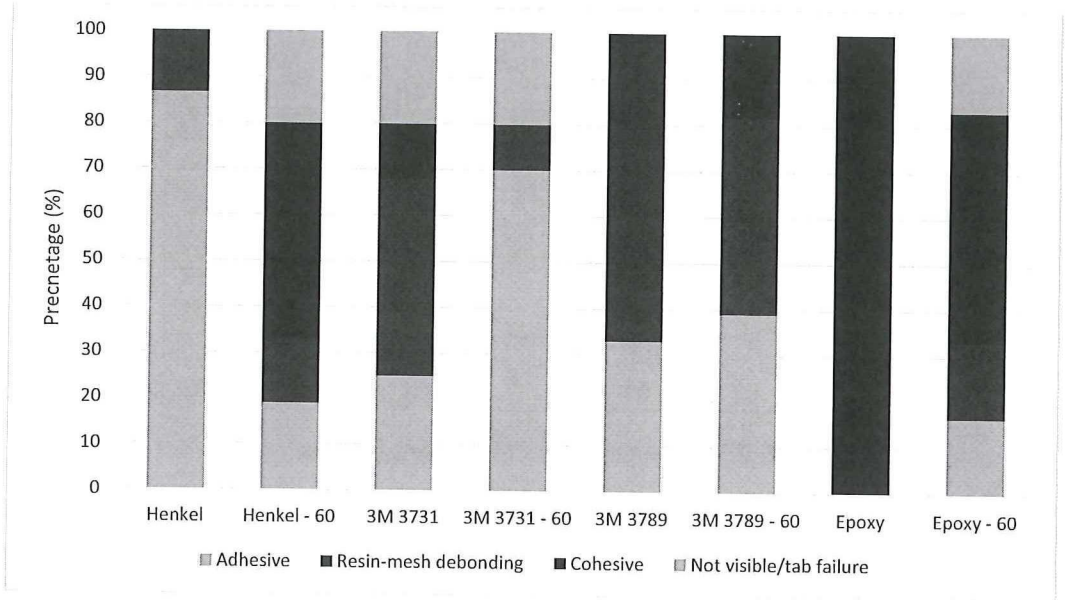

Figure 9.4: Overview of cumulative failure modes of test groups

For the thermoplastic adhesive, both adhesive failure and resin-mesh debonding are very prominent. Both occur in about the same amount, suggesting both modes initiate at similar load levels.

9.5.2 Microscopy analyses

The optical microscope was used to inspect prepared - and unprepared samples (process can be read in appendix H). Some results can be seen in figure 9.5. All adherents are CFRP epoxy material with a stainless steel mesh in a film of 3M 3731 (images a & b) or 3M 3789 (images c & d). Overall, it shows a void rich connection, which has a negative influence on bond strength. In section 10.6 it is discovered that the ultrasonic ethanol bath used for cleaning of the samples was a likely cause for the creation of voids. However, the next section discusses some changes that can improve the void content nonetheless.

9.5.3 Improvements

Based on these results, several improvements are suggested to improve both cohesive and adhesive bond properties.

During the manufacturing process, voids can develop by two ways; (1) a chemical reaction is triggered (by heat) causing gas to form, or (2), the air that is present in the mesh cannot (completely) escape. Improvements can be made to reduce 2 to a minimum. Air is present in the mesh because the mesh and adhesive layer are stacked during assembly. By pre-impregnating the mesh with resin, entrapped air is removed. Assembly should be performed in a flat mould to ensure an even pressure distribution.

Epoxy has a low surface tension, making it difficult to wet. A better surface pretreatment will improve wetting and adhesion. Of the methods available, UV exposure has the best

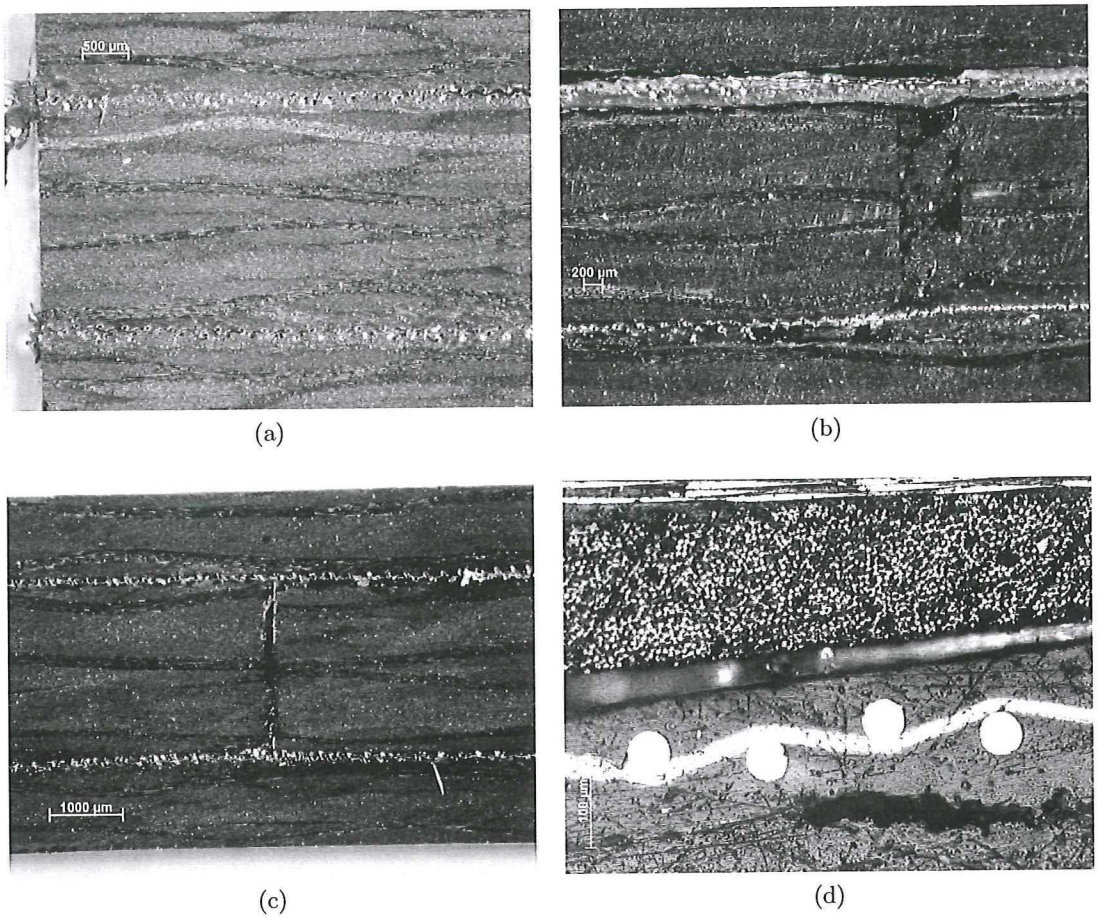

(a) (b)

(c) (d)

Figure 9.5: Microscopy photos of double lap joint connection. CFRP epoxy adherents with mesh an film of 3M 3731 (a & b) and 3M 3789 (c & d)

repeatability and is therefore found most suitable for this research. These improvements are incorporated in chapter 10.

9.6 Adhesive testing conclusion

Based on the manufacturing concepts from chapter 7, double lap shear samples are made and tested on shear strength. Carbon epoxy adherents were adhered using a thermoplastic film (pressed in the Joos press) and a metal mesh serving as heating element. The film was heated to 180°C in 20 seconds and cooled down under constant pressure of 0.017MPa.

Testing of the specimens shows typical thermoplastic adhesive shear strength values between 2-3MPa at RT. The V-Cart requires at least $2.0MPa$ (assuming the complete area is adhered), higher strength values (or a minimized scatter) are thus desirable. At 60°C the TP adhesive's shear strength decreased drastically. If an application requires stability at 60°C, another adhesive is definitely required.

Analysis of the results shows changes possible to improve adhesive strength and prevent resin-

mesh debonding. These include pre-impregnating the mesh and applying a pretreatment to the CFRP. These are explored in the next chapter.

The thermoset epoxy adhesive showed the largest shear strength values, by a large margin. Furthermore, strength values show no decline at 60°C. This makes it ideal from a strength and stiffness point of view. However, removal and re-use of the joint becomes problematic. The only suitable method is physical removal, which has a high chance of damage to the adherent. Furthermore, Donkervoort mentioned it did not see physical removal a feasible method.

Initial tests using single lap shear specimens show the Sabatack elastomer is not suitable for the V-Cart application. Despite its easy manufacturing process, shear strength values are too low. This cannot be compensated by an increase of the bonding area.

Part III

Detailed Design

Chapter 10

Improved adhesive testing

10.1 Introduction

Chapter 9 showed how the elastomer adhesive is not strong enough, how the TS adhesive is strong but difficult to remove, and how the TP adhesives reach slightly higher strength values than required but only at RT. This chapter aims to improve this last group. Several changes in the manufacturing process are thought to increase the strength values of the adhesive bond, making it applicable for several applications. The TP adhesives selected proved unable to keep their strength at 60°C, despite the claims from the manufacturer. A different adhesive would thus be required for the V-Cart chassis.

Several tests are performed to explore different properties of the reusable TP joint. Four sets of test samples are produced, differences in the manufacturing process aim to highlight different properties of the connection. All are manufactured with 3M 3789 adhesive because it proves most promising in the previous chapter.

Improvements obtained from the tests in chapter 9 are taken into account. This forms the benchmark test. The test is repeated at high temperatures to simulate removing the connection. To determine the influence of the mesh in the sample, similar specimens are made without mesh. Finally, a set of samples is disassembled and re-adhered, to determine whether the original strength can be reached after re-use.

10.2 Test methods

Many tests are available for joint strength determination, with many different geometries. A single lap tension test with $12.5mm$ overlap is commonly used. Failure is a combination of shear - and peel stresses (as a result of joint eccentricity). Such test methods thus cannot be used to obtain adhesive material properties, but serve as a suitable comparison method between adhesives.

10.2.1 Double lap shear

In chapter 9 double lap shear samples were used, with an aim to minimize joint eccentricity. However, several points indicate the resistance welding setup is less suitable for wide overlaps.

1. The $50mm$ wide mesh as used in chapter 9 has a relatively low electrical resistance. Power density in the adhesive layer is a combination of input current, electrical resistance and bonding area. For a given area and mesh, the output of the power source determines the maximum power density. Low current values result in long welding times. By decreasing joint width, electrical resistance increases, while reducing the bonding area, allowing for larger power densities for the same power source.
2. Copper blocks are pressed against the mesh using pneumatic cylinder, to close the electric circuit (figure 10.1). In the tests from chapter 9 the mesh was wider than the copper blocks. An additional wider copper plate was therefore placed in between the block and the mesh. It is hypothesized this results in inhomogeneity in the current input along the width of the mesh; the high clamping pressure of the copper blocks results in a worse connection at the edges. The mesh width is thus preferably below $30mm$.
3. A similar problem occurs for the crocodile beaks. During the welding process, the current is controlled in a feedback loop, using the electrical resistance of the mesh as input. Crocodile beaks are attached to the mesh to measure the electrical resistance (figure 10.1). These beaks are only $15mm$ long. A double lap joint typically has a wider overlap and thus a wider mesh. This requires folding of the mesh to fit inside the crocodile beak, resulting in an unreliable resistance measurement. The mesh width is thus preferably below $15mm$.

These factors, especially point 3, contribute to uncertainties in the manufacturing process of a wide (double) lap joint connection, making it unreproducible. A double lap joint was desired to reduce eccentricities. There are no geometric eccentricities, but differences in bond properties lead to eccentricities nonetheless. The overlap length should be shorter than $15mm$ to have a reproducible result. This is only possible for single lap shear samples.

The problem could also have been solved by modifying the setup to accept longer crocodile beaks. However, this is a new connection method with unknown properties. Therefore using simple test specimen is though to be more robust, to reduce the risk of deviations in the manufacturing process.

10.2.2 Napkin ring

Another adhesive test method is the napkin ring test. It produces a relatively uniform shear stress in the adhesive layer, yielding shear strength and modulus. However, it requires a machining of a thick substrate, which costs a lot of material and time. Therefore the method is not considered.

10.2.3 Single lap shear

To stay within the limits of the resistance welding setup, overlap length should be less than $15mm$ (figure 10.1). Typical single lap overlap values are $12.5mm$ and $25mm$, $12.5mm$ is

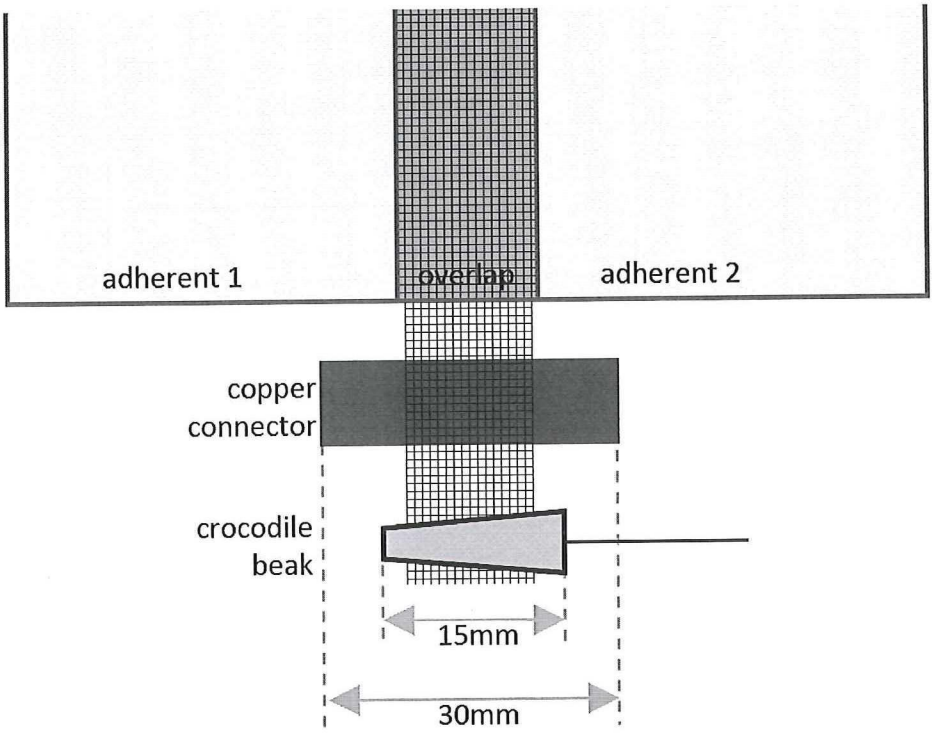

Figure 10.1: Schematic representation of the width of copper connector and crocodile beak for the resistance welding setup

thus the only option. Several geometries are possible for single lap shear, ASTM D1002 (for metals) or ASTM D5868 (for composites), ASTM D3165 and ASTM D5656 (for metals). The behavior under load is illustrated in figure 10.2.

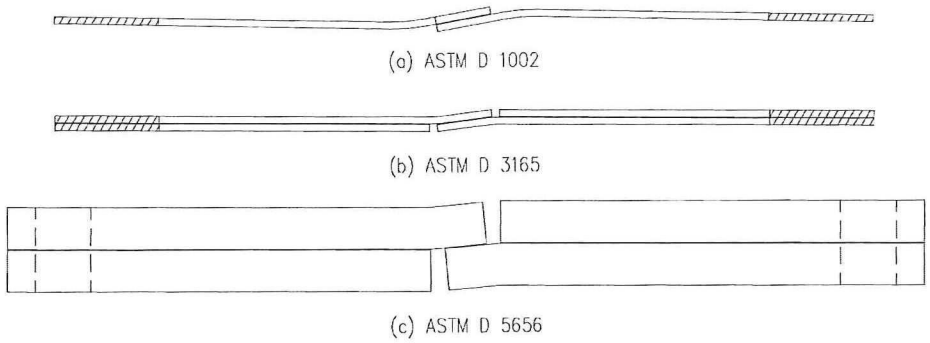

Figure 10.2: Test specimen deformation for various ASTM standards[39]

Peel stresses are lowest in ASTM D 5656 specimens due to the high bending rigidity. However for composites this methods is not often used, fabrication becomes a cumbersome process. ASTM D 1002 specimens have little bending stiffness and as result are exposed to high peel stresses. ASTM D 3165 specimens have similar bending stiffness as D 1002, but peel stresses are reduced by placing the load in line with the substrate.

Test name	Manufacturing	Test temperature (°C)	Number of times re-assembled	DIC	Number of test specimens
Benchmark	Resistance welding	RT	0	yes	6
Removability	Resistance welding	180	0	no	6
Re-usability	Resistance welding	RT	1	yes	6
Without mesh	Oven + adhesive film	RT	0	yes	6
Total number of specimens					24

Table 10.1: Test matrix summarizing the performed tests with 3M 3789 adhesive

10.2.4 Test samples

Specimens are manufactured in dimensions similar to the ASTM D 1002/D 5868 standard. By placing the clamps at an offset, bending moments are minimized. The joints are made by connecting two panels. Samples are cut from the connected panels.

10.3 Manufacturing

This section covers the manufacturing process of the test samples, highlighting the differences between the test groups. An overview is presented in test matrix 10.1.

10.3.1 Material

Manufacturing of CFRP One large CFRP panel is sufficient to provide all substrate material. The fabric has a satin weave, the top plies were therefore flipped w.r.t. the bottom plies to avoid residual stresses in the laminate. A peel ply was used to create a rough surface suitable for adhesion. Manufacturing was performed by vacuum infusion, the conditions are summarized in table 10.2.

Manufacturing of pre-impregnated mesh The mesh is impregnated in a Joos press. Mesh is cut to strips of 50mm wide and 300mm long. Tape was placed 192mm apart to control the flow of adhesive in length direction (the copper connectors are spaced 192mm apart in the resistance welding setup). Several methods to control the adhesive flow are explored in appendix F, using ordinary tape seemed most effective. 3M 3789 adhesive film (which is made from the original adhesive using the Joos press) of 0.20mm thickness was cut into rectangles of size 180 by 50mm. The mesh was placed in the Joos press with adhesive films stacked on top and below the mesh.

Under a constant force of 10kN, the material was heated to 190°C, held there for 2 minutes, and cooled down to RT. Thickness of the final product is determined by the mesh. The mesh

Item	Details
Fibres	Carbon [0°/90°] TenCate CD 0286 050 030
Lay-up panel	$[0/90]_4$
Resin	Bakelite EPR 04908
Hardener	Bakelite EPH 04908
Release agent	3 layers Marbocote 227CEE
Degassing pressure	3mBar
Infusion pressure	49mBar
Curing pressure	509mBar
Curing	16 hours @ RT + 5 hours @ 80°C
Cutting	Belt saw and Sepitom with diamond cutting blade
Panel size	192x150mm

Table 10.2: Manufacturing of single lap joint substrate material

is cut in strips of $12.5mm$ wide using a knife. Some small air bubbles are visible, but overall quality is good.

Pretreatment of CFRP A more elaborate pretreatment was performed to enhance adhesive properties. Specimens were adhered within four hours after the last step.

- 2 PF-SR (sealant remover & solvent cleaner) wipes
- 1 hour in oven at 50°C
- 10 minutes UV exposure at constant distance from lamb

10.3.2 Assembly

Assembly using resistance welding This production method is used for the benchmark, removability and re-usability samples. Using the resistance welding setup, two panels were pressed together with the pre-impregnated mesh in between, under constant pressure of 6.4 bar. A current of 13A ($35kW/m^2$) was used to heat the 3M 3789 adhesive in 30 seconds. Temperature was monitored using two thermocouples, reaching approximately 190°C. Pressure was released after the connection had cooled down to 30°C. Temperature curves can be seen in figure K.10.

Assembly in oven This production method applies to the samples without mesh. Without a heating element, a different manufacturing process is required. Note that this is not a realistic assembly method for the joint, it is solely used for comparison purposes.

Two CFRP panels were stacked in a mould with offset with an adhesive film in between (see figure 10.3). Perpendicular to the bond, three thin (approximately 2mm wide) strips of mesh were placed to eliminate bending of the top panel under pressure. Under a constant pressure of 950mBar, the whole was put in an preheated oven. In 11 minutes, T_{appl} was reached, and the connection was allowed to cool down. Temperature curves can be found in figure K.11.

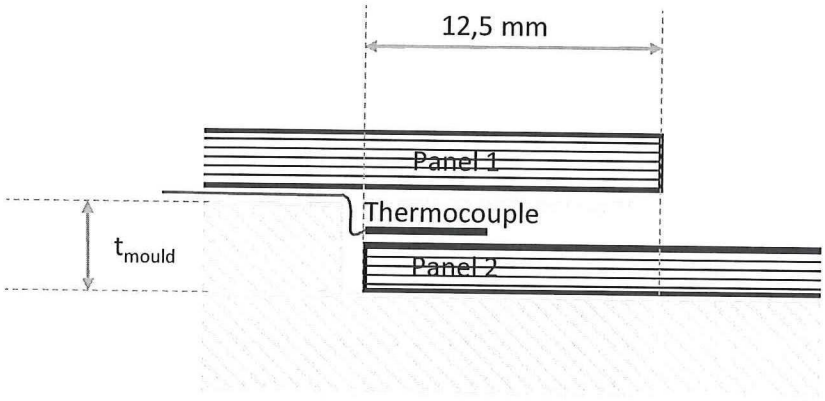

Figure 10.3: Schematic representation of manufacturing of single lap joint without mesh

Property	Value
Test bench	Zwick 250kN or 10kN
Test temperature	RT or 180°C
Number of samples	6
Strain rate	$1.3mm/min$
Test stop condition	F_{max} reached
Strain measurement	DIC + extensometers

Table 10.3: Test conditions for double lap joint shear testing

Assembly for re-usability test The re-usability test aims to determine the strength of the joint after the connection is disassembled and re-adhered. Manufacturing of the test samples therefore involves the same steps.

The adhesion process is performed using the resistance welding setup. The connection is removed by placing the panels in an oven preheated to 200°C for five minutes. Taking the panels apart requires no effort, the mesh is removed as well. Some areas feature adhesive residue, others areas are free of adhesive. Within an hour after the removal, the panels are re-adhered without cleaning or pretreatment.

Producing test samples Test samples are taken from the adhered panels using water-jet cutting by Van Nobelen. The heat generated by mechanical cutting is a potential cause for voids and damages in the connection. Although water-jet cutting utilizes an abrasive, the large amount of coolant reduces fluctuations in temperature of the adhesive layer as much as possible. Samples are identical in dimensions, cut to 25x188mm.

10.4 Test protocol

Test conditions were identical to those used in previous double lap shear tests (see table 10.3). However, to avoid peel stresses as much as possible, the clamps are placed at an offset. Conditions are summarized in table 10.3.

10.4.1 Test bench

To reduce the margin of error, it is best to select a test bench where failure of the sample occurs within 50-70% of the maximum load capacity of the bench. It is expected the strongest samples will fail at 2kN or lower. Of the test benches at my disposal, the 10kN bench is best suited. However due to unavailability it is decided to use the 250kN bench for testing. According to the calibration report, margin of error at $1000N$ is only 0.1%, which is acceptable.

The removability test was performed in a temperature chamber preheated to 180°C. By cutting the joint into samples, excess mesh was removed. This makes connection of a power source impossible; an external heating method is required. The expected failure load lies much lower than $1000N$, therefore it is performed in the Zwick 10kN bench. Samples were placed inside the chamber (pre-heated to 180°C) 15 minutes before testing. A thermocouple confirmed T_{appl} was reached after 15 minutes (heating the polymer to T_{appl} strongly reduces strength, while avoiding degradation).

10.4.2 Strain measurements

Strain can be measured using various devices. Extensometers are easy to use but introduce some inaccuracies for single lap shear tests, as a result of the rotation of the sample.

The KGR-1 extensometer is designed to measure the relative displacement between two points. By using three pins attached to the substrate, it aligns itself to the rotation and gives a better measure of strain. However, some error is also introduced due to slippage of the mounting pins and stretching of the adherent between the holes. Measures can be taken to reduce these discrepancies[39]. Unfortunately, the use of a KGR-1 extensometer requires much thicker substrates in order to drill holes. It was not possible for the specimens used.

DIC is a robust method for measuring strains in the material. One or more camera's take pictures at a set interval, comparison of these images enables the calculation of strain. The resolution of the camera (2048 by 2048 pixels) determines what the minimum measurable size change is. The speckle pattern can be seen as 'resolution of the material'. The combination yields the accuracies of the strain measurement.

2D DIC measurements are used in conjunction with an extensometer (albeit less accurate). First a white base coat was applied, then black dots using the airbrush at 2.5bar. It was deliberately not done vice verse, the white base coat allows for shorter shutter times of the camera and less noise.

10.5 Results

An overview of the results can be seen in table 10.4 and plotted in figure 10.4 (results of the removability test are omitted but discussed in section 10.6). A complete list of results is presented in appendix K.9.

Connection	Mean ultimate shear strength $[MPa]$	Standard deviation $[MPa]$
Benchmark	3.33	0.80
Re-use	3.90	0.27
Without mesh	6.30	0.89

Table 10.4: Strength values of single lap joints using CFRP adherents and 3M 3789 adhesive, tested at RT

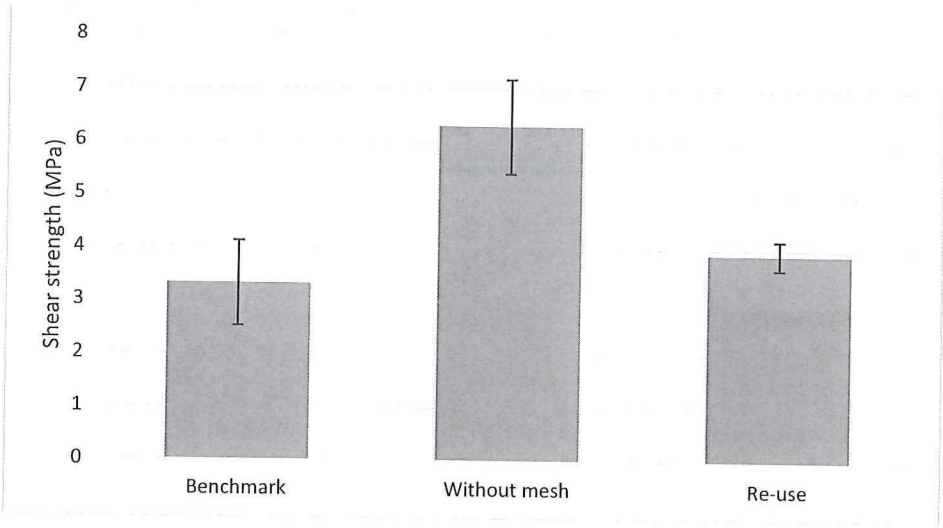

Figure 10.4: Mean shear strength data and deviation of single lap joints tested at RT

10.6 Discussion and quality assessment

10.6.1 Benchmark test

The original samples showed an average shear strength of $3.33MPa$. For the V-Cart application this satisfies the required $2.0MPa$ level. Theoretically, the manufacturing process could be performed cheaper and faster by using fewer adhesion areas. However, if a connection is designed using an average strength value and material coincidentally exhibits below average shear strength, the joint will likely fail sooner than expected. To prevent this, structures are often designed using the 99% or 90% strength value. This is the value 99% or 90% of the material should be able to withstand. Average shear strength is thus irrelevant if this goes together with a large scatter.

The benchmark samples show a relatively large scatter with the lowest strength level being $2.30MPa$. This is still higher than the V-Cart requirement. The tests from the previous chapter showed none of the selected adhesives had the appropriate temperature resistance required for the car chassis. If a suitable adhesive is found, it is therefore recommended to perform several shear strength tests to safely determine 99% or 90% values at several temperatures (for example at -15°C, RT and 60°C).

10.6.2 Removability test

The specimens tested at 180°C proved to be very weak in shear strength. Unfortunately, it is not possible to express this quantitatively.

Of the six samples, one fell apart in the temperature chamber and was not useable. Two were tested in the 250kN bench, due to unavailability of the 10kN bench. The failure load was much lower than expected. This makes the result unuseable; with forces below $20N$, the margin of error is too big. The final three specimens were tested in the 10kN test bench, reaching a maximum force of $1.1N$ or lower. The lowest calibration point of this bench is 1000N. Similar to the 250kN bench, measuring around $1N$ is unfounded.

If quantitative results are needed, the test should be repeated with a load cell suitable for smaller loads. However for the aim of the test this is not required; practically all strength is lost at 180°C.

10.6.3 Re-usability test

The specimens that had been disassembled and re-adhered exhibited no degradation in strength. In fact, average values were higher at $3.90MPa$, with less deviation. The groups are not statistically different however; the re-use group lies within the scatter of the benchmark group.

It shows the bond can be re-assembled without any structural consequences (when performed within an hour). How many times this process can be repeated without differences in strength is something for further research. It is hypothesized this number could be increased further when additional pretreatments are introduced between the assembly cycles. Longer time between disassembly and re-assembly is expected to influence the strength negatively, as it allows for more contaminants on the interface.

10.6.4 Dimensional scatter in adhesive thickness

There is always a slight variation between test specimens dimensions. The scatter within the bondline thicknesses of the samples was deemed too big to be ignored. The variation makes comparison difficult; samples with thinner bondlines fail at higher load levels[39].

Variation between resistance welded samples All test specimens were measured before testing using a digital caliper. Because the bondline thickness itself cannot be measured, the thickness of both adherents was subtracted from the combined thickness at the overlap. Most values were smaller than $0.20mm$ (the thickness of the mesh), this could have two causes:

- Manufacturing process. During assembly, it is possible that the combination of high pressure and high temperature compressed the adherents, causing a small local thickness decrease.
- Indentation of the mesh into the adherents.

This error was confirmed when viewing the samples under a microscope (see section 10.6.6). Bondline thickness of all samples was close to $0.20mm$.

Bondline thickness [mm]	Apparent shear strength [MPa]	Percentage [%]
0.2	20.9	100
0.1	21.4	102

Table 10.5: Increase of apparent shear strength for thinner bondlines using a linear extrapolation

Group	Apparent shear strength [MPa]	Percentage [%]
Benchmark	3.33	0.80
Without mesh	6.30	0.89
Without mesh corrected	6.18	0.87

Table 10.6: Correction of apparent shear strength for samples without mesh

Variation in samples without mesh The microscopy pictures show the samples manufactured without mesh featured notably thinner bondlines, around $0.10mm$. A thinner bondline will influence ultimate strength values positively, making comparing to the resistance welded samples difficult if differences are large enough. Samples of the *Without mesh* group have half the bondline thickness of the *Benchmark* samples, therefore some calculations are performed to make the results independent of bondline thickness.

A dataset from lap shear results is taken from research by Tomblin[39], where bondline thickness is varied for aluminium samples tested to ASTM D3165. According to his research, the trend in strength degradation remains the same for all adherent types. Tomblin used slightly different test specimens, but reported the difference between results of ASTM D 1002 and D 3165 samples to be negligible. A thermoset adhesive was used in his research. By making this comparison it is assumed the strength degradation trend is independent of adhesive type. This might not be completely true, however the difference in bondline thickness is deemed small enough (from $0.20mm$ to $0.10mm$) for the difference to be negligible.

Data points were taken and extrapolated to the thinner bondline regime. A linear extrapolation approximated the data points best, yielding a 2% increase in shear strength for the reduction in bondline thickness (table 10.5). More elaborate calculations can be found in appendix G.

Reducing the strength values obtained from the *without mesh* group with 2% enables the comparison to the other groups. Figure 10.5 shows two columns for the *without mesh* samples; the original column show the experimental results, the corrected column reduces these values by 2%. Results are also shown in table 10.6. Even with the compensation, the samples without mesh fail at much higher loads. This illustrates the negative influence the mesh has on bond strength.

The mesh influences bond strength negatively, but is required for assembly and disassembly. It is speculated using a coarser mesh has a positive effect on bond strength, assuming wire diameter stays equal. Less material is present in the adhesive layer, providing more direct contact. This effect requires experimental verification. Changing the space between the wire also influences the heat up of the polymer, this is discussed in the next chapter 11.

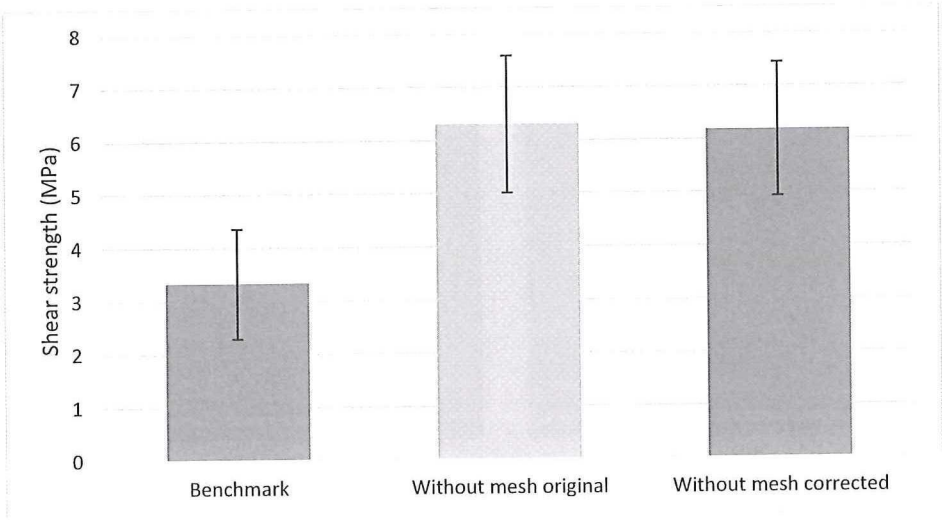

Figure 10.5: Mean shear strength data and standard deviation of of benchmark samples and samples without mesh

10.6.5 Failure analysis

The failure mechanisms of a specimen yields information about the 'weakest link' of a connection. Previously results (section 9.5) showed a large amount of both adhesive failure and resin-mesh debonding. Inspection showed failure of these samples was mostly resin-mesh debonding (figure 10.6).

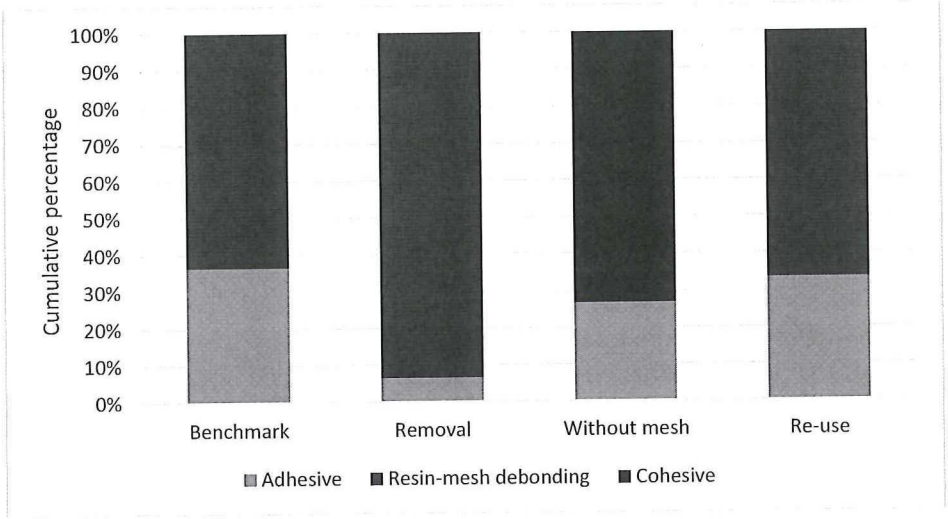

Figure 10.6: Cumulative percentage of failure modes per test group

Adhesive properties of the connection are improved by the UV treatment; adhesive failure is less prominent. It becomes clear that the resin-mesh debonding failure mode is most prominent by looking at the 'without mesh' shear strength results; bond strength is much higher.

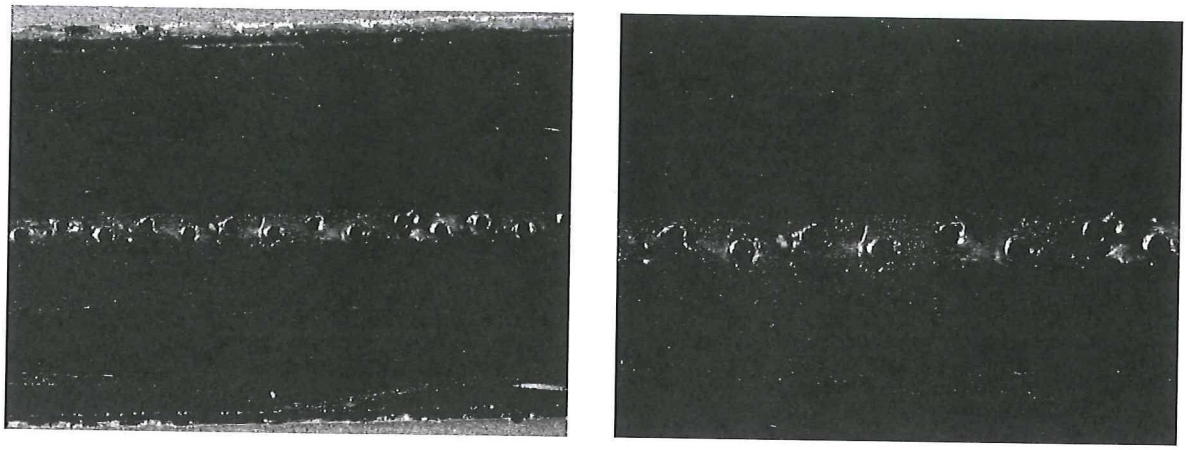

Figure 10.7: CFRP epoxy adherent with 3M 3789 adhesive containing a mesh. Small voids are visible

10.6.6 Microscopy analyses

Several untested specimens were used for visual inspection of the connection using a microscope. After preparing the samples, it was discovered that the ultrasonic ethanol bath (a critical step in sample preparation, appendix H) was a likely cause for dissolving the adhesive. As a result, voids were present in the adhesive.

Polyamide can dissolve in water and ethanol, especially at high temperatures [53]. Ultrasonic cleaning was performed at RT, but cavitation in the bath causes local heat up. When a cavity implodes, the area of low pressure causes a local increase of flow speed (approaching the speed of sound[54]). As a result, temperature is increased locally (temperatures larger than 1000K can be reached[54]) facilitating the dissolution of polyamide in ethanol. This was discovered when samples with a slightly exposed adhesive layer became tangible soft and tacky after the ethanol bath. At first, it was thought the polishing process caused voids, but this was not true; untreated, but cleaned samples exhibited the same voids. All pictures of the original samples can be seen in appendix I.

It is expected that deeper in the connection, less voids are present because the ethanol could not have penetrated that far. Two samples were sanded down to half their thickness (without using ethanol). The results in figure 10.7 show some voids are still present, but much less than the original samples. No hard conclusions can be drawn; either the joint contained voids (despite the precautions taken during assembly), or the images are not representative by the exposure to ethanol. It would require manufacturing the connection again and inspecting it without using ethanol to be certain. However, based on the reduction in voids deeper inside the connection, it can be assumed the connection is relatively void free.

Part IV

Final Design

Chapter 11

Application in sportscar chassis

Thus far, this research showed the potential of the reusable bond using test specimens. Considering the small bonding area of test samples, several changes are required to apply the connection in a sportscar chassis. These are discussed in this chapter.

11.1 Pressure

Assembling the joint requires the substrates to be pressed together. Intimate contact between two surfaces during adhesion is required for several reasons. First of all, it allows air to be pressed out from the connection. Insufficient pressure allows voids to be present, forming a weak boundary layer. At the same time, the filling of the crevices in the substrate provides mechanical interlocking, improving adhesion by the mechanical theory. For thermoplastic welding, high pressures ($> 5bar$) are typically used to aid diffusion. Polymer chain segments move across the interface to form a completely restored and strong bond.

The reusable bond uses a TP adhesive to join TS adherents. The different nature of the materials means diffusion will not occur. Pressure is only required for clamping and removing entrapped air, which is satisfied at much lower pressures than $5bar$.

Methods to apply pressure are discussed for two large panels and the V-Cart geometry.

11.1.1 Large structural joint

Composite panels are most often joined by giving them a short overlap, forming a single lap joint. Other configurations are a double lap joint or tapered lap joint. All require pressure perpendicular to the adhesive interface. For sandwich panels the same applies; often tapering is applied to prevent a large thickness step in the connection. Several methods are discussed to apply pressure to a large structure (the letters refer to the letters in figure 11.1).

a) G-clamps. This allows plate material to be clamped together. However, there is little control over clamping force, and these forces are concentrated around the clamping device. It is self-evident that for large panels, the clamps can only be attached at the edges of the overlap.
b) Clamping beam. Similar to option a, but by using two (metal) beams along the overlap pressure is more evenly distributed. When using the screws to tighten the system, the pressure applied to the connection can be controlled using a torque wrench. However, for long overlaps, bending of the beams will cause pressure to be largest at the edges.
c) Air/hydraulic pressure. Instead of screws, cylinders driven by air or hydraulic pressure can be used to exert pressure. This allows for better control over the applied pressure. It also allows cylinders to be placed in the middle of the overlap for a more even pressure distribution. However, an external frame in which the cylinders are mounted is required.
d) Robotic arm. Techniques have been developed for continuous resistance welding. By allowing the pressure system and heat source to travel along the bond, long welds are possible. Pressure is applied with a system similar to a rolling pin. It requires both connections of the heating element to be accessible from one side, and is thus more suitable for adhesion of stiffeners to a panel. It is a large investment, but can become profitable when very long connections are required, or for large series sizes.

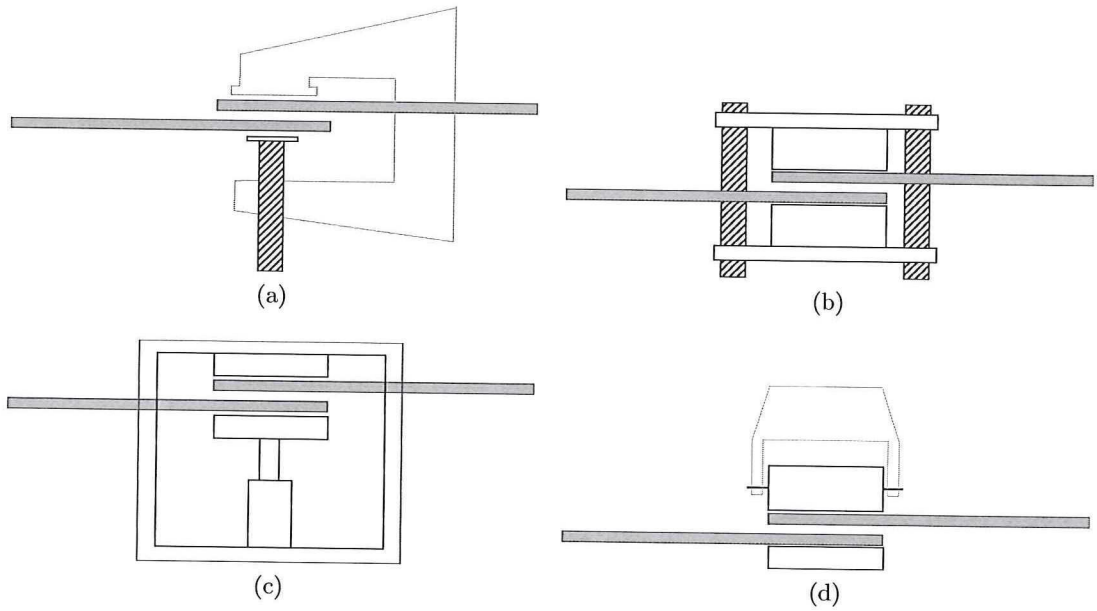

Figure 11.1: Clamping methods for flat composite sheets

11.1.2 V-Cart chassis

Clamping

Geometry of the front bulkhead joint in the V-Cart chassis is unconventional. For clarity, it is shown again in figure 11.2. Some changes to tooling of figure 11.1 geometry are required w.r.t. those discussed in the previous section. For a small series production as the Donkervoort car,

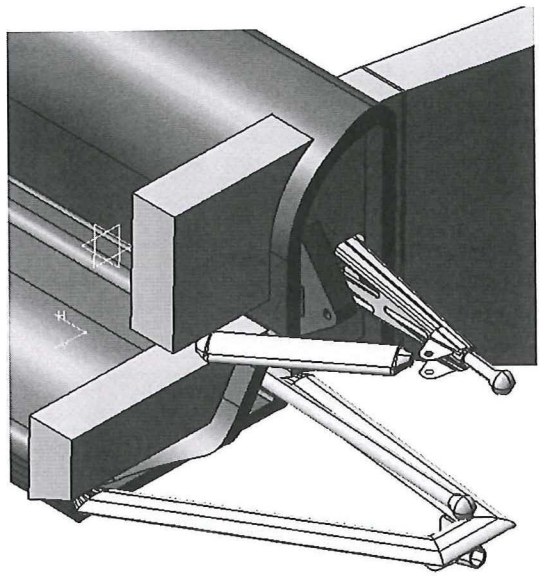

Figure 11.2: Detailed view of the front bulkhead joint geometry

a simple solution is probably the most cost effective: options (a) & (b). Tooling needs to form around the structure to be able to apply pressure, requiring custom made clamps for the curved and angled surfaces. An example can be seen in figure 11.3 for option (b), but it could be applied for option (a) & (c) as well. Note that the figure only shows clamping in y-direction, for pressure in the other directions a similar design can be used. Maximum surface pressure experienced by the bulkhead during driving is $8.0MPa$ (section 4.4.3), making it unlikely clamping would result in compressive damage to the structure.

Adhesion surfaces

As discussed in section 4.2, the adhesion of the complete bonding area becomes problematic due to the flat adhesion surfaces. Assuming a thermoplastic film of $0.20mm$ is applied, it seems most realistic to make the length and width dimensions of the hole in the bulkhead $0.40mm$ larger than the protrusion from the chassis beam. The adhesive films (containing mesh) can be placed in the open spaces and heated one by one to form the connection.

There will always be a small scatter in the dimensions. This results in residual stresses in the adhesive layer when areas from opposite sides of the chassis beam are both adhered to the bulkhead. The height of these stresses is a result of the scatter in dimensions. A large scatter could mean a gap in the adhesive layer. Therefore, this joining method is suitable when only two of the four surfaces of the chassis beam are adhered, but if the total bonding area is required this method is sub-optimal. A geometric-based solution is proposed in the next section, an adhesive-based solution is covered in 11.5.

Tapered surface

Considering the complexity of the tooling required to press the adherents together, other solutions might become more feasible. For example, by creating a slight local taper in both

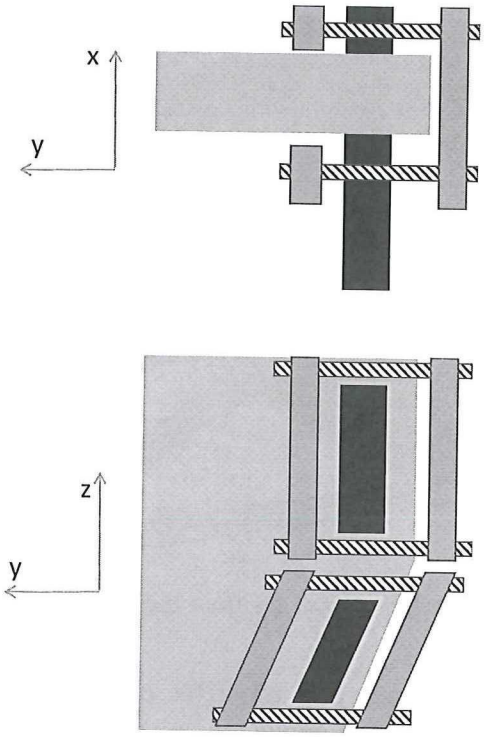

Figure 11.3: Schematic representation showing a top view (top) and front view (bottom) of a clamping structure for the V-Cart joint in y-direction

adherents, pressure is automatically applied by sliding the adherents together (figure 11.4). An ordinary clamping device is still required to press the adherents together, but the tapering allows pressure to be applied to multiple adhesion surfaces, something that was not possible with the original flat geometry. This also reduces the tolerance problem when the complete area is required for adhesion. A slight change in the geometry of the components is required, but given the advantage it would be a worthwhile change, especially when a large adhesive area is needed.

11.2 Mesh

Together with the adhesive, the mesh dictates most of the bond properties. This comes back in sizing of the joint, but also the manufacturing process.

11.2.1 Bondline thickness

The mesh dictates bondline thickness. With enough pressure present, the bondline thickness will eventually be twice the wire diameter (due to the crossing of the wires). Wire diameter therefore becomes the first selection criteria for a mesh.

Bondline thickness has a strong influence on shear strength[39](see appendix G). For structural applications high strength values are desired, and thin bondlines are preferred. Thicknesses

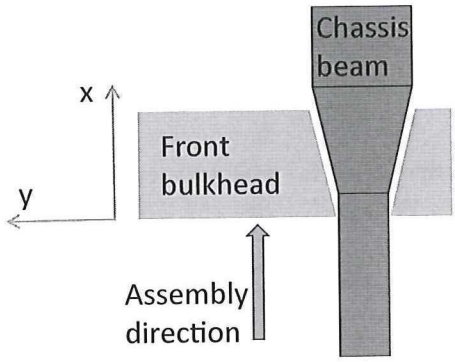

Figure 11.4: Schematic representation showing a top view of the front bulkhead and chassis beam with a tapered design. Note the taper is exaggerated for illustration purposes. The arrow shows the assembly direction of the front bulkhead w.r.t. the chassis beam

of $0.20mm$ are common and will be used for the reuseable connection. These thus require a d_{wire} of $0.10mm$.

11.2.2 Heat transfer

The mesh selected influences the power input to the adhesive. Heat generated by the mesh is given by combining Ohm's and Joule's law (equation (11.1)), where R is the resistance of the mesh. Several factors influence the electrical resistance (equation (11.2)), where R is the electrical resistance (in Ω), ρ the electrical resistivity, a material constant (in $\Omega \cdot m$), l is the length of the material (in m), and A is the cross-sectional area (in m^2).

$$P = I^2 \cdot R \tag{11.1}$$

$$R = \rho \frac{l}{A} \tag{11.2}$$

A lower input current is beneficial, as it requires a less demanding power source and is safer for workers. For the same power input, this can only be achieved by a higher electrical resistance. Assuming d_{wire} is constant, this is reached by a larger distance between the wires (Δ_{wire}), another mesh material, or longer wires. This last variable cannot always be changed.

Changing the wire spacing has more consequences. Due to the low heat conductivity of the polymer material it takes time for heat to dissipate through the material. As a result, for large values of Δ_{wire} large temperature gradients exist in the adhesive. Wire Weaving Co. LTD. (the company providing the wire mesh for this research) only offers a slight variation in wire spacing (from 218 to 263µm for $d_{wire} = 100\mu m$), but custom sizing is possible.

11.2.3 Large structural joint

As an example the influence of the mesh is elaborated for a large rectangular joint. A slight overlap of two panels results in a rectangular shaped interface. This thus requires a very wide

Mesh	Resistance [Ω]	Current [A]	Voltage [V]
Narrow	1.99	32.5	64.6
Wide	0.000447	2168	0.968

Table 11.1: Resistance and power values for different mesh widths of a 200x3cm welding area, $\Delta_{wire} = 0.234mm$, $d_{wire} = 0.10mm$ and power input density of $35\frac{kW}{m^2}$

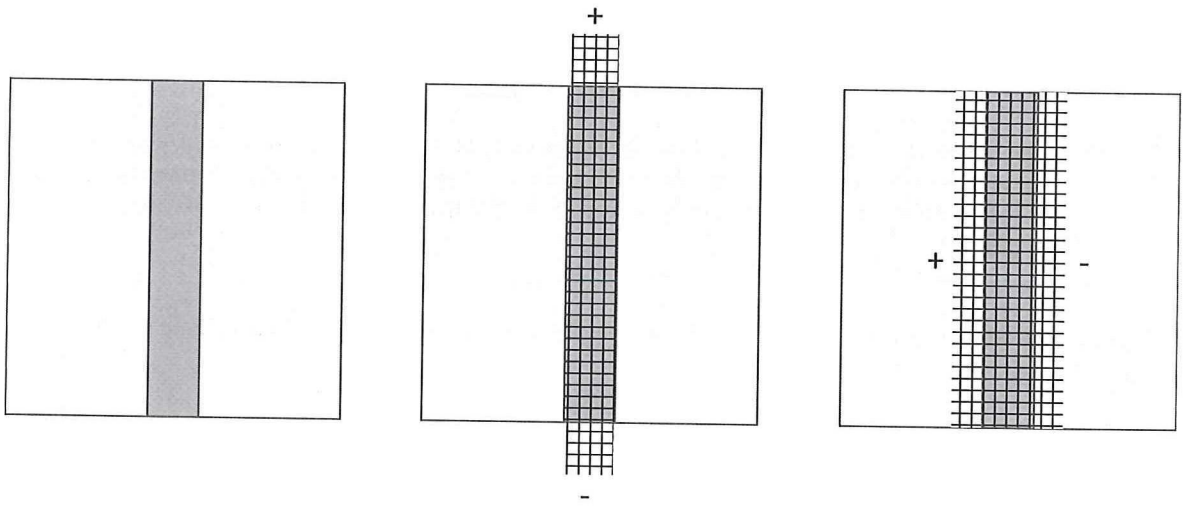

Figure 11.5: Top view of two panels in a single lap configuration with the darker area being adhered (left), with a narrow mesh (middle) and wide mesh (right). The '+' and '-' symbols show the connection with the power source

and short mesh, or a narrow and long mesh. Note that the bonding area is the same in both cases, the difference lies in how the mesh is connected to a power source (figures 11.5). The narrow mesh has the lowest resistance values. Furthermore, connecting the power source over a large area is much more complex. The narrow mesh is thus preferred.

Assume an bonding width of $2m$, with an overlap of $3cm$. Electrical resistance and power input values are given in table 11.1 for parameters identical to those used in section 10 ($\Delta_{wire} = 0.234mm$, $d_{wire} = 0.10mm$ and power input density of $35\frac{kW}{m^2}$). The wide situation is impractical given the power demands, requiring a high input current. However this choice is often restricted by geometry.

11.2.4 V-Cart chassis

The geometry (figure 11.2) of the V-Cart chassis poses some challenges. Assuming each surface is adhered separately, the largest surface is 200 x 30 mm, resulting in welding parameters in table 11.2. The lack of space at the thin edges makes welding with a narrow mesh impossible (figure 11.5). It would require leaving some mesh material exposed, introducing other problems (section 7.2.2). The wide mesh becomes the only solution, requiring more work and a different power source.

COMSOL simulations were performed to predict the heat up in the adhesive layer (more details can be found in appendix J). Such calculations can be performed analytically as well,

Mesh	Resistance [Ω]	Current [A]	Voltage [V]
Narrow	0.20	32.5	6.5
Wide	0.0045	217	0.97

Table 11.2: Resistance and power values for different mesh widths for V-cart joint, $\Delta_{wire} = 0.234mm$, $d_{wire} = 0.10mm$ and power input density $35\frac{kW}{m^2}$

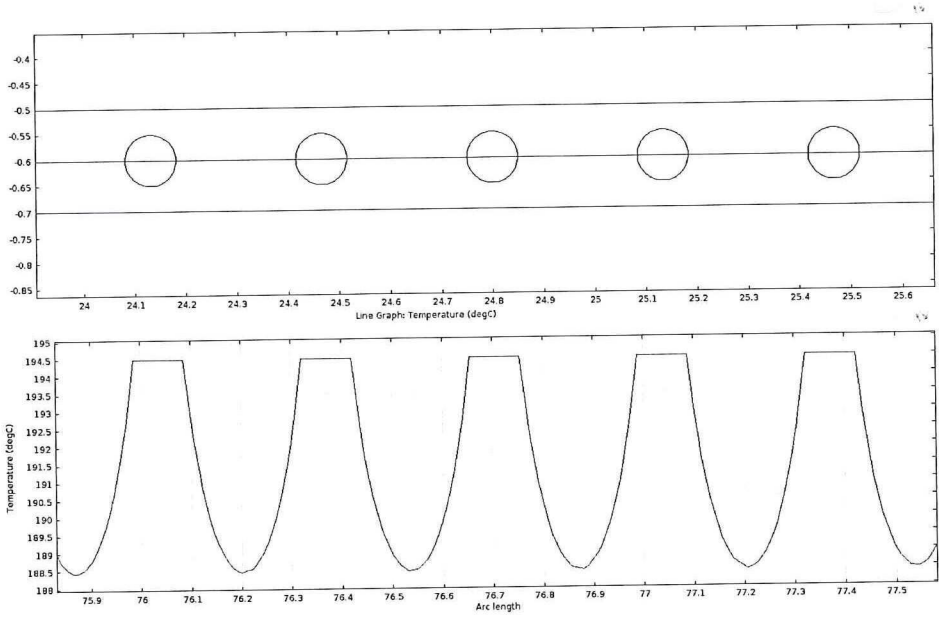

Figure 11.6: Schematic overview of a section of the COMSOL model geometry (top) showing the adhesive layer and steel mesh wires, and the temperature distribution along the red line (bottom).

but it is difficult to incorporate the heat dissipation through the adherents. The welding geometry is made, including the mesh, enabling us to see the temperature distribution inside the adhesive. Figure 11.6 shows a close up of the model on top, with the corresponding temperatures along the red line at the bottom.

A simulation is performed for the 200x30 mm bonding are of the V-Cart chassis. Using identical welding parameter as for the manufacturing of test samples ($P = 35\frac{kW}{m^3}, d_{wire} = 0.10mm, \Delta_{wire} = 0.234mm$), desired temperatures are reached after 25 seconds. This is slightly quicker than for the test specimens; there is relatively less surface area available for heat dissipation. The temperature profile along the adhesive bondline (figure 11.7) shows three downward peaks as a result of COMSOL refusing to recognize three out of 599 wires as heating elements. For the aim of this simulation, this has little influence.

The stable section in the middle of the figure reaches 195°C, but shows many oscillations. This is illustrated more clearly in figure 11.6. It is a result of the low thermal conductivity of the adhesive; the mesh heats up, but it takes time for the energy to dissipate through the adhesive. The oscillations show a maximum temperature difference of 6°C between mesh and adhesive. Temperature of the mesh is $200K$, while the adhesive is $194K$ at the lowest point. This is not a problem, but the temperature difference will likely become larger for a coarser

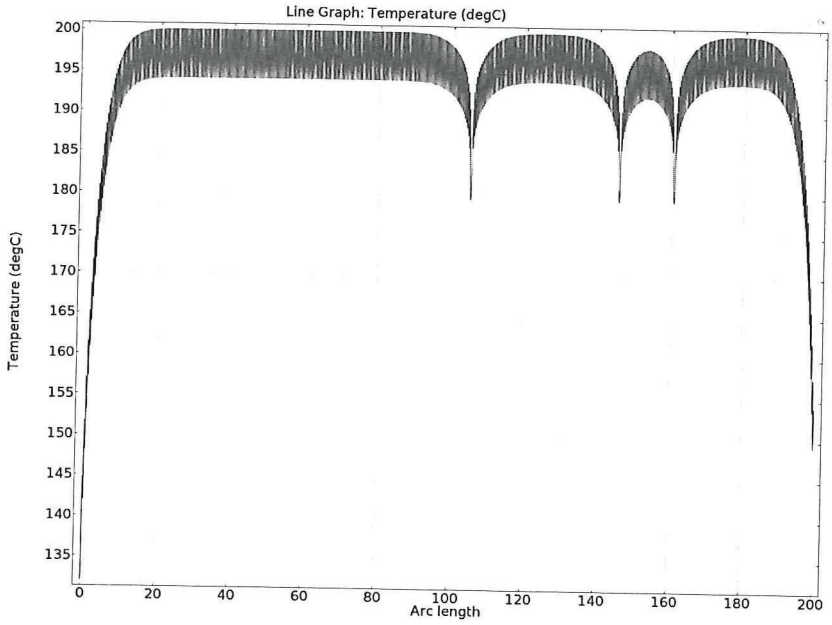

Figure 11.7: Temperature along a $200cm$ adhesive bondline after 25 seconds. Position along the width of the overlap is represented on the x-axis. Welding parameters: $P = 35\frac{kW}{m^3}, d_{wire} = 0.10mm, \Delta_{wire} = 0.234mm$

mesh.

Variations in welding parameters Lower input currents are beneficial. This can be achieved by increasing the space between mesh wires. Due to the low electrical conductivity of the adhesive, the temperature difference between mesh and adhesive increases. For successful adhesion, the minimum temperature in the adhesive should exceed the application temperature (170°C), while the maximum temperature should stay below the degradation temperature (380°C for 3M 3789, this depends strongly on the adhesive, as seen in chapter 6). Preferably, the maximum temperature stays below 300°C to prevent damage to the adherent.

Simulations are performed varying distance between mesh wires from $0.234mm$ to $10mm$. Corresponding temperatures are shown in table 11.3. The spacing of $2.0mm$ is the largest value satisfying the temperature demands when using 3M 3789. Note that the acceptable spacing value is thus strongly dependent on the materials selected. Power input density is identical regardless of spacing, average adhesive temperature should thus be similar as well. The heat up cycle takes 30 seconds, therefore peak temperature are only endured for a couple of seconds.

Temperature differences in the adhesive layer can (partially) be reduced using a lower power input density and longer welding times. For the same parameters as those used in table 11.3, power input density is reduced from $35\frac{kW}{m^3}$ to $20\frac{kW}{m^3}$ for the $2.0mm$ mesh spacing. Given the same minimum temperature, the temperature difference is reduced from 85°C to 49°C. Inherently to using a lower power input density, the time to reach this temperature increased from 25 to 47 seconds.

Mesh spacing $[mm]$	Mesh temperature $[°C]$	Lowest adhesive temperature $[°C]$	Temperature difference $[°C]$
0.234	200	194	6
0.5	211	194	17
1.0	230	191	39
2.0	269	184	85
5.0	409	165	244
10.0	667	134	533

Table 11.3: Temperature differences in adhesive for mesh spacing values, after 25 seconds of heating at $35\frac{kW}{m^3}$ with $d_{wire} = 0.10mm$

Thermal conductivity of the substrate is similar to that of the adhesive. As a result, the longer the welding time, the closer the temperature of the adherent will be to the adhesive temperature. This makes using a low power input density only feasible for strong thermally insulating substrates, or materials that are unaffected by welding temperatures.

11.2.5 Induction welding

The temperature distribution in the adhesive depends on the mesh dimensions, changing from resistance to induction welding will not influence this. For induction welding using magnetic hysteresis, heat up is determined by the mass fraction of particles in the adhesive. Similar to the mesh, a higher particle content is expected to result in smaller temperature fluctuation in the adhesive layer. At the same time, strength values are expected to be lower.

11.3 Environmental protection and aesthetics

Aesthetics are very important for a luxury product. Environmental protection is important to ensure safety and performance of the chassis during its life. Both have implications on the manufacturing process. The presence of a mesh sticking out from the overlap gives an unsatisfactory finish and exposes the adhesive to fluids. Several methods are discussed to prevent this. Having an adhesive that satisfies structural demands and is moisture resistant is best. If such an adhesive comes with other disadvantages e.g. high costs or difficult manufacturing, these measures allow for a structural adhesive without the moisture resistant properties.

11.3.1 Original state

Polymer properties are strongly influenced by moisture absorption (section 4.4.2). Under standard conditions, it takes years for moisture saturation to reach a $5mm$ depth[51]. This could be accounted for by modeling the outer edge of the overlap as a crack. However high temperatures and direct exposure to moisture speed up this process. To ensure structural safety frequent replacement of the bond or counter measures are required.

11.3.2 Sealant

Using a sealant is a common way to waterproof a joint, making it impenetrable to most fluids and environmental influences. A sealant is a polymer designed for fast curing and bonding to a wide variety of materials. Flexibility is important, allowing it to keep the seal under high strains.

Sealants give very good protection to the outside environment at low cost. However, disassembly is complicated if a mesh is used; the sealant needs to be removed to reach the mesh and connect a power supply. Furthermore, the mesh becomes covered in sealant, making it impossible to connect a power supply. Measures could be taken to protect the mesh from the sealant, for example using a plastic cover, but this seems cumbersome.

Alternatively, the excess mesh can be cut, after which sealant is applied. This complicates re-use of the joint; reheating becomes impossible. Assuming disassembly of the joint only occurs when one adherent requires replacement, holes can be drilled through the defective adherent to reach the mesh and apply an electric current. This method is only feasible if experience from repairs show re-use is seldom needed.

For the joining concepts that do not have a mesh sticking out, these problems are avoided. The sealant cannot interfere with the connection. Therefore, using a sealant is probably the best option, as long as it can easily be remove without damage to the adherent. Otherwise, it is also advised to use one of the solutions from the next section.

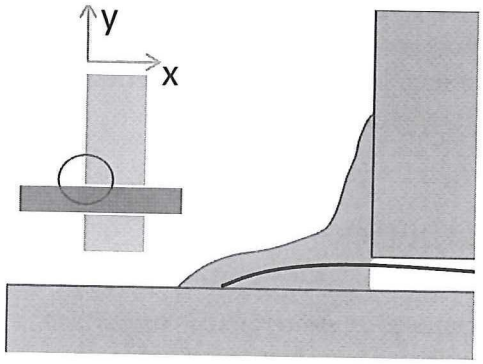

Figure 11.8: Sealant

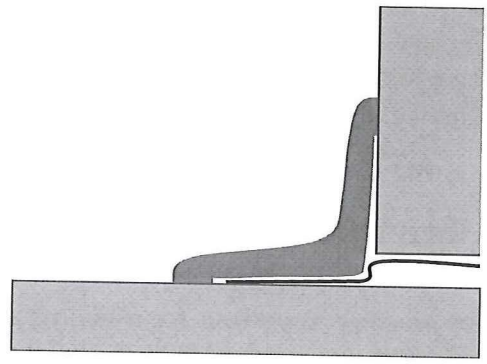

Figure 11.9: Adhered strips

Figure 11.10: The schematic representation in the top of 11.8 shows a top view of the bulkhead geometry, the circle shows the close-up area of figures 11.8, to 11.12

11.3.3 Rubber strips

Another method is covering the bond using rubber material. This is commonly seen in household appliances, where holes are covered with small rubber cylinders. The connection can be made form-closed, press-fitted or adhered. The dovetail joint requires a rubber strip with 90°angle.

Adhesion The strip can be adhered in place. This is most effectively done by using a small thin line of adhesive at the edge of the rubber strip (figure 11.9). As long as the rubber is

flexible enough, little strength is required from the adhesive. It potentially allows the joint to be completely sealed from the outside environment. However, note that this requires a waterproof adhesive. It seems cumbersome to use a second adhesive connection, but it allows the structural adhesive to be selected independent of its moisture resistance.

The environment between the rubber strip and adherent will have the same relative humidity as present at the moment of manufacturing. This can only contain a small amount of moisture due to the small volume, and therefore cannot influence the adhesive strongly.

Form-closed A form-closed connection could be achieved using a rubber strip, manufactured to fit precisely around the chassis beams. By using a small protrusion on the chassis beam, the rubber cannot slide away (figure 11.11). To provide a better seal, the strip is ideally placed under a compressive force by the protrusion. Assembly of this concept is easy, but it requires rubbers strips made to specifications, and extra steps during manufacturing of the chassis beams.

Similar to using adhesive, the volume under the rubber strip contains the same humidity as present at the moment of manufacturing. It is expected some exchange of moisture with the outside environment is possible, depending on how tight the connection is, thus providing less protection that the adhesion solution.

Press-fit A press-fit is achieved having small protrusions underneath the rubber strips, which fit in small holes in the substrates (figure 11.12). These holes introduce stress concentration and have to be taken into account during the design process. Furthermore, it is only possible for non-sandwich panels. Drilling of the holes exposes the core material, enabling moisture ingress.

Effectiveness of the seal is strongly dependent on the dimensional accuracy. If the protrusions are spaced wider than the holes in the substrate, the rubber buckles, allowing moisture to penetrate. Ideally a flexible rubber is used, putting the material under tension.

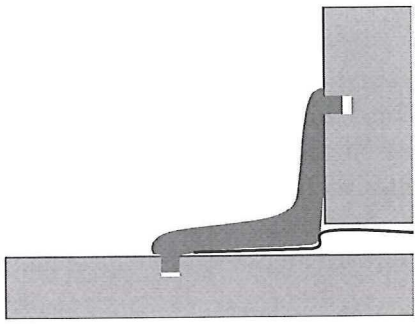

Figure 11.11: Form closed

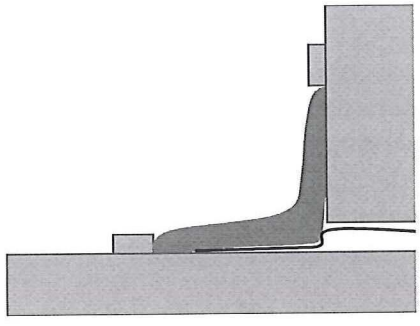

Figure 11.12: Press-fit

11.4 Repair methods

Aside from repairs to the engine or composite parts, the adhesive bond might require maintenance. A small crack could initiate, most likely along the resin-mesh interface. A propagating

crack could result in failure and should be repaired in time.

A repair should only be performed if needed. The aircraft industry applies the 'damage tolerant' design principle; the structure is able to sustain anticipated loads in the presence of fatigue, corrosion or accidental damage until this is detected and repaired. Applying such principle requires damage detection techniques available for the bond, which is complicated for the V-Cart connection. Visual-based inspection techniques are not possible, because it does not allow to see inside the overlap. Eddy current detection requires a electrically conductive material, which the polymer adhesive is not. Fokker bond inspection can only be applied to thin specimens, and the mesh inside the adhesive will make damage detection difficult. Ultrasound inspection is possible but not practical for the situation. It requires big and expensive tooling, and is not available with the chassis assembled.

A safe-life design seems better suited; products are designed to survive a specific design life with a reserve. The fatigue life is determined experimentally; after this period, the component is replaced. For the V-Cart chassis, this would mean the structure is disassembled and re-adhered. To keep the owners satisfied, this should not be needed at a time interval shorter than five years.

Repair consists of the steps described in previous chapters; heating the adhesive, disassembling the chassis, applying new adhesive and achieving adhesion by heating. Alternatively, the properties of the reusable bond could allow it to be repaired without taking it apart. With the chassis still assembled, the adhesive layer is heated. This activates the polymer, decreasing the viscosity. This causes cracks surfaces to reconnect, regaining strength upon cool down. Repair process by reheating would reduce both time and cost w.r.t. complete replacement. However, no tests have been done to study the effect of such procedure; future research is required. Also, it can only be effective if no large voids are present; no adhesive material is added and therefore void content cannot decrease.

11.5 Adhesive systems

This research focused on developing a re-usable adhesive bond. Several tests were performed showing favorable properties for numerous applications. Unfortunately, the adhesives selected did not have the thermal stability for its intended purpose in the V-Cart chassis. This does not mean the joining method is not suitable; other adhesives can be selected that do fit the requirements. This section explores some alternatives. As mentioned before, a thermoset adhesive is not considered because Donkervoort did not approve of a physical removal method.

11.5.1 Thermoplastic adhesives

A thermoplastic adhesive with larger thermal stability than 3M 3789, all other properties equal, is expected to fulfill the demands. Selecting an adhesive based on manufacturer specifications of datasheets has shown to be an unreliable technique; for all thermoplastic adhesives used 60°C was within operating range. Note that all polymers will lose strength at higher temperatures; testing at RT will always yield better results compared to 60°C. The challenge is finding a thermoplastic adhesive which still has a $2.0MPa$ shear strength at 60°C.

Browsing the datasheets of several manufacturers yields some alternatives. Henkel has a large range of thermoplastic adhesives under the name *Technomelt*. Technomelt PA 341 shows a relatively high softening point of 168°C, much higher than Technomelt Q 9268 H. As long as the adhesive becomes weak at 180°C, removal should not be a problem. Unfortunately, Henkel does not report shear strength data of its thermoplastic adhesives.

3M produces many thermoplastic adhesives under the Scotch-Weld Low-Melt and Hot-melt name. Given the low melting temperature range of the Low-Melt series (120-130°C) it is considered unsuitable. The two 3M adhesives used in this research features the second- & third-highest melting temperature of the 3M range. 3M 3779 with a reported thermal resistance of 150°C should show better shear strength than 3M 3789 at the same temperature. Strength level at 60°C is unclear.

11.5.2 Foaming adhesive

A select group of adhesives expands during the curing cycle, making it ideal for gap filling applications in the V-Cart chassis. It would allow the complete area to be bonded without tapering of the geometry or clamping measures.

Hexcel produces a number of foaming adhesives under the Redux name. These are delivered as roll of film, making it ideal for the current V-Cart geometry. Integrating a heating element becomes problematic, and is only possible by stacking a film and mesh together (as performed in chapter 9.2 with the corresponding risk of voids) or it should be performed by the adhesive manufacturer. Redux 212 still offers a $5.0MPa$ strength at 100°C, which would allow only part of the total bulkhead area to be adhered to the chassis beams to satisfy the strength requirement. It is assumed strength will degrade further for higher temperatures enabling removal. Note that removal is only possible if a heating element can be successfully integrated in the adhesive layer.

11.5.3 Reactive adhesive

Polyurethane-based polymers exist as reactive adhesive. The manufacturing process is typically performed as a conventional thermoplastic, using a glue gun. Heating triggers a chemical reaction which cross-links the polymer chains. As a result, bond strength and environmental resistance of the adhesive are enhanced. The reactive PUR adhesives produced by 3M should keep their strength at temperature up to 80°C, while offering better mechanical properties.

Manufacturing becomes more problematic. Inherent to the nature of the reaction, the process is not reversible. Manufacturing into a film should be done by the manufacturer. Otherwise, application is possible using a glue gun or as a spray. It is therefore uncertain if this can be applied in the V-Cart chassis. Furthermore, integrating a mesh or heating element in the connection becomes problematic, and might only be possible by stacking the mesh with an adhesive film. Spraying the adhesive can also be suitable if the bondline thickness can be controlled.

Chapter 12

Conclusions

The aim of this research was designing a reusable adhesive joining method suitable for the thermoset composite chassis of a small sports car. Load transfer between parts for composites is most effective by adhesives, but often complicates disassembly and maintenance.

A thermoplastic adhesive was used; strength is lost at high temperatures due to the lack of cross-links. Of all assembly concepts, resistance welding was found to be most suitable. It is a fast and simple process, with little investment costs, making it perfect for low production numbers.

A mesh serves as heating element and controls thickness of the bond. By pre-impregnating it with thermoplastic polymer adhesive, the void content is limited. Heating of the mesh decreases the viscosity of the polymer, allowing it to achieve good adhesion with both substrates. Extensive pretreatment including UV treatment of the CFRP was required to achieve acceptable adhesion values.

Strength tests were performed with single lap shear specimens according to ASTM D 5868, with an overlap of $12.5mm$ (a limitation of the resistance welding setup). Single lap testing introduces eccentricities and bending moments in the connection, meaning failure is not result of a single load case. Average ultimate strength value was found at $3.3MPa$, however there was a large scatter between results, from $2.3MPa$ to $4.3MPa$. This still satisfies the strength requirement for the V-Cart chassis. However strength is strongly reduced at 60°C; other adhesives are required for a successful bond in a car chassis. Other suggestions include tapering the V-Cart geometry or using a foaming adhesive.

Disassembling and reassembling the bond once does not result in strength degradation, even without an additional pretreatment. At high temperatures (180°C) the connection loses practically all its strength, easing disassembly. Without a mesh in the connection, the joint exhibits significantly higher strength values ($5.7MPa$ average). Resin-mesh debonding is the most prominent failure mode. Using a coarser mesh with identical wire diameter could solve this problem but introduces others. A combination of large mesh spacing and low thermal conductivity of the polymer results in large temperature difference in the adhesive during manufacturing.

Limitations of the connection are inherent to the chemical nature of polyamide. Low thermal resistivity limits the application of this specific joint to room temperature scenario's. Also, precautions are required to prevent moisture absorption. Other thermoplastic adhesives are to be selected for application in a small sportscar, where temperature resistance is important. Working principles are expected to remain the same. Some enhancements of the connection are discussed in the *Recommendations* (chapter 13).

Chapter 13

Recommendations

This research shows a detailed design for a reusable adhesive bond. It is part of larger project where it is applied to connect large structural composite parts of a sportscar chassis. Similarly, recommendations for future research can be divided in categories.

13.1 Reusable bond manufacturing

Several changes during manufacturing could potentially yield an increase in bond strength, for example using a coarser mesh. These changes should aim on preventing resin-mesh debonding. Induction welding is an interesting process. Despite the large initial investment required, the manufacturing process becomes easier, especially for complex geometries. It is unclear what, all other parameters identical, the influence of the process itself is on the bond strength. The use of induction welding in combination with magnetic hysteresis is expected to show some differences.

Furthermore, the selected adhesives experience glass transition at temperatures below the advised application temperature (170°C). Therefore assembly at lower temperature might be possible (if bond strength is not decresed), reducing energy cost and possible damage to structural parts.

13.2 Reusable bond properties

Several properties of the bond need to be discovered. The single lap test is a combination of load types. Achieving a better understanding of how the joint behaves under load types separately, allows us to make a better assessment of applications for the joint. These include compression, tension, pure shear, peel & cleavage tests. Results depend strongly on joint geometry and are best performed with an application in mind.

It terms of longevity of the joint, several things are open to investigation. First of all, it is unclear how the joint performs under fatigue loading. Thermoplastics are likely to exhibit creep at constant load levels, due to the lack of cross-links, reducing fatigue life further.

For wet applications, static strength and fatigue investigations are required. Using a sealant might be necessary for achieving good results, reducing the moisture degrading effect strongly. However, having a moisture resistant polymer is a more sound solution, reducing process steps at the same time.

Finally, it is unclear how many times the bond can be taken apart and reassembled without a large degradation in strength. If there is demand for a large number of cycles, this requires testing. Note that for applications in the V-Cart chassis, reuse of one to three times is likely enough.

13.3 Application in V-Cart

One promising application for the reusable joint was in a small sportscar with composite chassis. Although results from this research look promising, there are still some uncertainties, especially for longevity, resistance to elevated temperatures and moisture. These are covered by the recommendations mentioned above, and can most likely be solved selecting the right adhesive for the (sportscar) application.

Removal of the bond is, in the case of the V-Cart geometry, only possible by shear loading of the adhesive. A change in the geometry to enable peel loading would require less force for removal of the connection. Also, a completely different design using more conventional automotive elements might be more economical while achieving similar structural properties.

A consumer product needs to avoid failure at all cost. Although Donkervoort Automobielen B.V. can avoid some full scale test due to there small production numbers, additional experiments are required to guarantee safety. For example a full-scale strength test of the chassis. This is especially important as the joining method is new for the industry, and legislation is required for the vehicle to be road legal.

Bibliography

[1] 3M. Scotchweld 9323 b/a dataset, 1996.

[2] 3M. Thermoplastic adhesives catalogue, 2010.

[3] J.R. Abbott and B.G. Higgins. Surface tension of a curing epoxy. *Journal of Polymer Science Part A: Polymer Chemistry*, 26(7):4, 1998.

[4] T. J. Ahmed, D. Stavrov, H. E. N. Bersee, and A. Beukers. Induction welding of thermoplastic compositesan overview. *Composites Part A: Applied Science and Manufacturing*, 37(10):1638–1651, 2006.

[5] G. Altan and M. Topu. Fatigue and static performances of butterfly joints under hygrothermal exposure conditions. *Journal of Applied Polymer Science*, 127(5):3374–3381, 2013.

[6] Michael Ashby and David Jones. *Engineering Materials 2: An Introduction to Microstructures, Pocessing and Design, Third Edition.* Butterworth-Heinemann, 2006.

[7] ASTM. Astm d3528-96 standard test method for strength properties of double lap shear adhesive joints by tension loading. Technical report, American Society for Testing and Materials, 2008.

[8] Michael Austin. Car and driver - 2009 hyundai genesis 4.6 review, 2008. URL `http://www.caranddriver.com/reviews/2009-hyundai-genesis-46-road-test-review`.

[9] Pagani Automobili. Pagani official site, 2012. URL `www.pagani.com`.

[10] McLaren Automotive. Mclaren official site, 2012. URL `www.mclarenautomotive.com`.

[11] Y. Bai and T. Keller. Effects of thermal loading history on structural adhesive modulus across glass transition. *Construction and Building Materials*, 25(4):2162–2168, 2011.

[12] Yu Bai, Thomas Keller, and Till Valle. Modeling of stiffness of frp composites under elevated and high temperatures. *Composites Science and Technology*, 68(1516):3099–3106, 2008.

[13] Willard D. Bascom and Robert L. Cottington. Effect of temperature on the adhesive fracture behavior of an elastomer-epoxy resin. *Journal of Adhesion*, 7(4):333–346, 1976. Cited By (since 1996): 52 Export Date: 19 March 2013 Source: Scopus CODEN: JADNA Correspondence Address: Bascom, Willard D.

[14] Frank Markus Benson Koch, Edward Loh. The hypercar blueprint. *Motor Trend*, 2013.

[15] BMW. Bmw i3, 2013. URL `http://www.bmw.nl/nl/modellen/bmw-i/i3/showroom/duurzaamheid.html`.

[16] Donkervoort Automobielen B.V. Company website, 2013. URL `http://www.donkervoort.com/`.

[17] L. Ye C. Ageorges. *Fusion Bonding of Polymer Composites*. Springer, 2002.

[18] Hexion Specialty Chemicals. Datasheet of bakelite epr 04908, 2006.

[19] J. Coulon and H. Maillard. Plasma treatment of carbon/epoxy composites to manage surface adhesion. Technical report, 2011.

[20] A. J. Curley, H. Hadavinia, A. J. Kinloch, and A. C. Taylor. Predicting the service-life of adhesively-bonded joints. *International Journal of Fracture*, 103(1):41–69, 2000.

[21] Computer Department of Electrical and Colorado University Energy Engineering. Fundamentals of power electronics, 2005.

[22] Driven. Behind the scenes at pagani, 2012.

[23] M. Dub, P. Hubert, A. Yousefpour, and J. Denault. Current leakage prevention in resistance welding of carbon fibre reinforced thermoplastics. *Composites Science and Technology*, 68(6):1579–1587, 2008.

[24] M. Dub, P. Hubert, A. Yousefpour, and J. Denault. Resistance welding of thermoplastic composite skin/stringer specimens. 2009.

[25] World Car Fans. Porsche carrera gt - photos, 2003. URL `http://www.worldcarfans.com/204030112949/porsche-carrera-gt/photos`.

[26] Fein GmbH Elektrische Gereedschappen. Fein superwire, 2013. URL `http://www.fein.nl/nl_nl/autos/voertuigruiten-verwijderen/superwire-0298635/`.

[27] Joris van Gestel. *Thermal management of a composite sandwich engine bay wall: The futurue Donkervoort cars*. PhD thesis, 2012.

[28] B. Griffiths. F1-inspired monocell: Racing safety for the road: Composites world. *High-Performance Composites*, 18(5), 2010.

[29] Arnoud Haffmans. *Design of the front suspension mounting of a Donkervoort car with a CFRP chassis*. PhD thesis, 2012.

[30] A. Hassan, N. A. Rahman, and R. Yahya. Moisture absorption effect on thermal, dynamic mechanical and mechanical properties of injection-molded short glass-fiber/polyamide 6,6 composites. *Fibers and Polymers*, 13(7):899–906, 2012.

[31] Henkel. Technomelt q 9268h datasheet, 2001.

[32] HolidayCheck.com. Weather for abu dhabi, 2013. URL http://www.holidaycheck.com/climate-wetter_Abu+Dhabi-ebene_oid-id_1.html.

[33] HolidayCheck.com. Weather for sodankyla, 2013. URL http://www.holidaycheck.com/climate-wetter_Sodankyla-ebene_oid-id_20573.html.

[34] Meng Hou. Thermoplastic adhesive for thermosetting composites. Technical report, University of Queensland, Brisbane, 2012.

[35] R.M. IJperlaan. A review on possible joining methods suited for the production of the v-cart cfrp chassis. Technical report, TU Delft, 2012-04-19 2012.

[36] M. D. Islam, A. A. Alili, I. Kubo, and M. Ohadi. Measurement of solar-energy (direct beam radiation) in abu dhabi, uae. *Renewable Energy*, 35(2):515–519, 2010.

[37] K. M. B. Jansen. Heat transfer in injection moulding systems with insulation layers and heating elements. *International Journal of Heat and Mass Transfer*, 38(2):309–316, 1995.

[38] K. M. B. Jansen and A. A. M. Flaman. Construction of fast-response heating elements for injection molding applications. *Polymer Engineering and Science*, 34(11):894–897, 1994.

[39] P. Harter J.S. Tomblin, C. Yang. Investigation of thick bondline adhesive joints. Technical report, Wichita State University, 2001.

[40] Christos Kassapoglou. *Design and Analysis of Composite Structures*. 2010.

[41] A. Kochan. Lotus: Aluminium extrusions and adhesives. *Assembly Automation*, 16(4): 19–21, 1996. Cited By (since 1996): 2 Export Date: 13 February 2013 Source: Scopus CODEN: ASAUD Language of Original Document: English.

[42] Steven Label. Substrate surface energy, 2009.

[43] Glass Magic. Windscreen replacement, 2013. URL http://glassmagic.com/services/windshield-replacement.

[44] C. T. Moynihan, A. J. Easteal, J. Wilder, and J. Tucker. Dependence of the glass transition temperature on heating and cooling rate. *Journal of Physical Chemistry*, 78 (26):2673–2677, 1974.

[45] Sands Mechanical Museum. Lotus elise technical information, 2013. URL http://www.sandsmuseum.com/cars/elise/thecar/technology/technology.html.

[46] Natalie Neff. The hyundai genesis boldly goes where no korean car has gone before, 2008. URL http://www.garyromehyundai.com/genesis09boldlygoes.cfm.

[47] A. A. Obaid, J. W. Gillespie Jr, T. L. Pike, G. E. Thomas, Q. Nguyen, and L. E. Hornberger. Bond strength and durability of titanium joints using tp-8 adhesive under different environmental conditions. volume 52 of *SAMPE 2008 - 52nd International SAMPE Symposium - Material and Process Innovations: Changing our World*, 2008.

[48] Edward Petrie. *Handbook of Adhesives and Sealants.* McGraw-Hill Handbooks, 2007.

[49] Tim Pollard. Mclaren mp4-12c: the first official p11 story, 2009.

[50] H. Potente. Ultrasonic welding principles and theory. *Materials and Design*, 5(5): 228–234, 1984.

[51] R. T. D. Prabhakaran, T. L. Andersen, and A. Lystrup. Influence of moisture absorption on properties of fiber reinforced polyamide 6 composites. In *2nd Joint US-Canada Conference on Composites - American Society for Composites, 26th Annual Technical Conference: Canadian Association for Composite Structures and Materials*, 2011.

[52] J. G. Quini and G. Marinucci. Polyurethane structural adhesives applied in automotive composite joints. *Materials Research*, 15(3):434–439, 2012. Export Date: 18 March 2013 Source: Scopus.

[53] G. Reiter and G.R. Strobl. *Progress in Understanding of Polymer Crystallization.* 2007.

[54] P. Riesz, D. Berdahl, and C. L. Christman. Free radical generation by ultrasound in aqueous and nonaqueous solutions. *Environmental Health Perspectives*, VOL. 64:233–252, 1985.

[55] Sabatack. Sabatack 780 data sheet, 2011.

[56] Speedhunters. Pagani zonda factory tour, 2009. URL `http://www.speedhunters.com/2009/06/car_builder_gt_gt_pagani_factory_tour_pt_1/`.

[57] E. P. Weidmann T. Binner, H. Reister and J. Wiedemann. Aspects of underhood thermal analysis. Technical report, Daimler Chrysler AG, 2005.

[58] Jasper Terdu. *Design of an affordable high performance composite chassis.* PhD thesis, 2011.

[59] Georgia State University. Hyperphysics - hysteresis, 2013. URL `http://hyperphysics.phy-astr.gsu.edu/hbase/solids/hyst.html`.

[60] Cars Move Us. Carrera gt chassis, 2011. URL `http://www.carsmoveus.com/2012/01/carrera-gt-chassis/`.

[61] J.R. Vig. Uv/ozone cleaning of surfaces, 1984.

[62] Irene Fernandez Villegas, Lars Moser, Ali Yousefpour, Peter Mitschang, and Harald EN Bersee. Process and performance evaluation of ultrasonic, induction and resistance welding of advanced thermoplastic composites. *Journal of Thermoplastic Composite Materials*, 2012.

[63] Jack R. Vinson. Mechanical fastening of polymer composites. *Polymer Engineering and Science*, 29(19), 1989.

[64] J. Yan, X. Wang, M. Qin, X. Zhao, and S. Yang. Resistance welding of carbon fibre reinforced polyetheretherketone composites using metal mesh and pei film. *China Welding (English Edition)*, 13(1):71–75, 2004.

[65] B. Yang, W. M. Huang, C. Li, and L. Li. Effects of moisture on the thermomechanical properties of a polyurethane shape memory polymer. *Polymer*, 47(4):1348–1356, 2006. Cited By (since 1996):177 Export Date: 20 August 2014.

[66] Thomas Young. An essay on the cohesion of fluids. Technical report, The Royal Society, 1805.

[67] Ya-Jen Yu, Keith Hearon, Thomas S Wilson, and Duncan J Maitland. The effect of moisture absorption on the physical properties of polyurethane shape memory polymer foams. *Smart Materials and Structures*, 20(8):085010, 2011.

Part V

Appendices

Appendix A

Industry Analysis

This chapter deals with the current state of the art in the car industry. Both adhesive bonded joints in general and use of CFRP structures are explored.

A.1 Adhesive bonds in industry

Car Windshield In almost every car an adhesive is used for the connection between the windshield and the car's bodywork. Several materials can be used for the windows of a car, and the adhesive must keep its function under the influence of small deformations of the windshield and bodywork. This requires an elastic adhesive. Furthermore, thermal stability and environmental resistance are important features, and high strength before curing is beneficial. Sabatack produces a windshield adhesive on the basis of MS-polymer (Sabatack 760[55]), but polyurethane variants are also common. Application of an adhesive can be seen in figure A.1. Due to the high temperature resistance, the adhesive is often removed using a sharp knife or thin wire. Fein produces tooling designed specifically for removing a car's windshield[26]. It winches a steel cable through the adhesive layer.

Structural adhesive Several companies have experimented with applying adhesive bonded joints in an aluminium car chassis. The Lotus Elise (a small sportscar) uses aluminium extrusions bonded together to form a chassis[41] (figure A.2). Large flat areas provide space for applying adhesive. Small ridges as the edge make sure the adhesive cannot flow out when the adherents are pressed together. In order to avoid peeling forces and to keep the frame together before curing of the adhesive, rivets are added to the joints.

The Hyundai Genesis (a luxury sedan) uses adhesive in combination with mechanical fasteners for structural joining of chassis parts (similar to the Lotus Elise)[46]. The use of structural adhesive is uncommon for this type of car, but helped it achieve a torsional rigidity higher than the competition. Furthermore, it helped reduce noise and vibrations, which is very important in this segment[8].

Figure A.1: Application of adhesive for replacement windshield[43]

Figure A.2: Lotus Elise spaceframe [45]

A.2 CFRP structures in industry

The last decade has seen a large increase in the use of CFRP components for use in the automotive sector. This is especially so for luxurious sportscars; this reduces weight or increases stiffness, but also adds a form of exclusivity.

Porsche The Porsche Carrera GT is an exclusive supercar produced from 2004 to 2006. During this period, only 1270 cars were manufactured.

The chassis consists of two large hand laminated CFRP monocoque parts, manufactured by the ATR Composites Group in Italy. One tub-shaped part offers room for passengers and connects the front suspension, the other part houses the engine and connects the rear suspension. They are connected using aluminium inserts and bolts (figure A.3), allowing for easy disassembly. Judging from figure A.3, very little maintenance is possible with the frame intact. In order to provide sufficient crash safety, steel beam structures are added both at the front and rear of the car, with an aluminium traverse beam (figure A.4). These are designed for easy replacement, and to avoid damage to the CFRP structure.

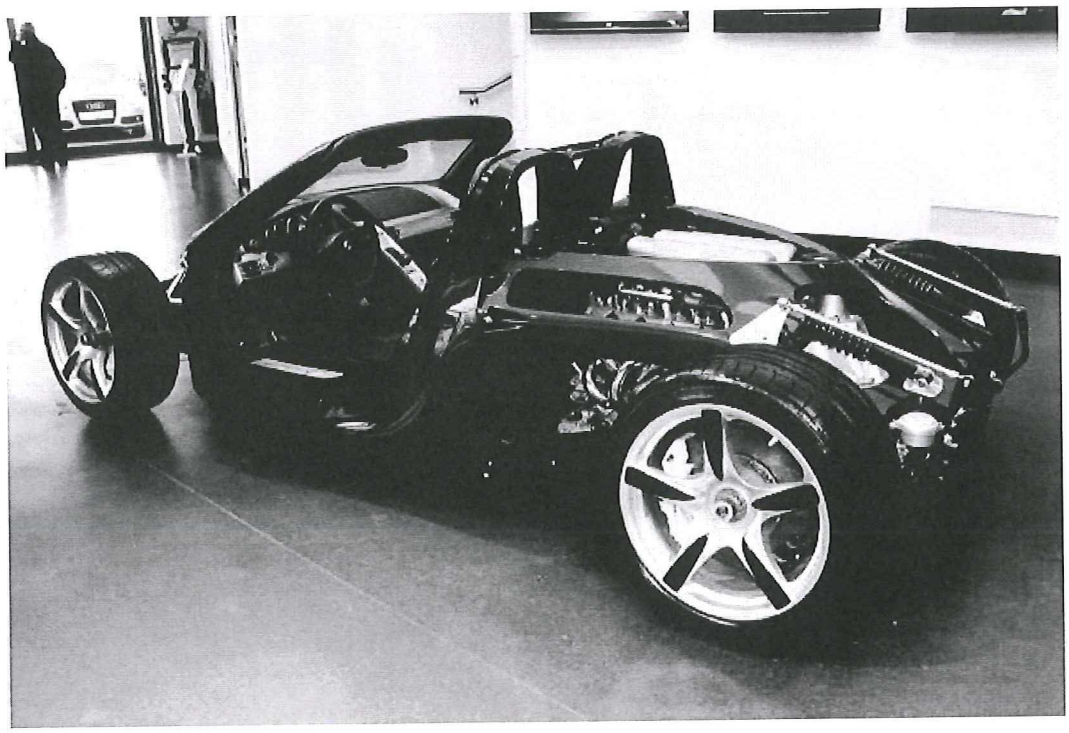

Figure A.3: Porsche Carrera GT chassis[60]

The next generation Porsche sportscar, the Porsche 918, features the same structure for the frame. However, in order to save weight, Porsche uses carbon instead of aluminium inserts for the suspension and powertrain mounting points[14].

McLaren The MP4-12C is McLaren's second production car. Assembled in Surrey, England, production started in 2011 and is still going on at present[10].

The McLaren MP4-12C is one of the cheapest cars having a CFRP load carrying structure. Similar to the Porsche, the McLaren has a CFRP 'tub' where the passengers sit in. McLaren have dubbed it the MonoCell[10], and can be seen in figure A.5. Production is done by RTM, which cuts down production time to four hours[49]. By avoiding hand lamination, costs can be reduced, and the product quality is very consistent[28].

The figure clearly shows the aluminium inserts present in the MonoCell. At the front of the tub, aluminium beam sections are connected to provide a crumple zone. An aluminium truss structure is bolted to the rear of the car. The rear suspension arms and engine are both connected to this truss structure. Loads are thus carried partly by the CFRP and partly by the truss structure.

Soon after the release of the MP4-12C, McLaren announced the McLaren P1. The P1 is a hybrid supercar; a twin-turbo V8 petrol engine and electric motor both power the rear wheels. Production is very limited at 375 units, with a starting price of €1.2 million.

Similar to the MP4-12C, the P1 features a CFRP tub structure. However, McLaren have elaborated the design of the MonoCell; it now includes a roof structure, forming a cage.

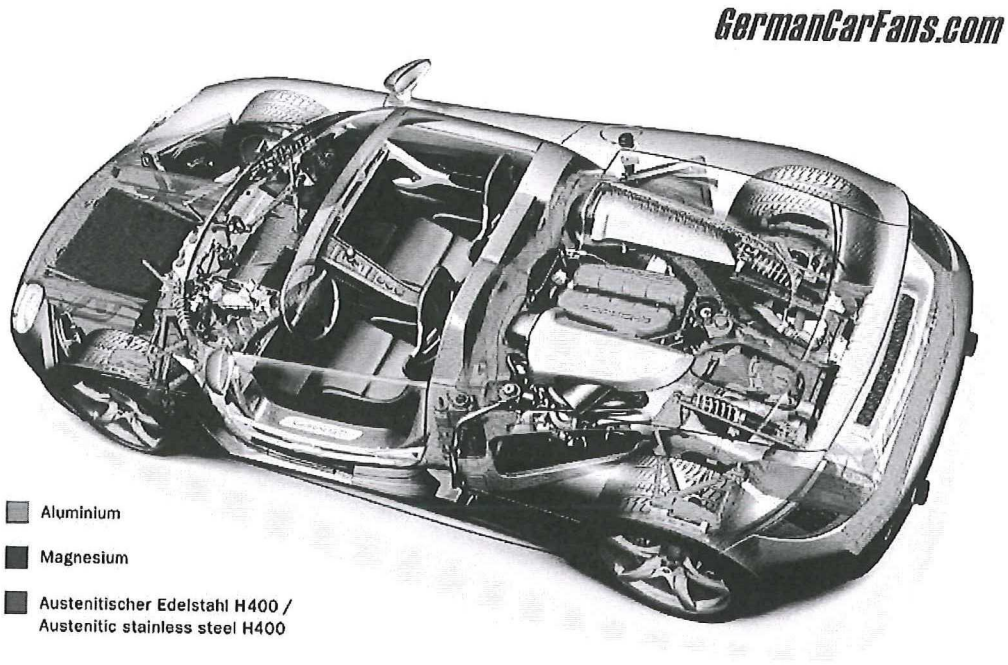

Figure A.4: Porsche Carrera GT materials[25]

Hence, they have called it the MonoCage. The use of composites also allowed part integration; the roof features a snorkel that draws in air for engine cooling[10]. Unlike the MP4-12C, the P1 does not have an aluminium truss structure for connection of the suspension arms and engine. CFRP structures are connected both at the front and rear of the MonoCage using bolts and aluminium inserts, as can be seen in figure A.6. All load carrying components of the car are thus made from CFRP. The outer surface of these parts also forms the bodywork of the car, reducing the amount of parts required.

Pagani Pagani Automobili is an Italian manufacturer of sports cars. It is a small company with 55 employees, focusing on producing exclusive sportscars in small numbers[9].

The Pagani Zonda was the first car produced by Pagani. Production started in 1999 and ended in 2011, but only a little more than 200 cars were built. The structure is similar to the McLaren MP4-12C. It features a CFRP passenger tub that includes a roof structure, made by hand lamination. A aluminium truss structure is bolted to the tub, providing connections for the engine and rear suspension. This can be clearly seen in figure A.7[56].

Pagani specializes in producing exotic CFRP parts. For example, the hood of the car features a clear division in the lay-up precisely in the middle, and the fibres line up perfectly between the left and right halve. This has no structural importance, but adds value to the customer; it is more exclusive and luxurious[22].

Last year (2012), Pagani started production of their next supercar, the Huayra. The general frame structure is still the same; a CFRP tub with aluminium beam section bolted to the rear. The composite parts feature a so-called carbotitanium weave; strands of titanium are

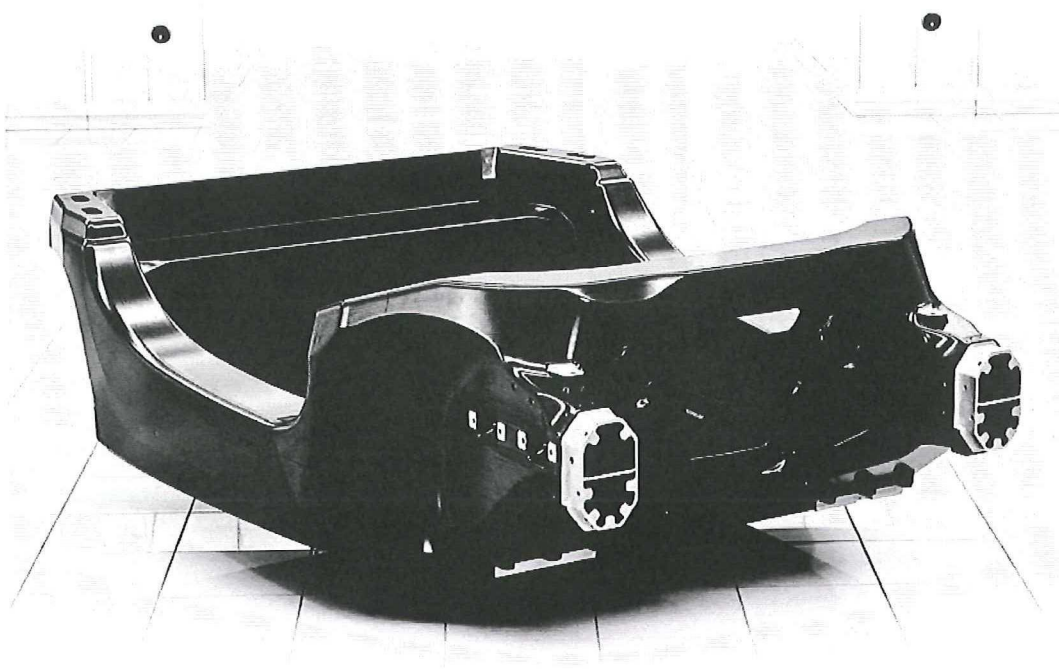

Figure A.5: McLaren MP4-12C MonoCell [10]

woven between the carbon fibres. However, it is unclear what advantage this brings to the structure.

BMW Saving weight is becoming increasingly important in the entire car sector to reduce energy consumption. This is especially true for electric cars, which have to carry a large amount of weight in batteries. BMW recently started production of their i3 full electric car, which uses CFRP structures to reduce weight.

Similar to the sportscars, the BMW i3 uses a carbon fibre tub structure to house the passengers. This includes a roof and trunk section. However, this is mounted on top of an aluminium beam frame, which houses the wheels, engine and batteries (see figure A.8)[15]. Using CFRP as material for the battery housing probably would have resulted in heat dissipating problems; batteries become warm during use and plastics have low thermal conductivity. How the connection between the aluminium and carbon structure is made is unclear.

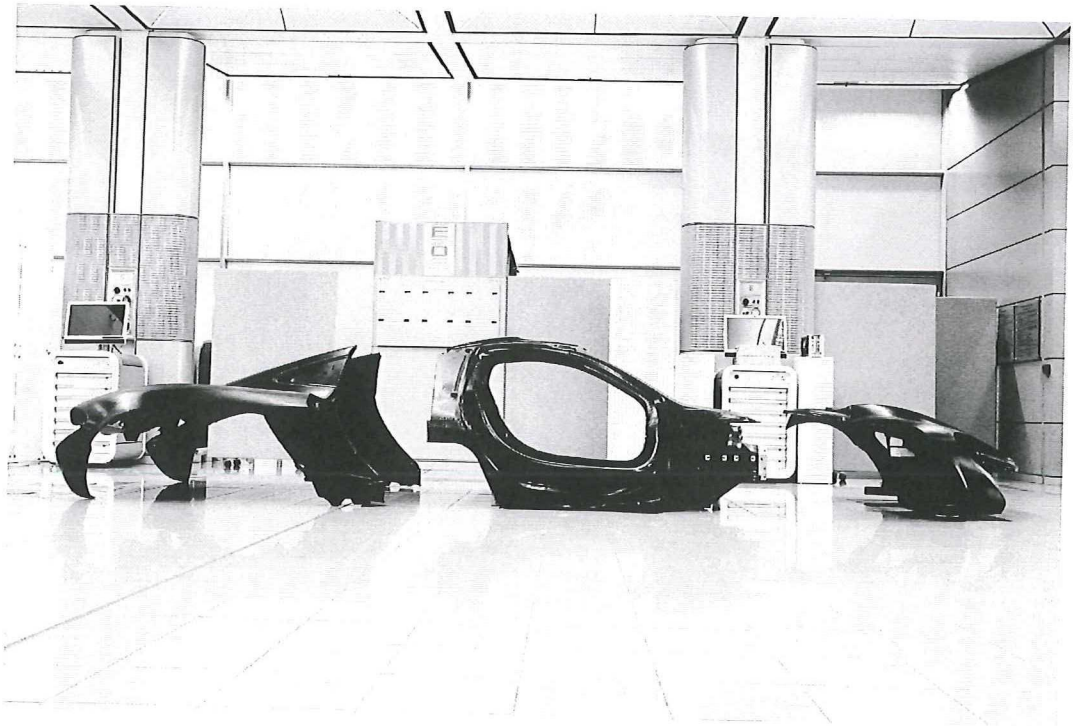

Figure A.6: McLaren P1 MonoCage and chassis[10]

Figure A.7: CFRP monocoque tub and aluminium truss structure of the Pagani Zonda[56]

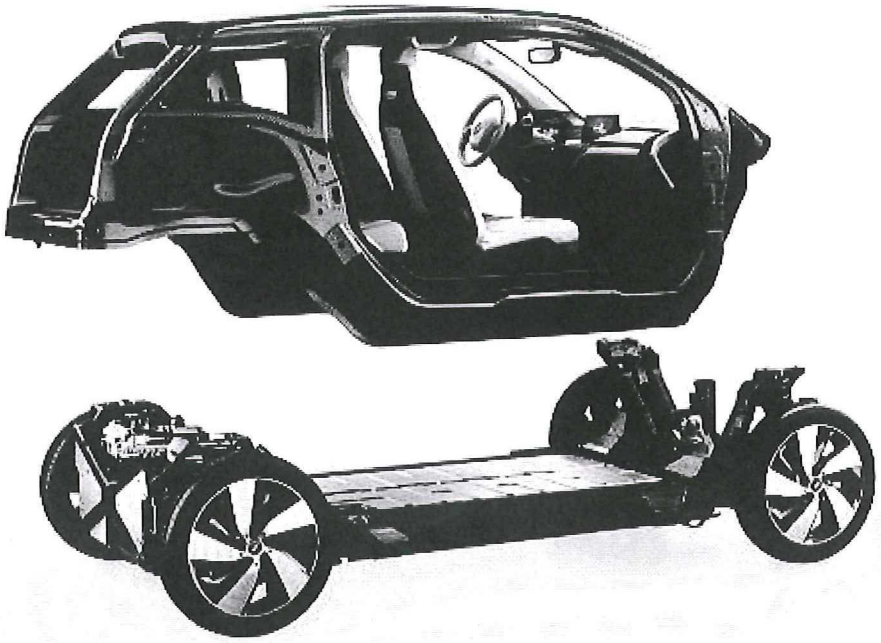

Figure A.8: CFRP and aluminium chassis structure of BMW i3[15]

Appendix B

Material data sheets

Throughout the report, many references are made to various adhesives and materials. To make looking up of the specifications easier, the datasheets are including in this appendix. The thermoplastic adhesives were selected after contacting their respective manufacturer.

B.1 3M

3M has a large collection of thermoplastic adhesives, based on various polymers. The catalog in figure B.1, which unfortunately was only available in Dutch, shows the range of thermoplastic adhesives.

B.2 Henkel

After having contacted Henkel, they proposed Technomelt Q 9268H[31] as an adhesive that would best suit the V-Cart demands (figure B.2).

B.3 Sabatack

Figure B.3 show the datasheet of Sabatack 780. It is an elastomer currently used by Donkervoort for connecting most CFRP panels to the steel beam frame. This datasheet was also only available in Dutch.

B.4 Hexion

Hexion is a large chemical company, production epoxy adhesive amongst others. The Bakelite EPR 04908[18] is a typical epoxy adhesive used at the TU Delft Aerospace faculty. Due to its excellent availability, it will be used for building several test samples.

Scotch-Weld™ Smeltlijmen

Product	Basis	Kleur	Temperatuurvastheid °C	Viscositeit bij 190 °C mPa s	Trekvastheid bij 22 °C MPa	Afschuifsterkte op douglasspar bij 22 °C MPa	Slagvastheid N m -18°C	Slagvastheid N m +22°C	Afpelkracht bij 22 °C N/cm	Geschikte lijmpistolen	SW EC-temperatuurmodule
3731	Polyolefine	beige	130	12.000	–	3,3	–	9,0	31	EC / PGII / TC Q	4 of 5
3738	EVA	lichtbruin	55	2.875	2,5	2,6	0,5	4,4	23	EC / PGII / TC / TC Q	4
Z 3748	Polyolefine	wit	80	5.000	–	2,2	2,3	8,3	31	EC / PGII / TC / TC Q	4
3762	EVA	beige	55	1.870	3,1	3,8	0,5	1,4	12	EC / PGII / TC / TC Q	3
3762 LM	EVA	beige	55	4.000**	–	3,3	1,1	1,4	10	EC / LT	1
3764	EVA	transparent	55	6.000	4,5	2,7	1,8	9,5	25	EC / PGII / TC / TC Q	4
3779*	Polyamide	amberkleurig	150	7.000	14,5	4,8	1,8	7,9	32	EC / PGII / TC / TC Q	5
3789*	Polyamide	amberkleurig	105	5.200	14,5	4,3	1,5	4,3	28	EC / PGII / TC / TC Q	5
A 3792	EVA	transparant	60	5.000	2,8	2,7	2,8	9,5	23	EC / PGII / TC / TC Q	4
A 3792 LM	EVA	transparant	60	10500**	–	2,4	1,1	1,4	22	EC / LT	1

* Vochtopname: altijd in de gesloten zak bewaren. Vocht door overdroging (ong. 60 °C) verwijderen.
** Viscositeit mPa s bij 120 °C
Houdbaarheid vanaf verzendingsdatum opslagruimte: 24 maanden

Verkrijgbaar in:
- Smeltlijmsticks in verschillende afmetingen = 5 kg en 10 kg
- Smeltlijmgranulaat
- Pistolen voor smeltlijm: zie pagina 42 en 43

Lijmkeuze

A Allrounder: krachtige uitvoering voor diverse toepassingen

Z Zeer krachtig of bijzondere eigenschappen

Figure B.1: The thermoplastic adhesives collection from 3M[2]

B.5 Other adhesive producers

Besides Henkel and 3M, Huntsman and Intercol were also contacted. These producers of adhesives both offered thermoplastic adhesives. Although the adhesive is used in a high-performance vehicle, it experiences relatively low shear stresses making it potentially suitable. However, both companies did not want the use of their thermoplastic adhesive for testing; they were not designed for CFRP adherents.

Technical Data

Colour:	white, nearly transparent
Density:	approx. 1.0 g/cm^3
Solids:	100 %
Viscosity:	24.000–30.000 mPa.s
Equipment:	Brookfield Thermosel
Spindle:	27
Temperature:	160°C
Softening point:	82–90°C
according to ASTM E 28	ring and ball
Application temperature:	170–190°C
Open time:	approx. 30 s (3 mm joint on wood at 20°C; processing temperature 180°C)
Application temperature:	–20–80°C
Short exposure (up to 1 h):	100°C

Figure B.2: Henkel Technomelt Q9268H datasheet

Basis	MS-Polymeer, (lucht) vocht-uithardend
Dichtheid (EN 542)	ca. 1.389 kg/m^3
Vaste-stofgehalte	ca. 100%
Velvormingstijd (23 °C, 50% RLV)	ca. 8 minuten
Open tijd (23 °C, 50% RLV)	ca. 10 minuten
Kleefvrij (23 °C, 50% RLV)	na ca. 4 uur
Doorhardingssnelheid (23 °C, 50% RLV)	ca. 4 mm/24 uur
Hardheid in Shore A (EN ISO 868)	ca. 55
Volumeverandering (EN ISO 10563)	< 5%
Modulus bij 100% rek (ISO 37/DIN 53504)	ca. 1,5 N/mm^2
Trek bij breuk (ISO 37/DIN 53504)	ca. 3,0 N/mm^2
Rek bij breuk (ISO 37/DIN 53504)	ca. 350%
Afschuifsterkte (ISO 4587)	ca. 1,8 N/mm^2
Verwerkingstemperatuur	minimaal + 5 °C tot maximaal + 35 °C
Opslagtemperatuur	minimaal + 5 °C tot maximaal + 25 °C
Temperatuurbestendigheid	minimaal - 40 °C tot maximaal + 120 °C
Korte temperatuurbestendigheid	tot maximaal +180 °C (tot 30 minuten)

Figure B.3: Sabatack 780 datasheet

Product physical properties: (at time of manufacturing)			
Property	**Unit**	**EPR 04908**	**EPH 04908**
Viscosity at 25°C	mPa·s	500 ± 250	10 ± 5
Epoxy equivalent weight	g/equiv.	165 ± 3	
Amine equivalent weigth	g/equiv.		50
Density at 20°C	g/cm^3	1.15 ± 0.02	0.93 ± 0.02
Refractive index at 25°C		1.540 ± 0.003	1.468 ± 0.003
Mixing viscosity at 25°C	mPa·s	130 ± 10	
Pot life at 25°C	minutes	300 ± 50	
T_G (TMA)	°C	82	

Properties of the cured, non-reinforced resin system: (curing: 4h at 70°C + 6h at 80°C)		
Property	**Unit**	**Value**
Density	g/cm^3	1.15
Tensile strength	MPa	74
Tensile strain	%	9.4
Modulus in tensile	MPa	2900
Flexural strength	MPa	112
Modulus in flexure	MPa	3100
Water absorption after 24h 23°C	pbw	0,180
Water absorption after 168h 23°C	pbw	0,432

Properties of the cured, reinforced resin system (curing: 4h at 70°C + 6h at 80°C)		
Property	**Unit**	**Value**
Tensile strength	MPa	447
Flexural strength	MPa	588
Modulus in flexure	MPa	23400
ILSS	MPa	40
T_G (DMTA)	°C	89

Figure B.4: Hexion Bakelite datasheet

Appendix C

Failed CFRP thermal stability tests

Several tests were performed to determine the thermal stability of CFRP epoxy. As described in section 6.1, only the in-plane shear strength test produced adequate results. Results from the open-hole tensile strength test and ILSS test are discussed in this section, as well as why results were not deemed usable.

C.1 Open-hole tensile strength test

An open hole tensile test is performed. This is similar to a tensile test, except there is a hole in the middle of the rectangular sample. It requires the loads to distribute around the hole, which is a function of the resin. Failure is thus resin-dominated.

Test specimen The rectangular test specimens consist of plies of woven carbon, forming a quasi-isotropic laminate. After the curing cycle some small voids were visible in the material, as a result of a leakage somewhere in the vacuum bag. However, it was decided to still use this material, as the voids were distributed uniformly over the material, and the void content seemed low.

Four groups, each consisting of six specimens, were cut manually using a Secutom with diamond cutting blade to 200 by 15mm. This caused a small scatter in the sample's dimensions. All samples were measured using a digital caliper for accurate dimensions. Each group received a different heat treatment to simulate the temperature excursion experienced during manufacturing (table C.1). In the middle of the sample a hole with a diameter of 5mm was drilled using a drill bit for metal. Before drilling, tape was placed over the material to prevent damage.

It is hypothesized exposure to temperatures in the order of 200°C cause slight degradation to the resin. Longer exposure times would result in more degradation. As a result, strength values decline, resulting in a average strength of the groups sorted in descending order being $1 \approx 2 > 3 > 4$.

Group	Temperature (°C)	Duration (min)
1	-	-
2	90	10
3	200	10
4	200	30

Table C.1: Heat treatment of open-hole tensile strength specimens

Test procedure The tensile tests were performed in a 250kN Zwick test bench, at RT. Strain rate was constant at $1.3\frac{mm}{min}$, the test is stopped when the maximum force is reached. An extensometer is used for strain measurement.

The ultimate open hole tensile strength can be calculated using equation (C.1). Here σ_{OHTu} is the ultimate open hole tensile strength in $[MPa]$, F_{max} is the maximum load prior to failure in $[N]$ and A is the cross-sectional area disregarding the hole in $[mm^2]$.

$$\sigma_{OHTu} = \frac{F_{max}}{A} \tag{C.1}$$

Test results & discussion Test results are shown in table C.2 (a complete list of results can be found in appendix K.1).

Group	Ultimate open hole strength $[MPa]$	Standard deviation $[MPa]$
1	287	8.1
2	254	7.8
3	270	5.4
4	254	7.0

Table C.2: Ultimate open hole tensile strength of CFRP samples

Although group 1 showed highest strength values, the trend between the other groups was not clear. This could mean a false hypothesis, or something gave an unrepresentative result. The latter was believed to be the case. The void content, although low, could have influenced the test. The load is distributed around the hole, forming a stress concentration around it. This is primarily done by the resin. Voids near the hole cause this distribution to be different than for a void free laminate, resulting in different stress peaks. This makes comparison unfounded.

The test could be repeated with a satisfactory laminate. However, another piece of plate material was already available. The different lay-up did not allow for open hole tensile strength testing. It seemed easier to use the material with another test, as described in the next section.

C.2 ILSS by short beam strength

Interlaminar shear strength (ILSS) test is a small scale form of a three point bending test. Using rectangular specimens with fibres in the 0°direction, a bending moment causes shear stresses between the laminate plies, forming a crack.

Test specimen A panel of UD CFRP with 3mm thickness was left from a previous project. Samples were cut manually using a Secutom with diamond cutting blade, to 20 by 10mm. All dimensions were determined more accurately using a digital caliper. Similar to the previous test, several groups were made with specimens receiving different heat treatments (table C.3).

Group	Temperature (°C)	Duration (min)
1	-	-
2	90	15
3	200	15
4	200	30

Table C.3: Heat treatment of ILSS specimens

Test procedure The tensile tests were performed in a 10kN Zwick test bench, at RT. The span was set to 14.95mm, with the loading nose compressing at a constant rate of $1.0\frac{mm}{min}$. The test is stopped manually when the first signs of failure are clear, often a cracking noise accompanied by a dip in the load-strain curve. This might not be the ultimate strength of the sample, but is is important the test is stopped here. Continuing might introduce other failure modes, while the test specifically aims to initiate interlaminar failure. Possible failure modes are illustrated in figure C.1.

Interlaminar shear strength is calulated using equation (C.2). Here σ_{ILSS} is the interlaminar shear strength in $[MPa]$, F_{max} is the maximum load before failure in $[N]$ and b and h are specimen width and thickness respectively in $[mm^2]$. Note that only results of specimens that failed by interlaminar shear can be used.

$$\sigma_{ILSS} = 0.75 \cdot \frac{F_{fail}}{b \cdot h} \tag{C.2}$$

Test results & discussion Many samples were tested. Inspection of the failed samples showed most did not fail by interlaminar failure; it was flexural failure dominant (figure C.1, making the results not usable. In order to achieve a better efficiency of the test, dimensions of the samples were altered slightly but this did not alleviate the problem. Some extra material was made but the same problems remained. As discussed in section 6.1, three tests were selected to achieve the same goal. The in-plane shear strength test was performed which fulfilled the objective.

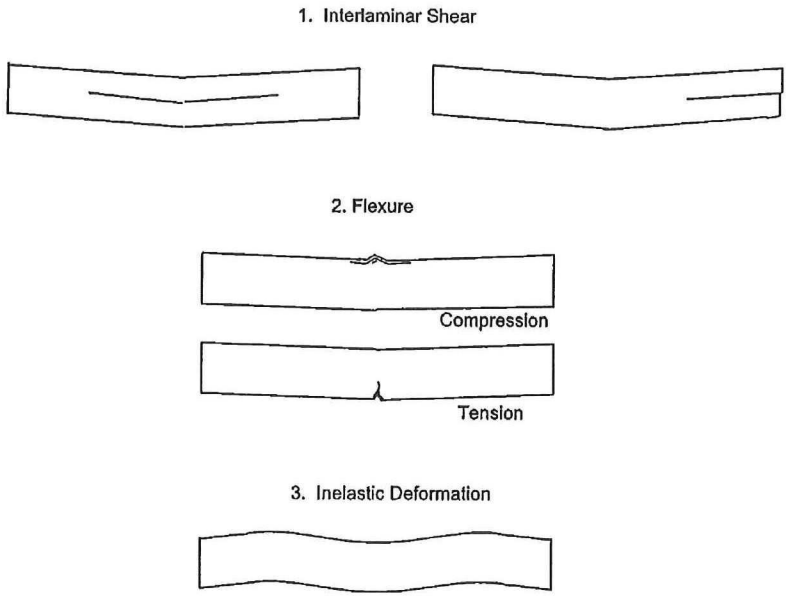

Figure C.1: Possible failure modes of interlaminar shear test

Appendix D

Concept selection elaboration

D.1 House of Quality elaboration

This section explains in more detail the relationships between the technical - and consumer requirements of the House of Quality analysis is section 8.2. Several requirements did not have a relationship, and are therefore not mentioned.

High performance There is a strong relationship between the performance of the car and high strength & stiffness combined with a low weight. Increased safety has a moderate relationship, because increasing the safety of the chassis (for example for side-impact) will also result in larger torsional stiffness.

Unique product A strong relationship is given for the high strength & stiffness efficiency and aesthetics; both are ways to distinguish a car from its competitors. This is also true for increased safety, especially when high stiffness is combined with a high level of safety. A low part count and automated production can also be unique to the consumer, and are given a weak relationship.

Feeling of safety Significantly increasing the chassis' safety will improve the feeling of safety to the driver, resulting in a strong relationship. A weak relationship is given for strength & stiffness efficiency, low part complexity and fit for maintenance; all can increase the perception of production quality and hence safety.

Beautiful product The surface finish has a large influence on the exterior of the car, hence the strong relationship. Medium relationships are present for a low part count and low part complexity, because both will result in a simple and clean structure. Finally the automated processes can create smooth patterns with constant quality, giving it a weak relationship.

High quality For a consumers point of view, a feeling of high quality is achieved by great safety and automated production. Both add a sense of a well designed product and high repeatability to the car, giving it a moderate relationship. High strength & stiffness achieves the same but the effect is less strong, hence the weak relationship. A good surface finish also gives a sense of attention to detail, resulting in a weak relationship.

Low-cost insurance Insurance costs will most certainly be lower for a car that is easy to maintain, giving this a strong relationship. Medium relationships are present for low part count and low part complexity, as this reduces the costs of repairs. If the chassis is based on a modular design, parts can be exchanged, reducing costs. Finally, easy access to components reduces the time needed for repairs and thus costs of labor.

Easy maintenance Easy access to components will reduce time and effort required for maintenance. The same is true for low part complexity and a design fit for maintenance, resulting in strong relationships. A low part count also aids with this but is given a medium relationship.

Relatively low cost Low cost is achieved by reducing the part count and part complexity. Also, easy access to components will result in reduced production times, hence the strong relationships. Using a modular design, many components and tooling can be shared, as well as investment and development costs. However this also requires a substantial initial investment, therefore a moderate relationship is considered. A design fit for automation can reduce labor, but requires a large investment in machinery, giving this a weak relationship. If the design is optimized for maintenance, components will be more easily accessible, easing production. Therefore a weak relationship is considered.

D.2 Trade-off elaboration

The classification of each category in the trade-off analyses is discussed in more detail. In order to make comparison easier, the concepts (discussed in section 7) were numbered as in table D.1.

Number	Concept
1	Ultrasonic welding
2	Resistance welding using mesh
3	Resistance welding using heating element
4	Induction welding using mesh
5	Induction welding using magnetic hysteresis
6	Thermoset epoxy

Table D.1: Numbering of concepts

Strength & stiffness efficiency Ranking the concepts on strength is not possible without any test data. However using some qualitative assumptions, the concepts are arranged to their expected strength level. Note that the relationship between the scores might not represent the same ratio in the quantitative strength values.

Concept 1: score 0 (baseline). Using the thermoplastic adhesive can provide suitable strength and stiffness. However, only spot welds are possible for ultrasonic welding, resulting in a small bonding area.
Concept 2, 4 & 5: score 2. All concepts allow for bonding over a large area, enhancing strength levels of the connection. The connection is still made using a thermoplastic adhesive.
Concept 3: score 0. Concept 3 uses the same the same thermoplastic adhesive. However, the heating layers are not necessarily design for load transfer, introducing more failure possibilities. Furthermore, the bondline becomes slightly thicker, resulting in larger peel stresses. Therefore the score is lower than concepts 2, 4 & 5.
Concept 6: score 3. Thermoset epoxy adhesive is both stronger and stiffer than thermoplastic adhesive. A much stronger bond is thus achieved.

Low part complexity *Concept 1: score 0 (baseline).* The ultrasonic welding setup contains little complex parts. However the thermoplastic film needs energy directors to concentrate the heat up.
Concept 2 & 4: score 0. The thermoplastic film for resistance/induction welding does not require energy directors, but a mesh inside. This is assumed to be equally complex as the baseline.
Concept 3: score -3. The heating element is a thin layer consisting of several very thin polymer layers. Attaining a reproducible layer thickness is quite difficult.
Concept 5: score -2. This heating layer requires small metal particles dispersed inside the thermoplastic film, in a uniform distribution. Only at higher temperatures will the viscosity of the adhesive be low enough to allow mixing.
Concept 6: score -1. Epoxy bonding requires precise mixing of resin and hardener to achieve the desired material properties.

Aesthetics *Concept 1: score 0 (baseline).* Ultrasonic welding has no material sticking out from underneath the overlap, achieving a clean appearance.
Concept 2: score -1. Mesh has to stick out from under the overlap, to be able to reheat the joint. This could be hidden using for example rubber flaps, but it still makes for a worse appearance.
Concept 3, 4, 5 & 6: score 0. Similar to the baseline, no material sticks out from under the overlap.

Increased safety *Concept 1: score 0 (baseline).* Safety is increased by preventing the joint from failing. This is mostly reflected by the strength of the adhesive connection (under environmental influences). Same scoring is therefore applied as with the *Strength & stiffness efficiency* requirement
Concept 2, 4 & 5: score 0.
Concept 3: score 0.
Concept 6: score 3.

Fit for maintenance *Concept 1: score 0 (baseline).* The thermoplastic adhesive is easily weakened by increasing its temperature. However, the lack of a local heating method makes this complex.
Concept 2 & 3: score 3. The resistive heating allows for easy removal of the bond.
Concept 4 & 5: score 2. Inductive heating allows for easy heating and disassembly. However, especially for large bonding areas, disassembly has to take place in phases.
Concept 6: score -3. Disassembly by heat is not possible. A sharp knife or blade is required, which might be troublesome if there is little space around the joint.

Low part count *Concept 1: score 0 (baseline).* Ultrasonic welding requires a thermoplastic film and tooling.
Concept 2, 4 & 5: score -1. Part requirements are similar to ultrasonic welding. However, the thermoplastic layer requires additives to transfer heat, hence the slightly lower appreciation.
Concept 3: score -3. Applying a heating element to the substrates effectively doubles the number of adhesive connections. The different nature of the connections also results in a large number of parts, resulting in the lowest rating.
Concept 6: score -1. The epoxy adhesive requires mixing of two substances, preferably in combination with glass beads to control bondline thickness. Therefore it is judged similarly to the adhesive films with additives.

Access to components *Concept 1 to 6: score 0.* The manufacturing methods have little influence on space around the joint. Therefore, all concepts are judged equally. The result should be discussed because it is part of the trade-off analysis.

Fit for automated production *Concept 1: score 0 (baseline).* Ultrasonic welding is easy to automate. However, only spot welds can be created. Welding of a large area can only be achieved by placing several spot welds next to each other, which is a time-consuming process.
Concept 2: score -1. Resistance welding can be automated, but requires considerations in the geometry of the adherents to make it accessible for the tooling.
Concept 4 & 5: score 1. Induction welding can be automated.
Concept 3 & 6: score -3. Bonding using thermoset epoxy is a delicate process, requiring the adhesive to be smeared on the substrate. It is therefore difficult to automate, especially for small series sizes.

Fit for modular design *Concept 1: score 0 (baseline).* Ultrasonic welding can be changed in size. Due to the aforementioned limitations of the process, scaling up to large bonding areas is difficult.
Concept 2: score 2. Changes in dimensions are no problem. A different mesh or power source might be required to meet the desired power input density.
Concept 3 & 6: score 3. Scaling presents no problems.
Concept 4 & 5: score 1. Scaling is easy, however heating in phases might be needed to achieve the full bond. The magnetic field is strongest around the coil, adhering larger areas takes a long time.

Appendix E

Adhesive test with single lap shear

Single lap shear test were performed with all adhesives, prior to testing using double lap shear test specimens. Goal of the test was to determine bond strength values of using a TP adhesives for joining TS composite substrates. It is an uncommon joining method, and strength values are unknown. At the same time, a relatively simple test can show several improvements that could be incorporated for the final design.

E.1 Proposed test

A single lap shear test was selected, it is a simple and widely used test for determining adhesive strength values. The test was performed according to ASTM D5868. To form test specimens, two panels of size 100x150[mm] were adhered over the long edge with an overlap of 25[mm]. Test specimens had 175x25[mm] dimensions.
Adhesive was applied using a glue gun. The quick cooldown of the hot thermoplastic on the RT substrate complicates manufacturing. Therefore the thermoplastic adhesives were manufactured using two methods; (1) substrates at RT & (2) substrates pre-heated to 80°C. This results in test matrix E.1. Several samples were also created with Pattex thermoplastic household adhesive, allowing me to get acquainted with the assembly process.

E.2 Manufacturing of samples

Manufacturing of substrate CFRP was used as adherent material, its manufacturing conditions are summarized in table E.2.
The joint interfaces were given a pretreatment before assembly consisting of several steps. Adhesion of the two panels was performed within four hours after the final step.

1. Placing tape 25mm from edge of the panel
2. Sanding the adhesion area with P240 sanding paper
3. Degreasing the adhesion area with PF-QD (quick drying cleaning solvent)
4. Drying the panels in the oven at 50°C for 1 hour

Assembly of joint at room temperature (group 1) Assembly of the joint was done in a special mould, made from a 15mm thick aluminium plate. Wooden sticks and aluminium

Adhesive	Substrate temperature (°C)	Number of test specimens
Pattex	RT	5
Sabatack 780	RT	6
Henkel	RT	6
	80	6
3M 3731	RT	6
	80	6
3M 3789	RT	6
	80	5
Total number of specimens	46	

Table E.1: Test matrix for single lap shear

Item	Details
Fibres	Carbon [0°/90°] TenCate CD 0286 050 030
Lay-up	$[\pm 45, 0/90, \pm 45, 0/90, \pm 45]$
Dimensions	600x600[mm]
Resin	RIM 235
Hardener	RIMH 237
Release agent	2 layers Marbocote 227CEE
Degassing pressure	3mBar
Infusion pressure	49mBar
Curing pressure	499mBar
Curing	5 hours @ 80°C
Cutting	Belt saw and Sepitom with diamond cutting blade
Specimen panel size	100x150[mm]

Table E.2: Manufacturing of single lap joint adherent material

sheets were used to align the adherents and ensure a constant bondline thickness (see figure E.1).
Adhesive was smeared on the adhesion area of the lower panel using the glue gun. The upper panel was aligned and placed in the mould with a 2kg weight on top. Solidification was a quick process; as a result the pressure was often not enough to distribute the adhesive. Cool down took several minutes in the mould, tape was removed afterwards.

Assembly of joint at 80°C (group 2) Before assembly, the mould was placed in an oven at 80°C for 15 minutes, together with the adherents and weight. The thick aluminium mould acted as a temperature buffer, preventing cool down of the substrate. After applying adhesive with the glue gun, it was clear the adhesive cooled down much more slowly compared to group 1 samples. This allowed the adhesive to flow much better over the bonding area after applying the upper panel (with the same 2kg weight). Test specimens were cut from the material using a Secutom with silicon carbide blade.

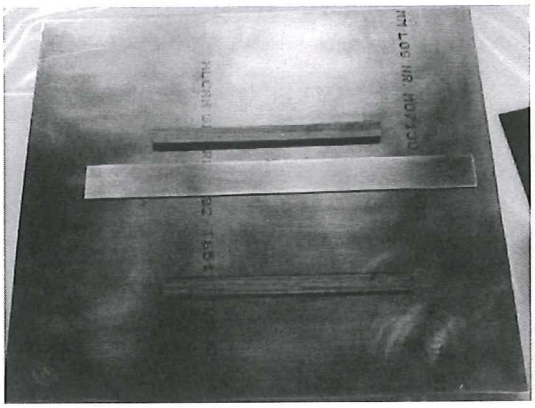

Figure E.1: Aluminium mould for single lap joint

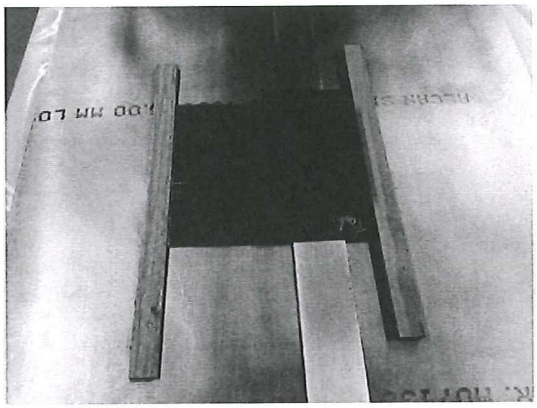

Figure E.2: Assembly of a single lap shear joint

Adhesive	Assembly temperature [°C]	Average shear strength $[MPa]$	Standard deviation $[MPa]$
Pattex	RT	2.30	0.27
Sabatack 780	RT	0.74	0.07
Henkel	RT	1.18	0.14
	180	2.52	0.13
3M 3731	RT	0.54	0.14
	180	1.35	0.33
3M 3789	RT	1.30	0.19
	180	2.33	0.16

Table E.3: Test results for single lap shear samples

E.3 Test protocol

Tests are performed in a 250kN Zwick test bench, with offset clamps to decrease joint eccentricity. Loading had a constant strain rate of $1.00mm/min$, and stopped when the measured force had decreased to 50% of F_{max}. Testing took place at RT.

E.4 Results & discussion

Shear strength values are calculated using equation (E.1).

$$\sigma_{ult} = \frac{F_{max}}{l \cdot w} \tag{E.1}$$

Where σ_{ult} is the ultimate shear strength of the connection, F_{max} the maximum force and l and w are the length and width dimensions of the adhesion area. The results are shown in table E.3 and plotted in figure E.3, where the error bars represent minimum and maximum values. The 1 & 2 behind the adhesive name indicate temperature of the mould during manufacturing: RT (1) or preheated (2).
The shear strength plot shows a large difference between the adhesives. Sabatack is a flexible elastomer, exhibiting low strength values as expected. The thermoplastic adhesives show a

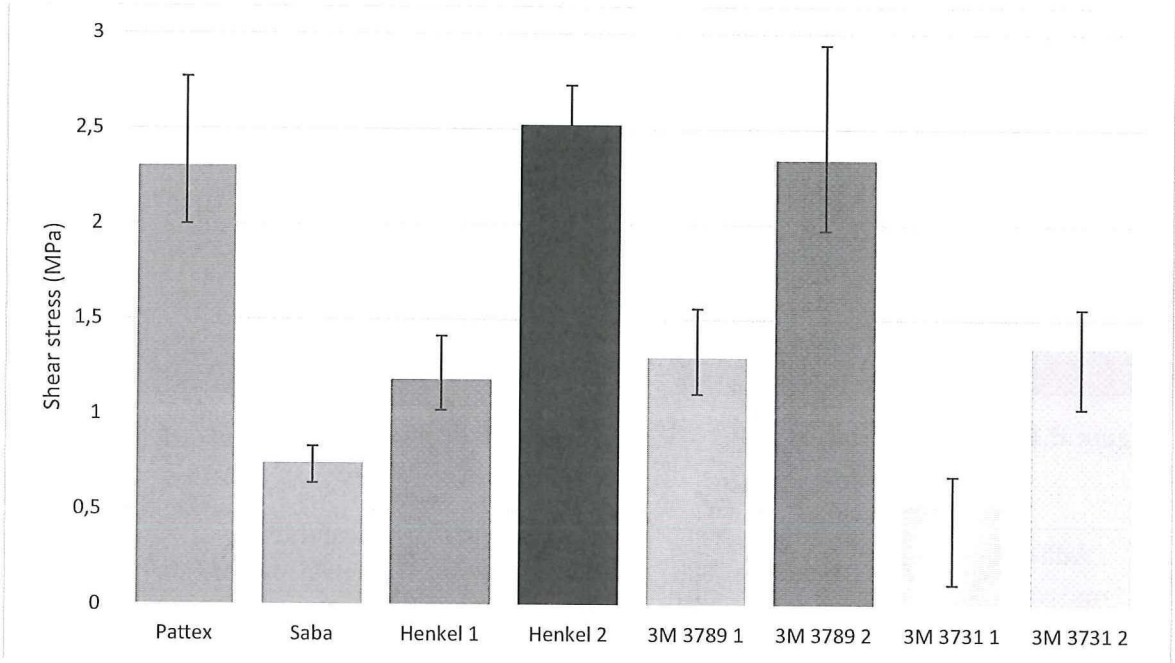

Figure E.3: Average, maximum and minimum shear strength results for single lap shear specimen

large variety; between adhesives but also between group 1 and 2. Closer inspection reveals group 2 specimens have thinner bondlines than their group 1 counterparts. This geometry change decreases the eccentricity reducing the bending moments and making for a stronger connection[39]. This makes comparison of result between groups unfounded. For a completer view, all data points are plotted in figure E.4.

Conclusion The variance in bondline thickness is too large to draw good conclusions. The tests show manufacturing conditions have a large influence on adhesive properties; keeping viscosity of the adhesive low seems critical. A heating element in the connections allows for better control and hence better reproducibility of the joint.
Furthermore, the test show the elastomer (Saba) adhesive has very little shear strength. Based on the strength values obtained it seems to be unrealistic to be applicable in the V-Cart chassis.

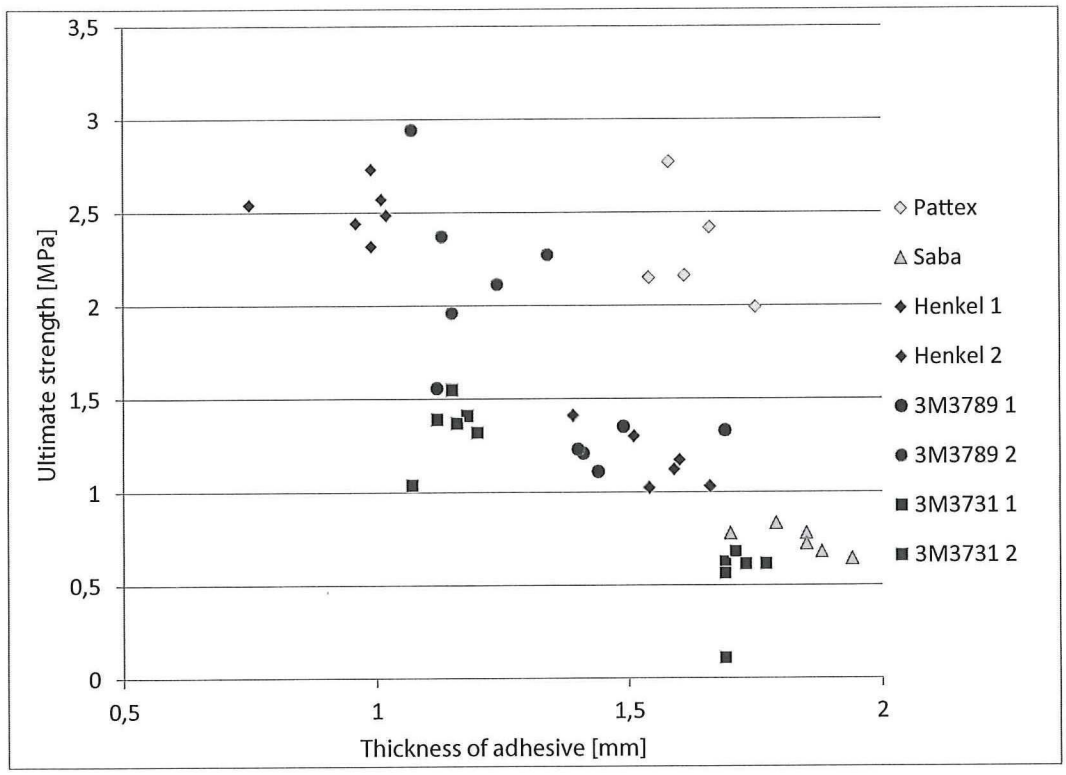

Figure E.4: Shear strength and bondline thickness values of single lap shear specimen

Appendix F

Pre-impregnation of mesh

The mesh is impregnated with resin to prevent voids in the adhesive layer. This is done by putting the mesh in a hot press together with an adhesive layer, exposing the material to a heating cycle. During this process, the flow of the adhesive needs to be controlled. Impregnation of the whole mesh would prevent an effective connection to the power source. Several methods are discussed in this chapter.

Problem statement Due to the low viscosity at high temperatures, the adhesive flows in an uncontrolled manner during the heating cycle (illustrated in figure F.1). The excess adhesive in width (x-direction) is no a problem; the mesh will be cut to size in x-direction. In the length (y-direction) this cannot; the copper contact points and crocodile beaks are at a fixed position and require a clean mesh. The distance between the copper contact points is 192mm, clean mesh is required beyond those points.

Proposed solutions Several solutions are tested. A mesh of size 100x50mm with a wire diameter of $0.20mm$ was used. This is a different mesh than the one used for structural testing (with wire diameter of $0.10mm$). There was only a small amount of this $0.10mm$ mesh available, therefore it had to be used sparingly to make sure all structural tests could be performed with the mesh.
In the middle of the mesh, on both sides, thermoplastic adhesive films of 50x50mm with a $0.20mm$ thickness were placed. Several solutions were applied on the edges of the mesh. All samples were heated using the same cycle, described in section 10.3.1.
Proposed solutions:

1. Tape
2. Tape with additional layer of release agent
3. Bee's wax
4. Release agent

Results The solutions had varying success. Using tape hindered the flow of the adhesive. However, the adhesive still managed to creep in between the layers of tape and mesh. Applying a layer of release agent on the tape made sure the adhesive did not stick to the tape, but could not prevent adhesive from entering between the tape and mesh. This resulted in a thin

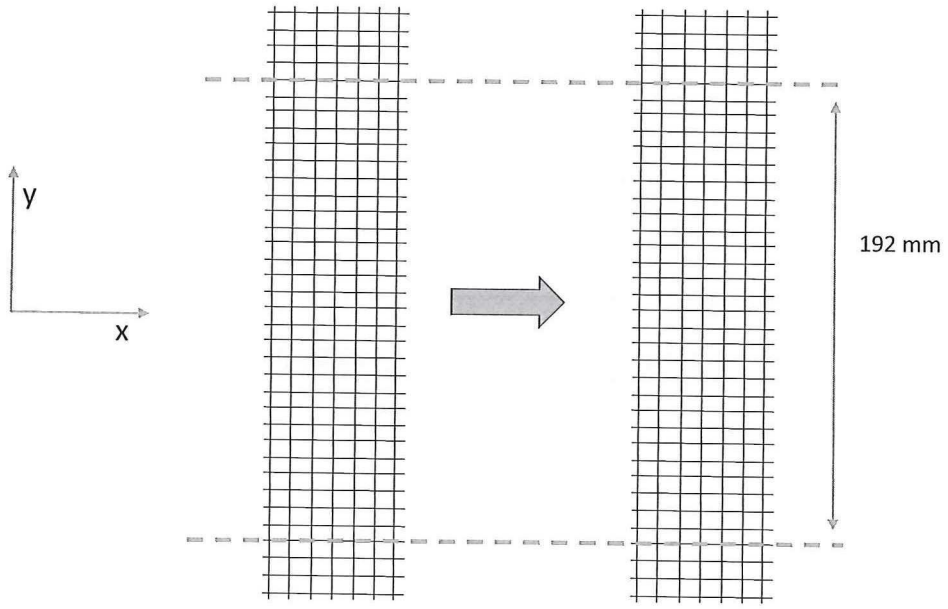

Figure F.1: Schematic representation of the uncontrolled flow of the adhesive layer before (left) and after (right) hot pressing

layer of adhesive present within the mesh. Given the large space between the wires this can be removed manually using a needle, but this would not be a feasible option for production. Nevertheless, for both solutions the removal of the tape showed a clean mesh area underneath, allowing good contact with the copper connector.
Bee's wax is typically used to fill up holes in moulds, to prevent resin from building up. Therefore it also seemed suitable to prevent the adhesive from flowing. However, at the high temperatures in the hot press, the wax's viscosity decreased considerably. As a result it was unable to control the flow of the adhesive.
Applying only release agent was least successful. As expected, it did not stop the flow of adhesive. The release agent was supposed to make it easy to peel off the excess adhesive. However, due to mechanical interlocking of the adhesive around the wires, this was not possible

Conclusion Using tape seems the most effective way to prevent adhesive from reaching unwanted places. The viscosity of the adhesive at 190°C is low enough to flow in between the mesh and the layers of tape, but the contact surface underneath the tape is still acceptable for the purpose.
The tests were performed using a mesh with large wire diameter. It is expected the solution with tape will work even better for smaller wire diameters. This reduces the size of the open space between the wires, requiring a lower adhesive viscosity to penetrate between the layers of tape. Figure F.2 illustrates this, the white area represents the open area of the mesh between the layers of tape.

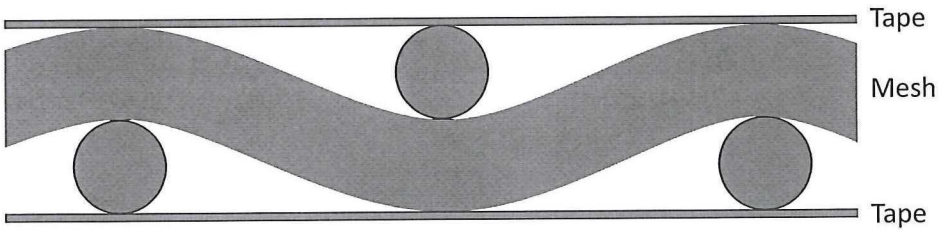

Figure F.2: Cross-section of the mesh with tape layers on top and below. The white area shows open space in the woven mesh, enabling adhesive to pass through. This space becomes thinner for smaller wire diameters.

Appendix G

Bondline calculations

A difference in bondline thickness of the single lap specimens makes direct comparison difficult. Thicker bondlines decrease joint strength by increasing the load path eccentricity, thus increasing the peel stresses in the joint. This section discusses calculations performed to make a better comparison between the *Benchmark* and *Without mesh* samples. By comparing the results to an existing data set of single lap shear tests with varying bondline thicknesses, the variable can be filtered from the results. This chapter is an elaboration on section 10.6.

G.1 Literature results

An existing data set was taken from a study by Tomblin et. al.[39]. In his research, many single lap shear tests are performed, varying (amongst others) adhesive, substrate material, substrate geometry, and bondline thickness. A data set for aluminium ASTM D3165 test specimens adhered with Hysol EA9394 adhesive is used. This has several differences compared to the single lap shear tests performed in this study:

1. Substrate material
2. Substrate geometry
3. Adhesive material

The test results are still deemed useful for comparison for several reasons:

1. This research used CFRP epoxy adherent material. Tomblin performed tests with several substrate materials. When plotting shear strength to bondline thickness, trendlines were similar regardless of the material used. Although at different shear strength values, but the trends were similar. Tomblin performed extensive tests with aluminium adherents (but very little with CFRP adherents), therefore these results were taken.
2. This research uses ordinary single lap specimens (section 10.2.3). Tomblin used ASTM D3165 shaped specimens (figure 10.2), minimizing peel stresses in the adhesive layer. However, by placing the clamps of the test bench at an offset, a similar effect is achieved. Furthermore, shear strength results using ASTM D1002 varied only slightly from D3165.
3. Tomblin used a thermoset epoxy adhesive, while this research uses a thermoplastic adhesive. This comparison thus assumes the dependence of shear strength on bondline thickness is the same regardless of adhesive nature. Unfortunately, little research is

Specimen	Max. App. Shear Stress $[MPa]$	Avg. Bondline Thickness $[mm]$
1	21.04	0.356
2	20.65	0.356
3	20.30	0.330
4	16.82	1.13
5	17.10	1.12
6	16.46	1.18
7	10.80	2.16
8	10.51	2.17
9	10.76	2.18
10	8.32	3.05
11	8.62	3.10
12	8.07	3.15
13	8.39	3.16
14	8.08	3.15
15	8.63	3.11

Table G.1: List of apparent shear stress results of aluminium ASTM D3165 substrates/Hysol EA9394 paste adhesive[39]

done involving bondline variations for thermoplastic adhesive to thermoset composite substrates. Although some small differences can be expected, it is thought to have little influence on the outcome. Especially while the difference in bondline thickness is already quite small.

G.2 Data Set

Apparent shear strength values of single lap ASTM D 3165 adhered with Hysol EA9394 paste are used as data set[39]. Original values can be seen in table G.1, converted to SI units.
By plotting these values and adding a trendline, apparent shear strength can be determined for values outside these points. Bondline thickness values from the table are slightly higher than the values from this research, thus requiring extrapolation. This is done in figure G.1. Tomblin suggests a linear relationship between shear strength and bondline thickness. Several trendlines were plotted and the linear line indeed seemed to fit best. Its equation is given in equation (G.1).

$$y = -4.4515x + 21.785 \tag{G.1}$$

G.3 Results

Apparent shear strength values can be taken from figure G.1 for different bondline thicknesses. These results are taken for values of $0.20mm$ & $0.10mm$ (corresponding to the bondline thicknesses in this research) and shown in table G.2.
This would thus suggest a 2% increase in shear strength when bondline thickness decreases

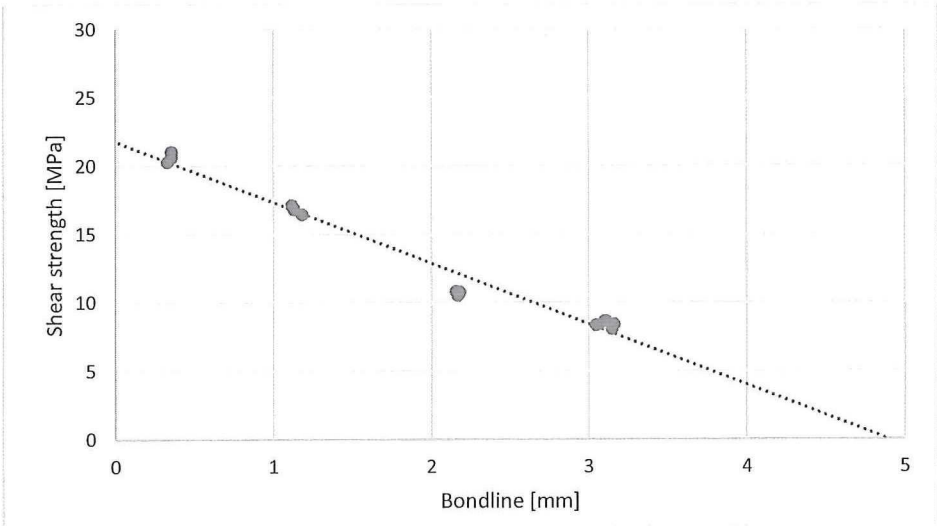

Figure G.1: Extrapolated trendlines for apparent shear strength values

Bondline thickness [mm]	Apparent shear strength [MPa]	Percentage [%]
0.2	20.9	100
0.1	21.4	102

Table G.2: Increase of apparent shear strength for thinner bondlines

from $0.20mm$ to $0.10mm$. Results from the samples *without mesh* are lowered by this percentage to compare them to the *benchmark* data, see figure G.2. The results can also be seen in table G.3.
The result is a reduction of the average apparent shear strength value from $6.30MPa$ to $6.18MPa$ for the *without mesh* group. Compared to $3.33MPa$ for the benchmark samples, strength values are still much higher. Even when considering the scatter in results, it can be concluded the samples without mesh showed higher shear strength. This is thus not solely a result of the thinner bondlines. The behavior was expected, as resin-mesh debonding proved a common failure mechanism in the benchmark samples.

Group	Apparent shear strength [MPa]	Standard deviation [MPa]
Benchmark	3.33	0.80
Without mesh	6.30	0.89
Without mesh corrected	6.18	0.87

Table G.3: Correction of apparent shear strength for samples without mesh

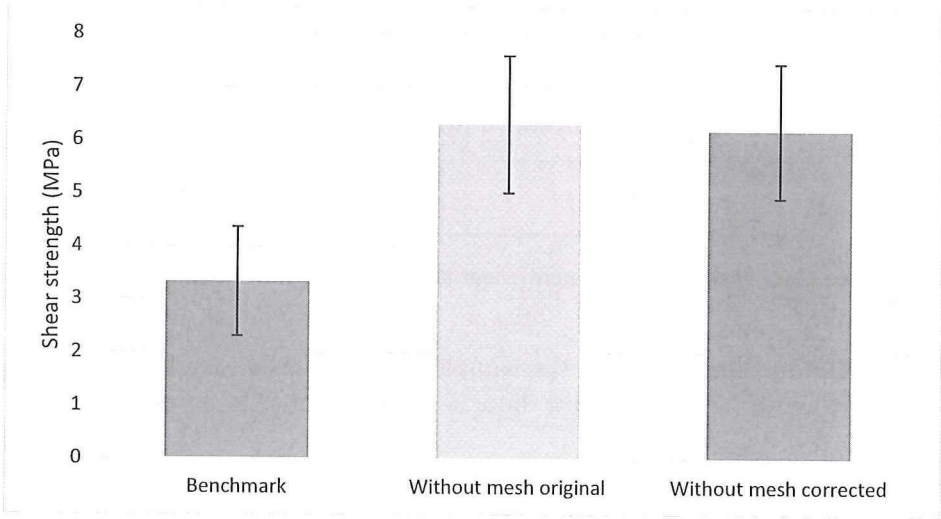

Figure G.2: Mean shear strength data and deviation of test specimens

Appendix H

Manufacturing of microscopy samples

Before viewing a sample under the microscope, several preparations are required. Thin plate material is difficult to handle. Furthermore, the viewing surface might not be perpendicular to the lens. This chapter describes several steps to turn the test samples into samples that can be viewed under the microscope.

Preparation Samples are cast in resin to make them easily yieldable. The material is cut to size to fit in the casting tube using a Secutom with silicon carbide blade. Cleaning was done in an ultrasonic bath with ethanol for five minutes.

Embedding To make the samples easier to yield, they were embedded in a cylinder of resin. A transparent resin was used to allow light of the microscope to pass through. Technovit 4071 was mixed in a 2:1 volumetric ratio for powder:liquid, and left to cure for five minutes at RT. Curing took place in a plastic cylinder (which was later removed), with the samples present.

Polishing There are many scratches present in the sample's surface, distorting the view. Using a Struers Pedemat, these were removed by polishing. This consisted of many steps, from coarse to fine sanding papers, and varying pressures (see table H.1).

Polishing step	Sanding paper	Force [N]	Lubricant	Pretreatment
1	P180	Manual	Water	-
2	P320	10 → 30	Water	-
3	P1000	10 → 30	Water	-
4	P2400	10 → 30	Water	-
5	Polishing 1	30	Ethanol	1' ethanol bath
6	Polishing 2	30	Ethanol	1' ethanol bath
7	Polishing 3	30	Ethanol	1' ethanol bath

Table H.1: Overview of polishing steps for the preparation of microscopy samples

Appendix I

Microscopy photos of single lap shear samples

Microscopy photos of the lap shear samples show a large void content in the adhesive layer. As discussed in section 10.6.6, it is thought this is a result of the ultrasonic ethanol cleaning process, which dissolves the adhesive at high temperatures. However, until identical samples are manufactured without exposure to ethanol, it is not possible to give absolute certainty. Nevertheless, the images and are still useful for several purposes. For example, the lack of adhesive allowed easy determination of the bondline thickness.

Figure I.1 shows the samples where ethanol was used during preparation (chapter H). All pictures show the CFRP epoxy adherents and the top and bottom, with the adhesive layer in the middle. Images (a) & (b) show samples from the *benchmark* group, the darker areas show many voids are present. Images (c) & (d) show samples from the *without mesh* group, the dark line in the middle is a large void where adhesive has disappeared.

Figure I.2 shows resistance welded samples sanded down about $3mm$ without ethanol. The sanding was performed identical to the process as described in appendix H. Only the last three steps from table H.1 were omitted; the polishing paper require lubrication with ethanol. The void content slightly below the surface is much lower. Image (a) shows a void free interface. In images (b) and (c) the dark areas show a few voids, but much less compared to I.1. A close-up in image (d) clearly shows a void rich area.

Sanding the samples down even further to half of the original sample thickness, relatively void poor areas were found (figure I.3). The resistance welded samples show very few voids (the dark areas). The void content clearly decreases deeper inside the connection, suggesting it originated from the ethanol penetration. However this cannot be known for certain without manufacturing of a similar connection without exposing it to ethanol.

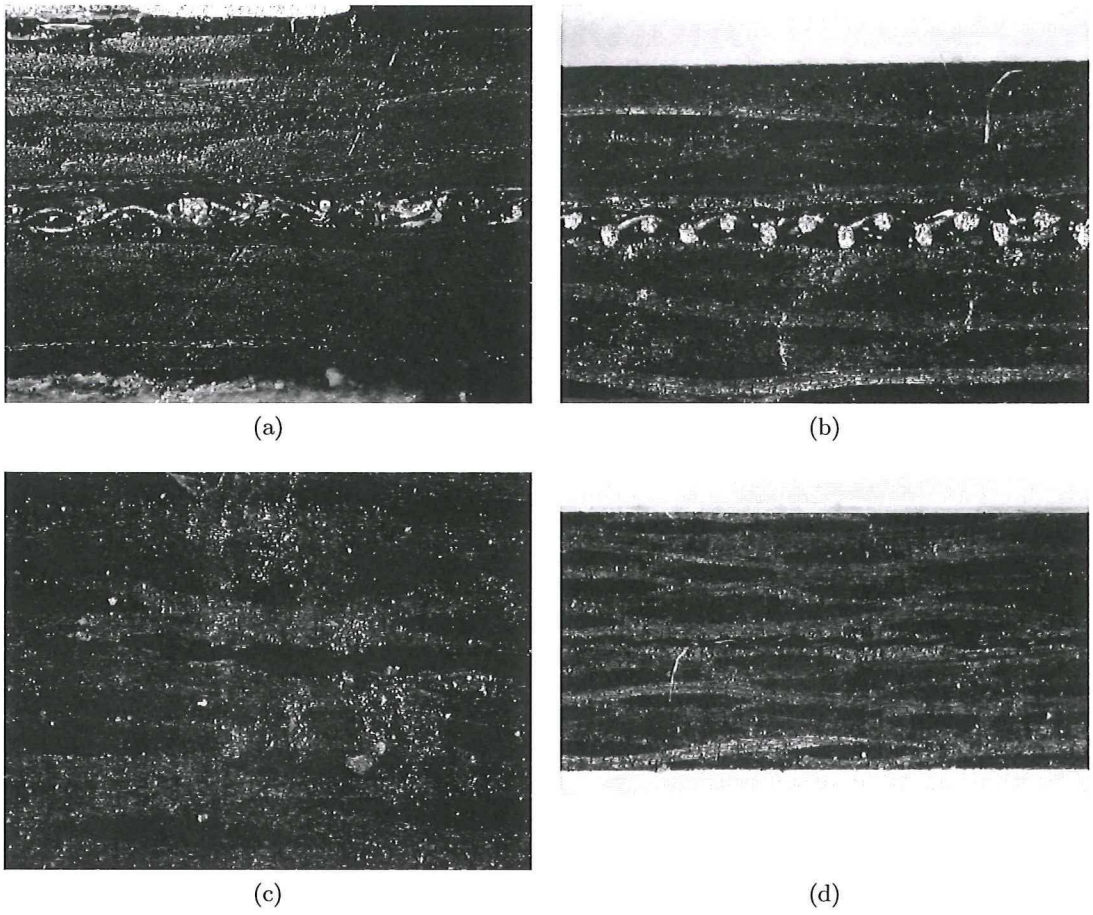

(a) (b)

(c) (d)

Figure I.1: Microscopy photos of single lap joints prepared using the ethanol bath. Photos are taken at the edges. The top and bottom of the image show the CFRP epoxy adherents. In the middle the mesh and adhesive layer are visible, dark areas are voids in the adhesive layer.

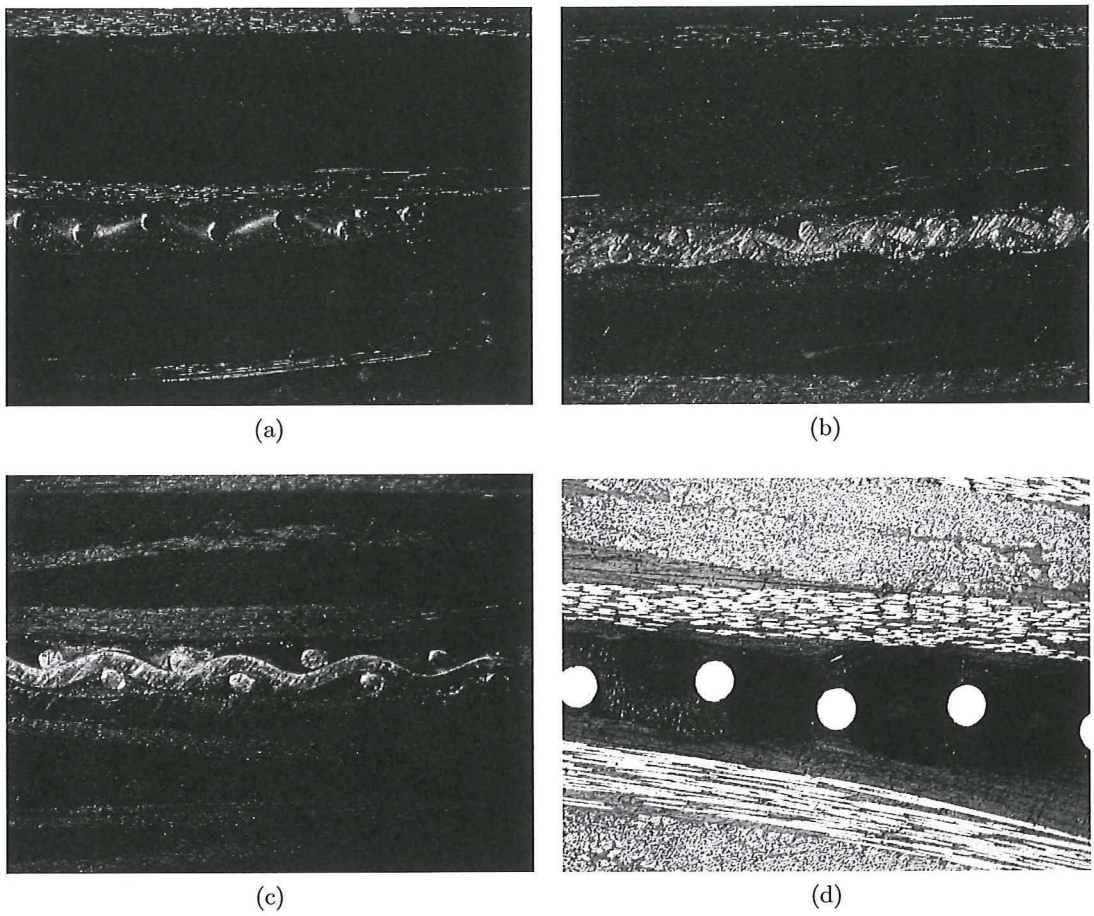

(a) (b)

(c) (d)

Figure I.2: Microscopy photos of single lap joints prepared using the ethanol bath. Images are taken at the edge after sanding them down $3mm$without ethanol. All samples are manufactured using resistance welding.

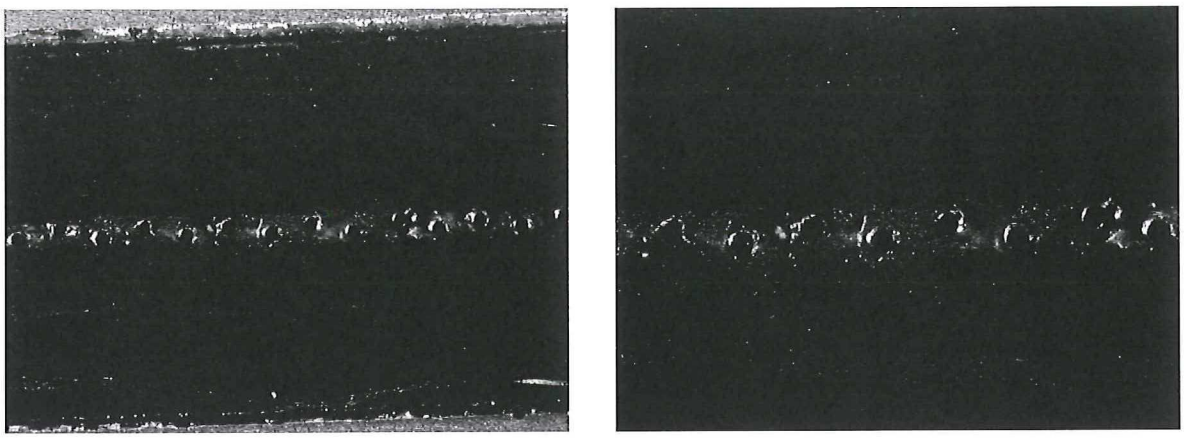

Figure I.3: Microscopy photos of single lap joints prepared using the ethanol bath. Images are taken at the edge after sanding them down to half of the original thickness, without ethanol.

Appendix J

COMSOL simulations

Throughout the project, several simulations were performed using COMSOL Multiphysics 4.3b. Especially phenomena as heat transfer during assembly are difficult to calculate and are better approximated using simulations. Values obtained need to be validated in order to confirm reliability. Once a reliable model is established, it allows welding times to be predicted for different geometries. Less tests have to be performed to 'streamline' the welding process; approximate values are already known.
With a constant power input density, the adhesive is heated to $T_{application}$. Using a simple calculation with material constants shows the adhesive material (used for test samples) can be heated in less than 2 seconds. However this ignores heat dissipation to the surrounding CFRP material, which is complex for calculations by hand. This can easily be included in a simulation.

J.1 Resistance welding model

A time-dependent 2D heat transfer model was selected. A side view of the single lap test samples was built, including the wooden support blocks and mesh in the adhesive (see figure J.1). Parameters used are presented in table J.1.

J.2 Model validation

Running the model renders a temperature distribution. This can be represented graphically by taking the values across the center line of the sample. Figure J.2 shows a close up of the COMSOL geometry, with temperature values taken along the red line through the center plane of the the adhesive layer. The corresponding temperature profile is also illustrated.
Applying a power of $P = 35\frac{kW}{m^3}$, the temperature distribution after 28 seconds is shown in figures J.3. It shows that temperatures of 200°C are reached in the middle of the overlap. The mesh was refined until the solution converged.

Temperature in the adhesive layer was measured during manufacturing using a thermocouple (chapter 10). By plotting this data next to that obtained from the COMSOL model, the accuracy of the model can be validated. Data from three panels is plotted over time. For the

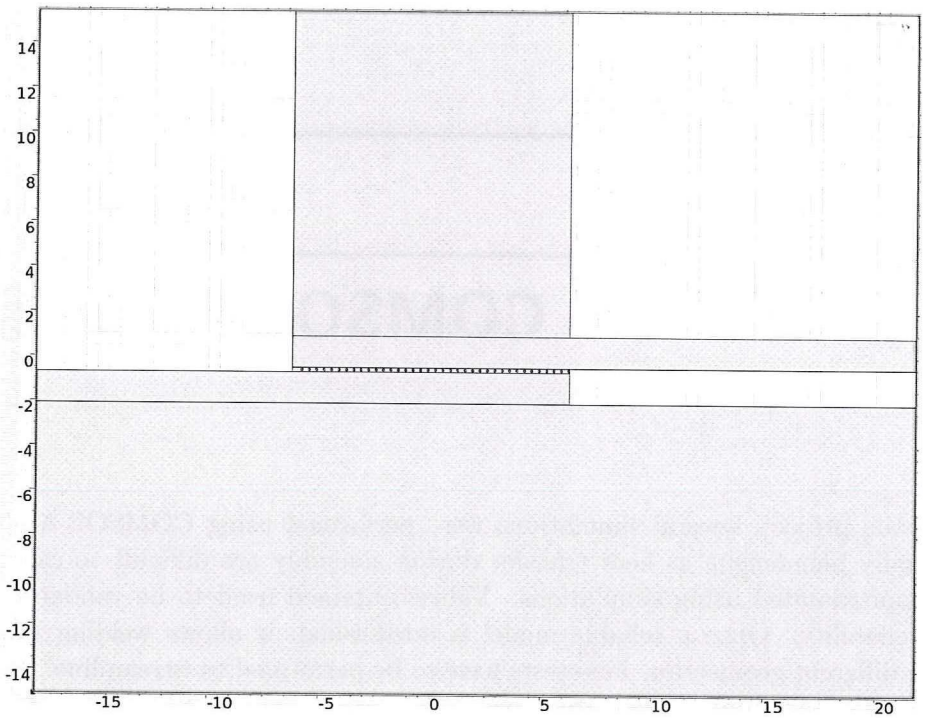

Figure J.1: 2D single lap joint model, excluding surrounding air

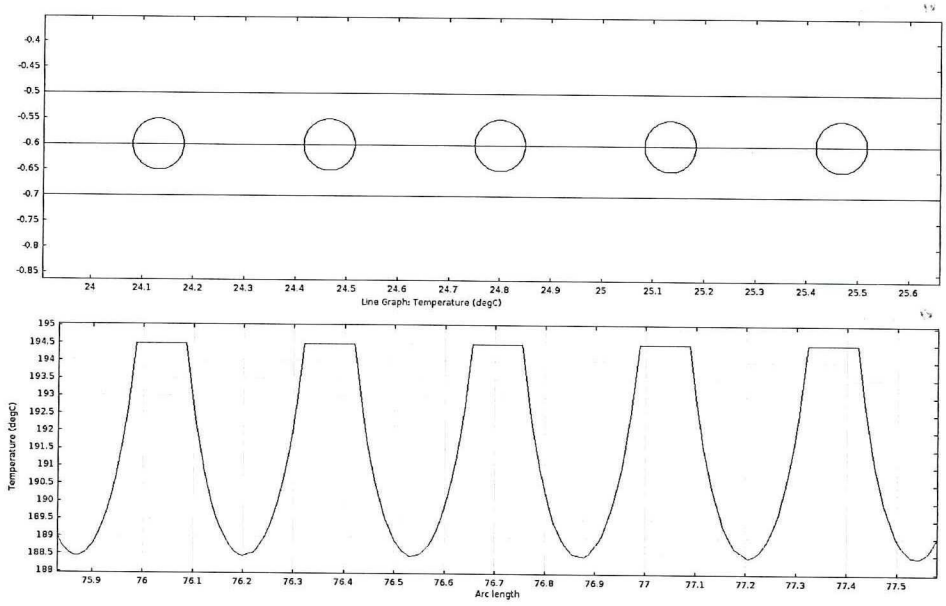

Figure J.2: Schematic overview of the COMSOL model geometry (top) showing the adhesive layer and steel mesh wires, and the temperature distribution along the red line (bottom).

Item	Details
Model	2D time dependent
Physics	Heat transfer in solids
$c_{p,mesh}$	$475[\frac{J}{kg \cdot K}]$
k_{mesh}	$44.5[\frac{W}{m \cdot K}]$
ρ_{mesh}	$7850[\frac{kg}{m^3}]$
$c_{p,adhesive}$	$1666[\frac{J}{kg \cdot K}]$
$k_{adhesive}$	$0.22[\frac{W}{m \cdot K}]$
$\rho_{adhesive}$	$1100[\frac{kg}{m^3}]$
$c_{p,CFRP}$	$1400[\frac{J}{kg \cdot K}]$
$k_{CFRP,in-plane}$	$2.1[\frac{W}{m \cdot K}]$[27]
$k_{CFRP,out-of-plane}$	$0.22[\frac{W}{m \cdot K}]$[27]
ρ_{CFRP}	$0.16[\frac{kg}{m^3}]$
$c_{p,wood}$	$1300[\frac{J}{kg \cdot K}]$
k_{wood}	$0.0001[\frac{W}{m \cdot K}]$
ρ_{wood}	$7850[\frac{kg}{m^3}]$
Initial values	293.15[K]
Mesh type	User-controlled triangular
Time dependent study	0 to 30 seconds, 1 second step size

Table J.1: Simulation parameters of single lap model with mesh

model, temperature values of a point on the red line from J.2 next to the mesh are taken. The result is shown in figure J.4.
The graph shows differences and similarities. All four lines reach approximately the same final temperature. Although all panels were manufactured under the same conditions and using the same welding parameters, temperature curves are different. Panel 4 quickly reached a high temperature, while for panels 2 and 3 a sudden rise in temperature can be seen halfway through the process. This could be a result of data capturing; this happens every 1.5 seconds, the first step even takes 3 seconds, explaining the erratic nature of the curve. Data from the model lies in between the curves. Nevertheless, within the modeled time-frame, data of the model resembles the measurements well enough for the intended purpose; determining the final temperature in the adhesive layer.

J.2.1 Thermal conductivity

The mesh heats up by the application of power. This heat dissipates through the adhesive as a function of the thermal conductivity of the polymer. Polymers typically have a low thermal conductivity. Heat transfer (along the red line from figure J.2) increases for larger temperature differences or larger κ values.
The low thermal conductivity values result in temperature differences within the adhesive. This is visible in figure J.2; further away from the mesh, temperatures quickly decrease. It explains the wave shape in the figure showing the temperature distribution (figure J.3). This can be reduced by selecting an adhesive with larger thermal conductivity values, or by reducing the space between the mesh wires.

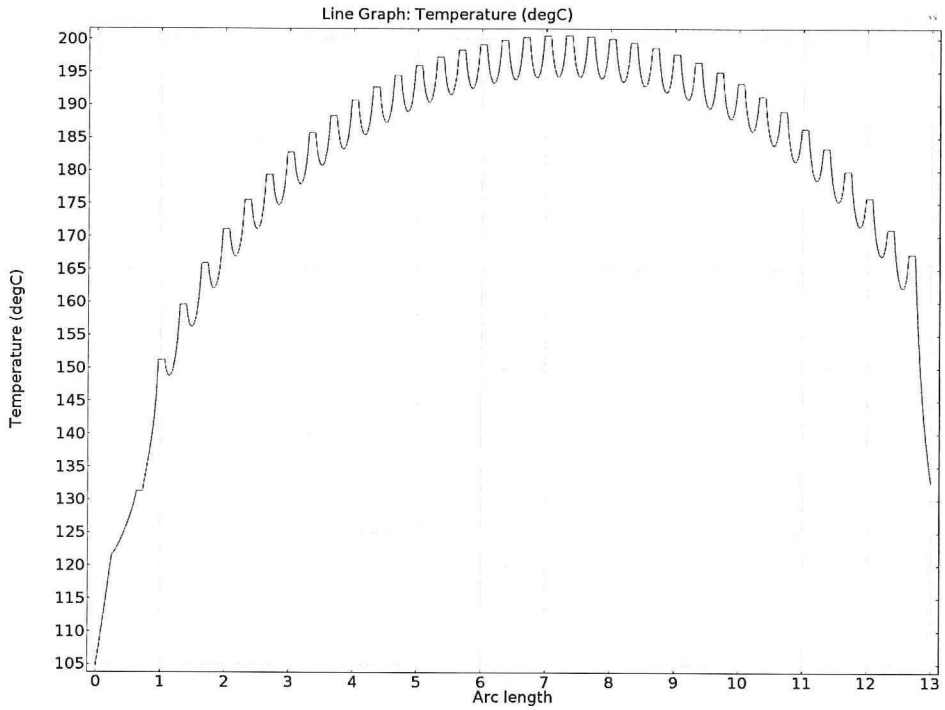

Figure J.3: Temperature distribution along the adhesive layer after 28 seconds. Position along the width of the overlap is represented on the x-axis. Welding parameters: $t = 28s, P = 35\frac{kW}{m^3}, overlap = 12.5mm, \Delta_{wire} = 0.234mm$

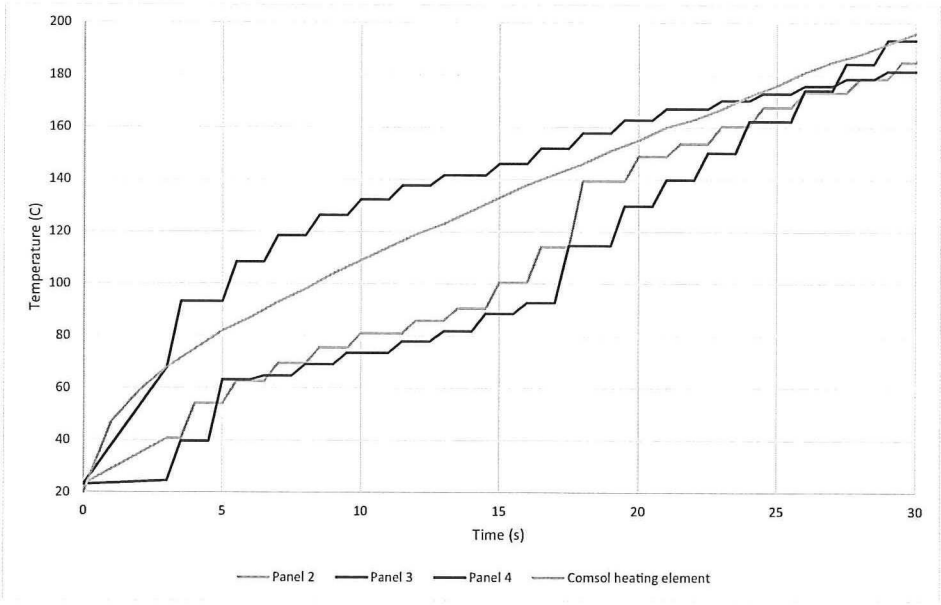

Figure J.4: Temperature data from thermocouples during manufacturing of single lap samples, together with temperature data from simulation

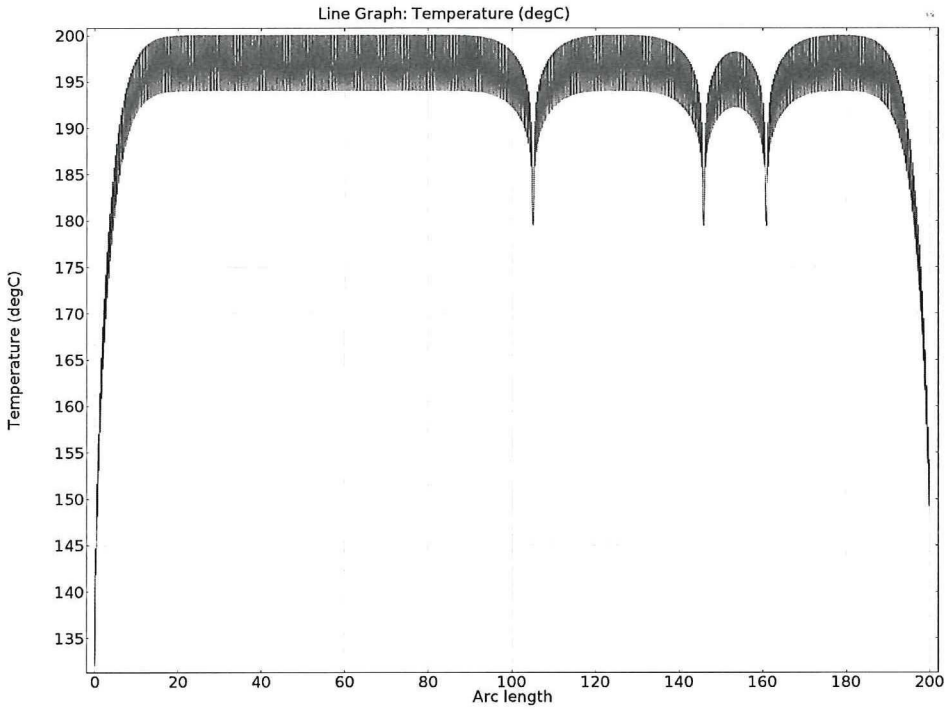

Figure J.5: Temperature distribution along the adhesive layer after 25 seconds. Position along the width of the overlap is represented on the x-axis. Welding parameters: $t = 25s, P = 35\frac{kW}{m^3}, overlap = 200mm, \Delta_{wire} = 0.234mm$

J.3 Geometric changes

J.3.1 Overlap length

To make the connection suitable for other applications, different overlap lengths are required. A longer overlap length reduces average shear stress (although maximum stress values stay the same), potentially allowing for better load transfer. The overlap length influences the temperature distribution in the adhesive. It is expected larger overlap lengths result in shorter heat up times by the higher $\frac{Volume}{Area}$ ratio for the adhesive, and thus relatively less opportunities to dissipate heat.
This can be confirmed using the model. Overlap length is increased to $200mm$, temperature distribution after 25 seconds is shown in figure J.5. Compared to the $12.5mm$ overlap, similar temperatures are reached in a shorter time. Note the three downward peaks; these are a result of COMSOL refusing to include three wires as heating elements. Given the abundance of wires in the $200mm$ overlap, this has little influence on the aim of the simulation.

J.3.2 Mesh spacing

The spacing between the mesh wires has a large influence on the heat up process. As discussed in section 11.2, large Δ_{wire} values give the mesh a high electronic resistance, allowing for higher power input densities. However, temperature differences in the adhesive may exacerbate. At the same time, the spacing of the mesh is thought to influence the strength of the connection. Resin-mesh debonding is a prominent failure mechanism, this is potentially

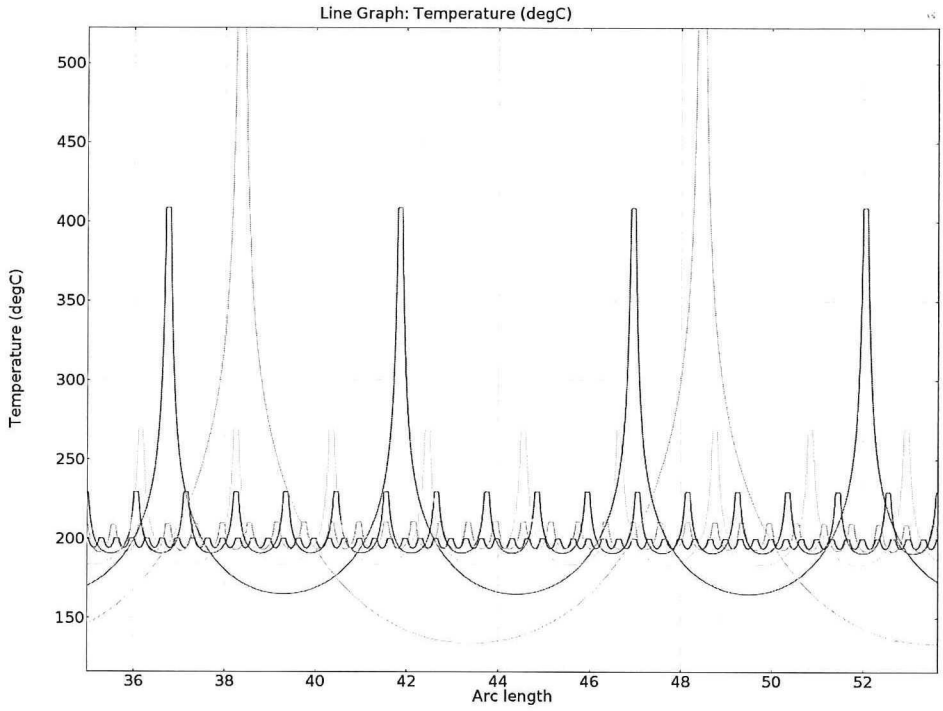

Figure J.6: Temperature distribution along a part of the adhesive layer for various mesh spacings, after 25 seconds. Dark blue is 0.234mm, green is 0.5mm, red is 1mm, light blue is 2mm, purple is 5mm and orange is 10mm. Welding parameters: $t = 25s, P = 35\frac{kW}{m^3}, overlap = 200mm$

reduced by selecting a coarser mesh.
The COMSOL model cannot give conclusive information about strength values, but can be used to see how changes in Δ_{wire} influences heat-up. A parametric sweep is performed, varying the mesh spacing with values $0.234, 0.5, 1, 2, 5$ and $10mm$. Power input density was constant, larger spacing thus meant a larger current per wire. Figure J.6 shows a close up of the corresponding temperature distributions, taken along the red line of figure J.2. Temperature differences within the adhesive are listed in table J.2.
The figure shows large temperature difference within the adhesive arise as spacing is increased. This is a result of the low thermal conductivity of the adhesive, presenting a problem. The connection must be assembled within a temperature window. The minimum temperature of every point in the adhesive must be higher than the application temperature, while the maximum temperature must not exceed the degradation temperature. For large spacing values, the processing window becomes very small or is not available.
If 3M 3789 is used as adhesive material, temperatures may not exceed 380°C to prevent degradation (section 6.2). At the same time, the lowest temperature must be higher than 170°C to enable good adhesion. Looking at the table, this is only satisfied for mesh spacing values from $0.234mm$ to $2.0mm$. Larger spacing values could potentially be applied using a lower power input densities with longer weld times, allowing more time for the heat to dissipate through the material. However, since the CFRP adherents have similar thermal conductivity as the adhesive, this also results in higher temperatures in the adherents. High temperatures can initiate damage, and must therefore be avoided.

Mesh spacing $[mm]$	Line colour	Mesh temperature $[°C]$	Lowest adhesive temperature $[°C]$	Temperature difference $[°C]$
0.234	dark blue	200	194	6
0.5	green	211	194	17
1.0	red	230	191	39
2.0	light blue	269	184	85
5.0	purple	409	165	244
10.0	orange	667	134	533

Table J.2: Temperature differences in adhesive for mesh spacing values, after 25 seconds of heating at $35\frac{kW}{m^3}$

J.3.3 Power input density

A comparison is made to see the influence of power input density on the temperature difference in the adhesive layer. Two simulations are performed with identical welding parameters except for the power input density. The resulting temperature distributions show that for the lower power input density, temperature differences within the adhesive were smaller. For example, for a $200mm$ overlap with $2mm$ between wires, using a reduced power input density of $P = 20\frac{kW}{m^3}$ results in $T_{max} = 234°C$, reducing the temperature difference from 85°C to 49°C. However, this requires an increase in the welding time proportional to the reduction in power input density (from 25 to 47 seconds).
Using a lower power input density allows the temperature within the adhesive to be controlled better, reducing temperature differences. At the same time, the adherents will reach higher temperatures too. Furthermore, longer manufacturing times are not beneficial, and if the power input density is too low, the right temperature might not be reached at all. The ideal manufacturing conditions thus depend strongly on the materials used, but also on the application.

J.3.4 Adhesive material

Material properties of the adhesive have a strong influence on the heating process. This is mostly dictated by the heat capacity and thermal conductivity. For example, the polyamide adhesive has a heat capacity of $1666\frac{J}{kg \cdot K}$. A change in this property requires more or less total energy input (depending on the change), resulting in longer or shorter welding times to reach the same temperature. The effect is relatively small if a fine mesh is applied; the steel also requires heating energy. When increasing the heat capacity of the polymer to $2100\frac{J}{kg \cdot K}$, average temperatures after 25 seconds of heating at $35\frac{kW}{m^3}$ lie only 3°C lower (for a mesh with $\Delta_{wire} = 0.234mm$ and $d_{wire} = 0.10mm$). Similarly, temperatures are 3°C higher for a heat capacity of $1200\frac{J}{kg \cdot K}$.
Thermal conductivity is expected to have a similar influence on the temperature distribution as varying the spacing of the mesh. This property also varies per polymer, and can be altered using additives. Using a polymer with higher thermal conductivity can be a solution if larger mesh spacing values are required.

Appendix K

Test Data

This appendix shows the original test data obtained during several experiments.

K.1 Open-hole tensile strength test

Table K.1 and K.2 show the original and summarized testdata of the open hole tensile strength test.

K.2 In-plane shear strength tests

Table K.3 and K.4 show the original and summarized testdata of the in-plane shear strength tests.

K.3 TGA tests

The temperature where degradation starts is taken as the point where sample weight has reduced to 95%. Therefore, a horizontal line indicating 95 weight-% has been added to each graph. The intersection with the weight-% shows the degradation temperature.
A summary of the obtained values is shown in table K.5, the original graphs can be seen figures K.1 to K.5.

Specimen group	Force $[N]$	Area $[mm^2]$	Open-hole tensile strength$[MPa]$
1	11771	41.3	285
	12277	40.5	303
	12072	42.3	285
	12453	43.1	289
	11064	39.9	278
	11495	40.9	281
2	10529	41.6	253
	11139	43.3	257
	11402	42.7	267
	11875	47.3	250
	10214	41.7	245
	10115	41.7	243
	10874	42.0	259
3	11592	43.3	268
	11302	43.1	262
	11887	40.2	271
	12477	44.6	279
	11718	43.1	272
	11137	41.8	266
4	12042	49.2	245
	11417	43.5	262
	11222	43.9	256
	10402	42.7	243
	11348	43.7	260
	10381	40.7	255

Table K.1: Test data from open-hole testile testing of CFRP

Specimen group	Mean open-hole tensile strength$[MPa]$	Standard deviation $[MPa]$
1	287	8.1
2	254	7.8
3	270	5.4
4	254	7.0

Table K.2: Summarized results of open-hole test data

Specimen group	Force $[N]$	Area $[mm^2]$	In-plane shear strength$[MPa]$
1	3866	33.2	58.2
	4574	34.4	66.4
	4456	35.3	63.2
	4061	32.5	62.5
	4306	33.9	63.6
	4126	32.5	63.4
2	4929	36.3	67.8
	4678	33.0	70.8
	3738	33.3	56.1
	4367	34.1	64.1
	3698	32.4	57.0
	4618	33.7	68.5
3	4032	32.0	63.1
	3476	30.0	58.0
	4289	32.9	65.1
	4203	34.2	61.4
	4063	31.0	65.6
	4529	34.9	64.8
4	4347	34.3	63.4
	3962	29.7	66.7
	4237	31.4	67.4
	4405	33.8	65.2
	5002	34.8	71.9
	4079	32.5	62.7
5	226	33.9	3.33
	443	30.3	6.97
	102	32.5	1.57
	106	34.9	1.52
	94	34.4	1.37
	85	34.1	1.26

Table K.3: Test data from in-plane shear strength testing of CFRP

Specimen group	Mean in-plane shear strength$[MPa]$	Standard deviation $[MPa]$
1	62.9	2.4
2	64.1	5.7
3	63.0	2.7
4	66.2	3.0
5	2.67	2.1

Table K.4: Summarized results of in-plane shear strength test data

Material	T_{deg} (°C)
Ten Cate carbon fibres with RIM 235 & 237H resin	315
3M 3731	300
3M 3789	380
Henkel Technomelt Q 9268 H	280
Sabatack 780	225

Table K.5: Test results of TGA testing

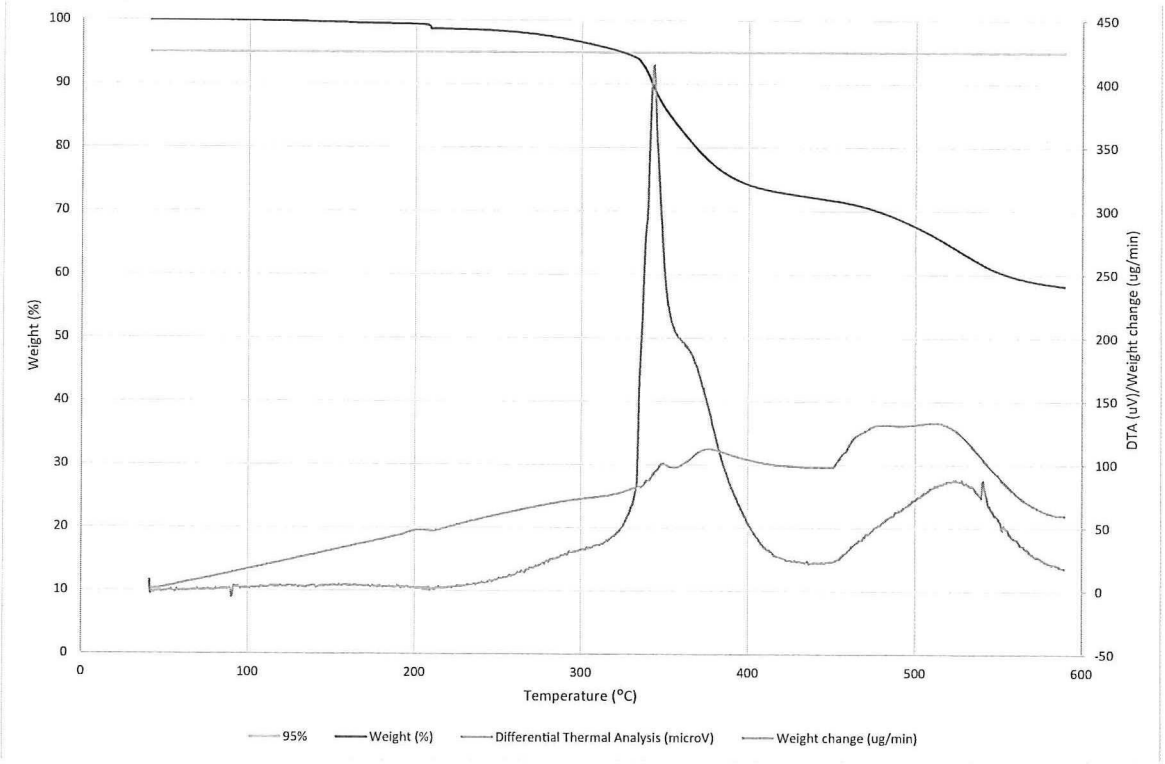

Figure K.1: TGA result of carbon fibre infused with RIM 235 epoxy

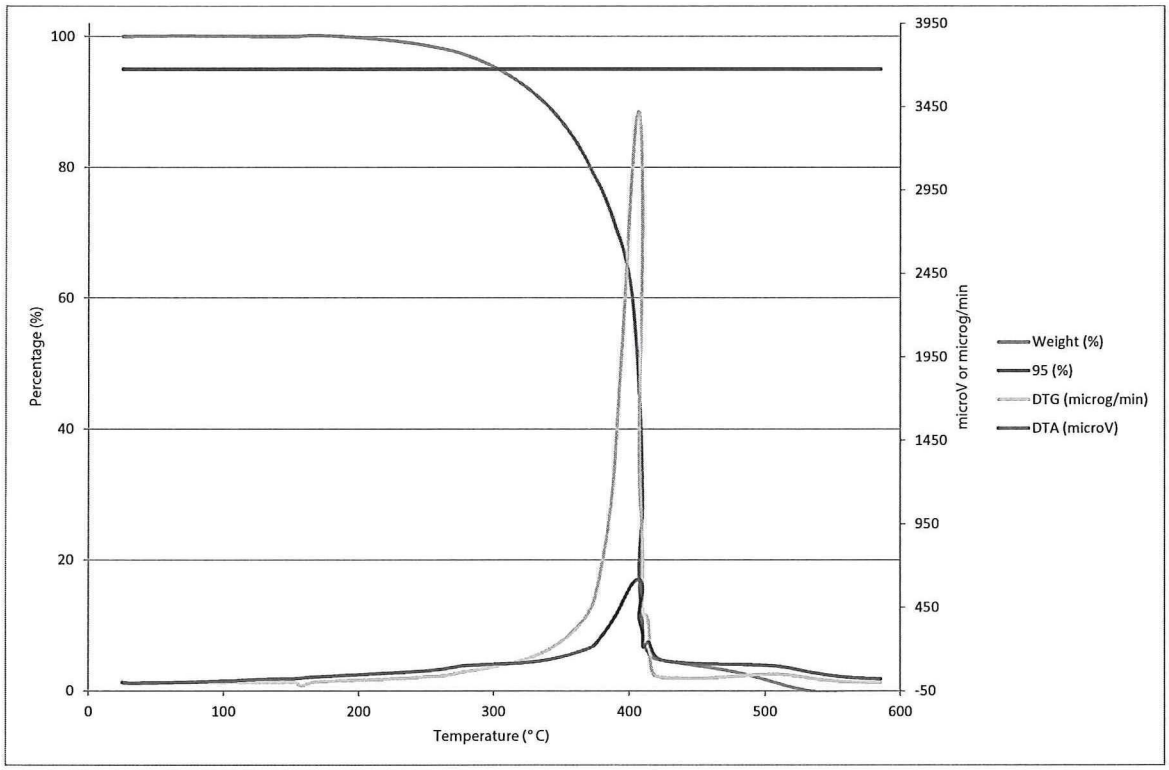

Figure K.2: TGA result of 3M 3731 thermoplastic adhesive

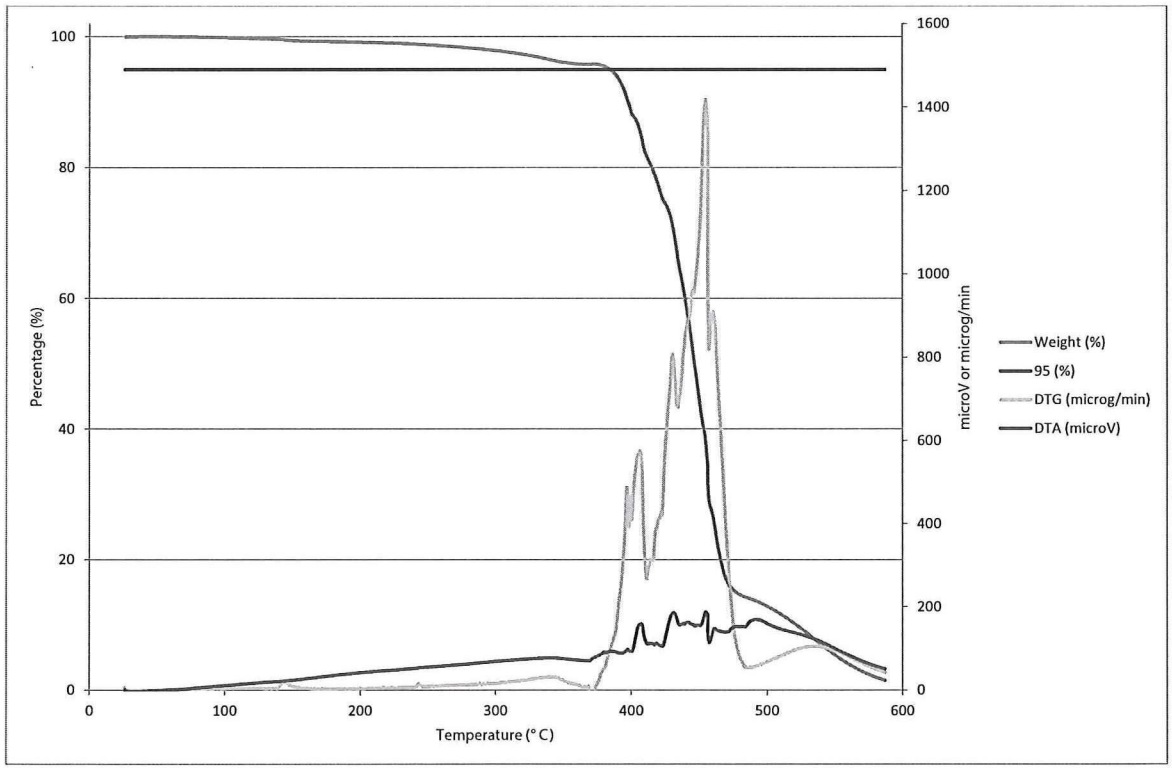

Figure K.3: TGA result of 3M 3789 thermoplastic adhesive

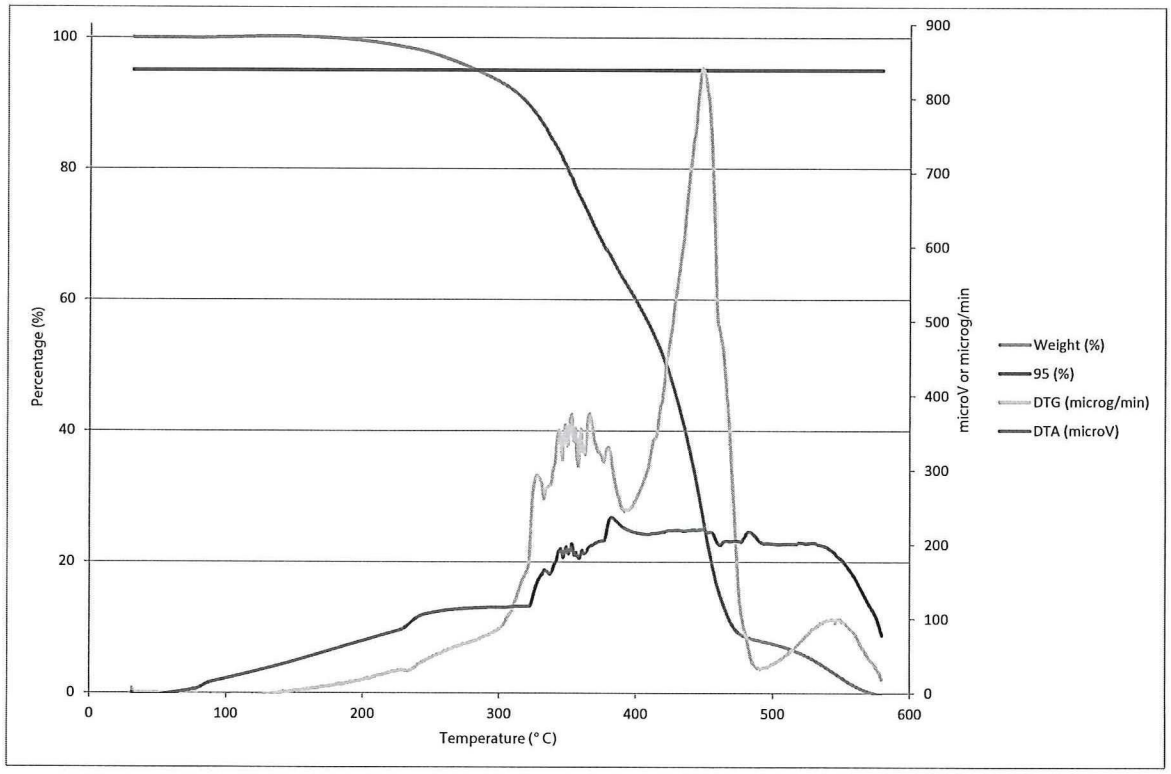

Figure K.4: TGA result of Henkel Technomelt Q 9268 H thermoplastic adhesive

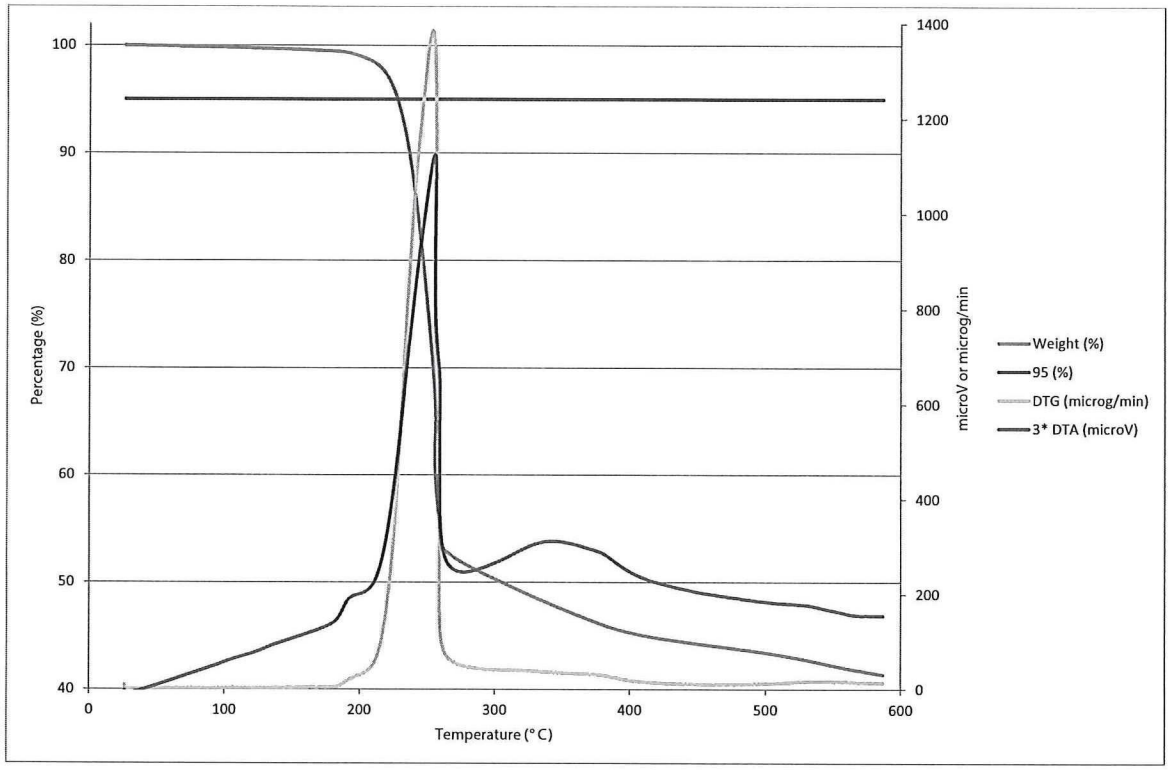

Figure K.5: TGA result of Sabatack 780 elastomer adhesive

K.4 DSC tests

DSC tests were performed to determine the T_g of the material. The device heats the sample at a constant rate while carefully monitoring the energy input. Results are shown in figure K.7 to K.9. The energy required to heat the sample per °C is shown by the DSC curve, the DDSC curve is the derivative of this.
When a polymer goes through this transition the amount of energy required to heat the material decreases. This results in two changes in the steepness of the energy curve. The glass transition temperature is taken as the median point of the transition region. This is shown in figure K.6 for 3M 3731. It illustrates how determining an exact temperature for the onset is difficult, influencing the obtained value of the T_g. The outcome from the graph is deemed accurate to ± 1°C.
Another source of uncertainty comes from the adhesive itself. If material changes during the heating cycle are completely reversed after cool down, the two DSC curves should overlap perfectly. However this is not the case. The adhesive consists of many substances, and is not a 'pure' polymer. Some of these substances undergo changes which are not reversible. As a result, the two DSC cycles undergo T_g at different temperatures. This is best visible in the 3M 3731 curve, where the difference is about 5°C. Values are determined from the first curve; these are thought to come closest to manufacturing conditions.
A summary of the obtained values is shown in table K.6, the original graphs can be seen figures K.7 to K.9.

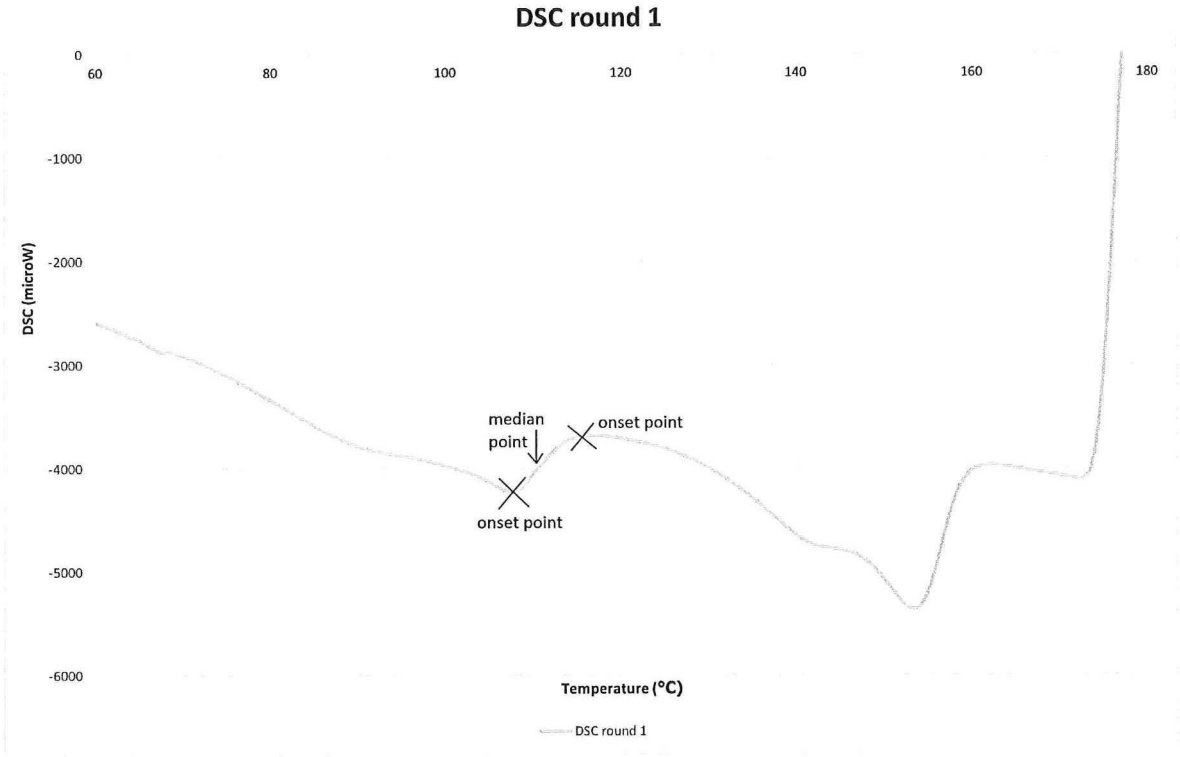

Figure K.6: Determination of T_g for 3M 3731 adhesive from the first DSC cycle

Adhesives	T_g (°C)
3M 3731	110
3M 3789	140
Henkel Technomelt Q 9268 H	80

Table K.6: Test results of DSC testing of adhesives

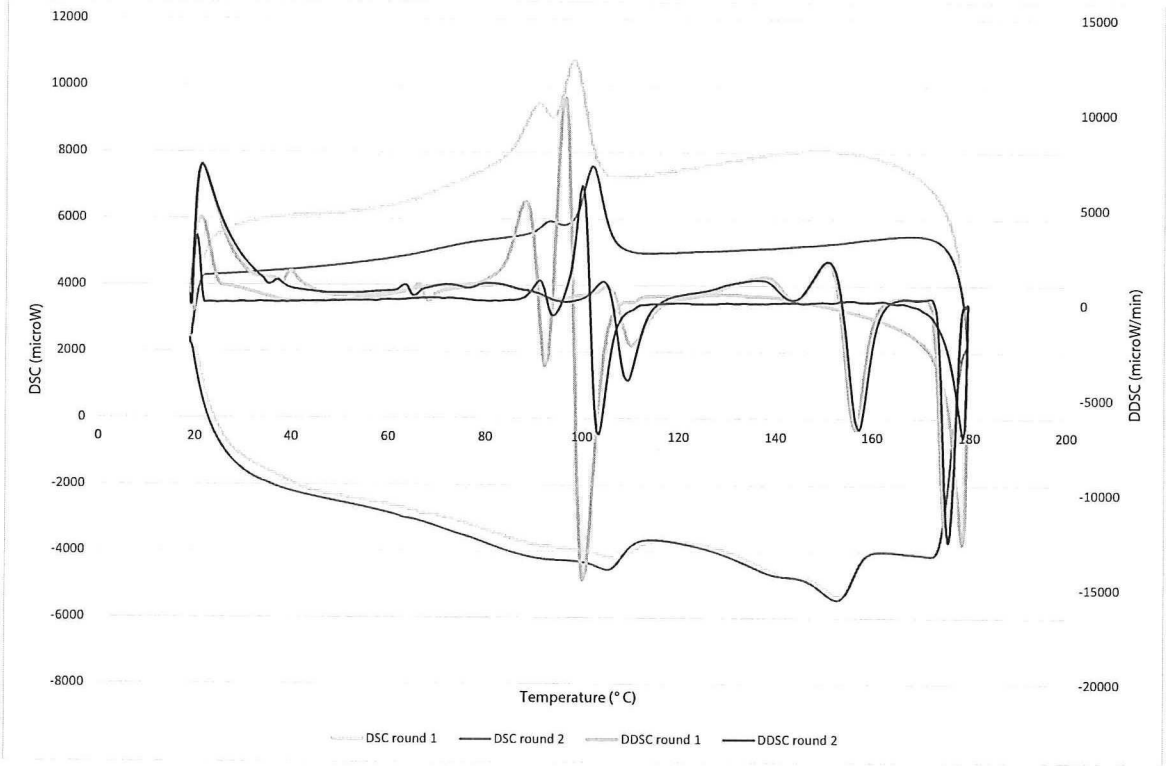

Figure K.7: DSC result of 3M 3731 thermoplastic adhesive

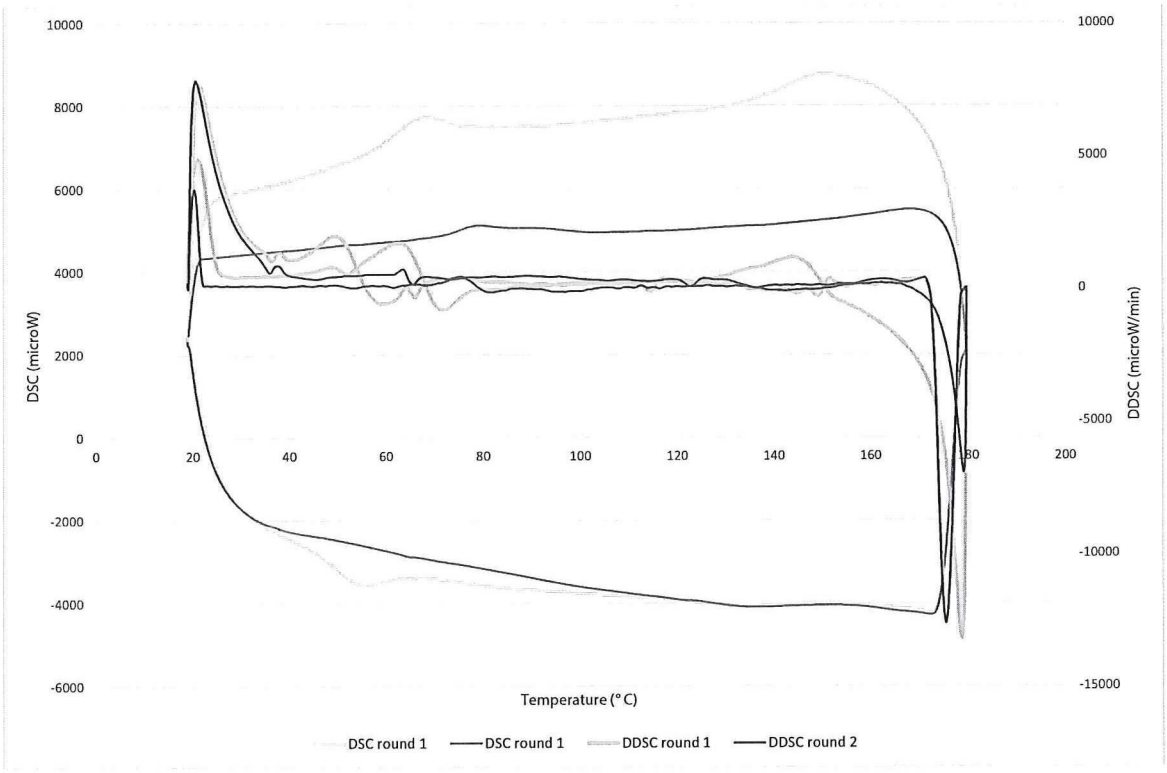

Figure K.8: DSC result of 3M 3789 thermoplastic adhesive

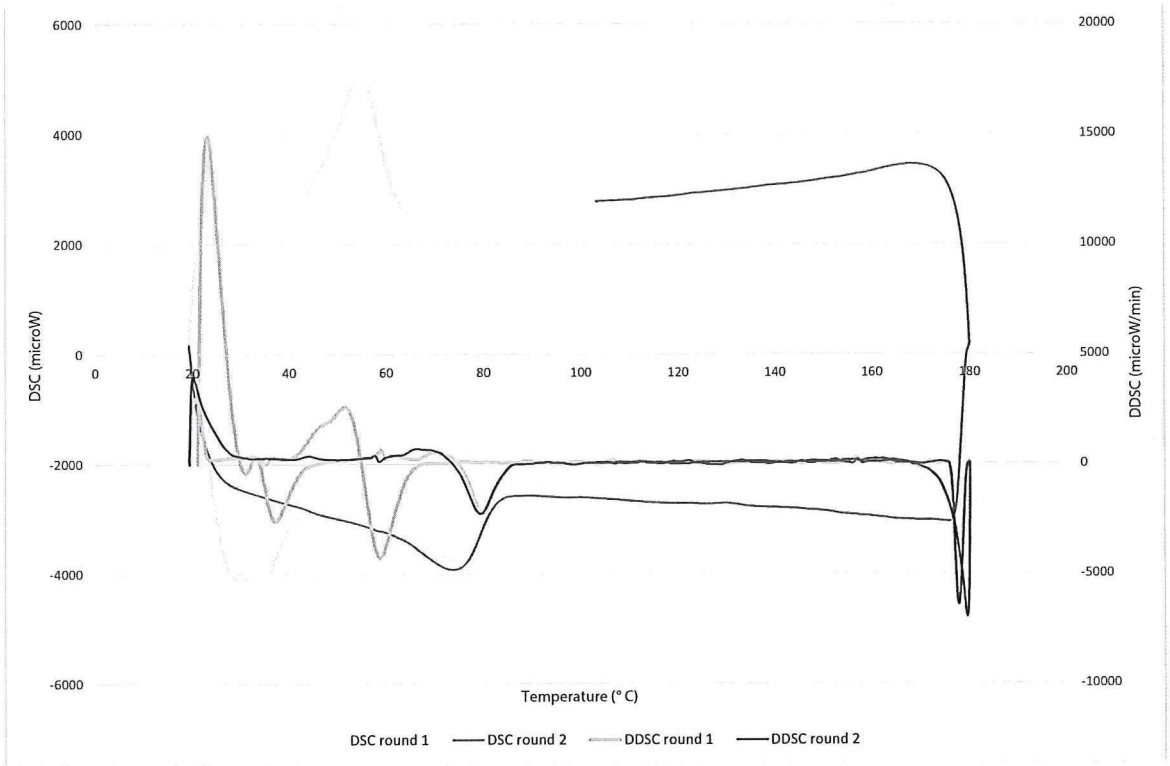

Figure K.9: DSC result of Henkel Technomelt Q 9268 H thermoplastic adhesive

K.5 Manufacturing data

Figure K.10 shows the heat up curves of the manufactured single lap shear specimens using the pre-impregnated mesh. Aside from numerous test runs, this process was performed four times for the four test sample groups (from chapter 10). Unfortunately, one of the data files was lost, therefore only three curves are shown. The fourth curve shows simulated data obtained from the COMSOL model.

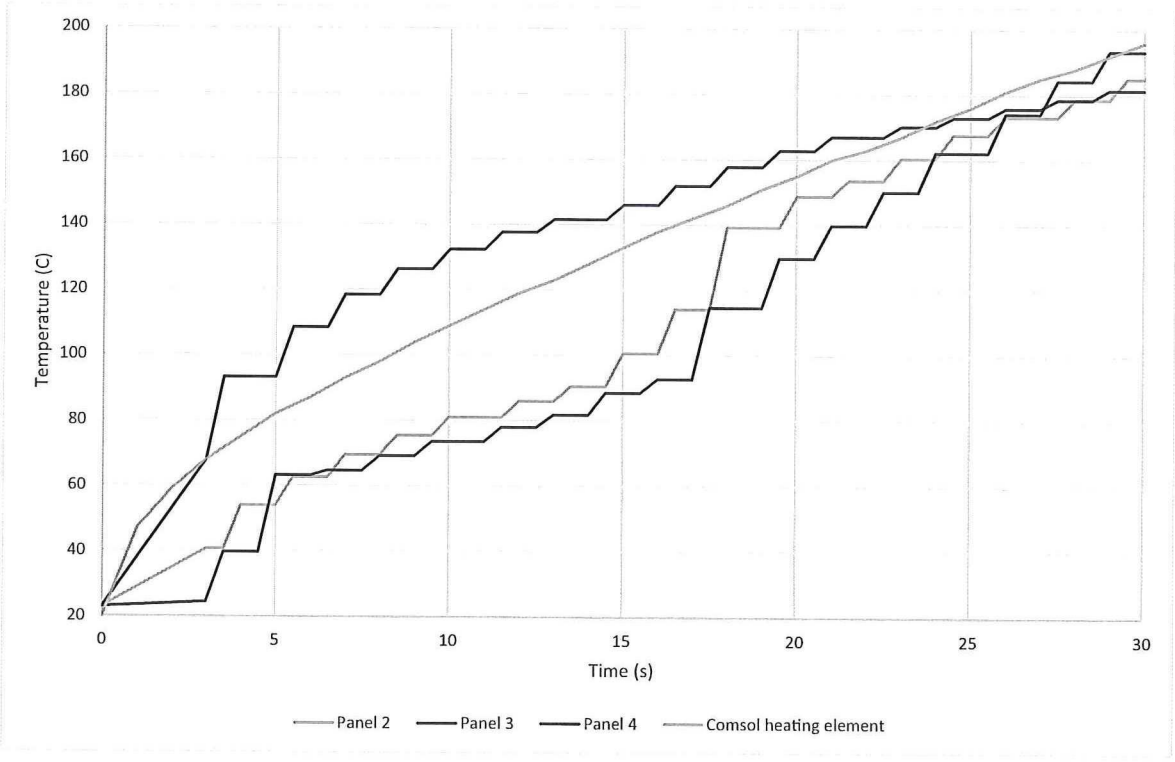

Figure K.10: Temperature profiles of the single lap joints manufactured using resistance welding set-up together with simulated data from COMSOL

Figure K.11 shows temperature and pressure cycle of the single lap joint without mesh, manufactured in the oven. Shortly after the panels were put in the oven, the vacuum pump broke down. It was rapidly replaced, but caused a disturbance in the pressure curve nonetheless. Due to the relatively low pressure difference and short duration, it was thought not to have a large influence on the specimen quality.

K.6 Double lap shear tests

A complete list of results of the double lap shear tests (from chapter 9) are shown in table K.7 and K.8.

Adhesive	Test temperature	Maximum force [N]	Bonding area [mm^2]	Shear strength [MPa]	Adhesive failure [%]	Resin-mesh debonding [%]	Cohesive failure [%]	Undetermined [%]
Henkel	RT	3777	1168	3.24	85	15	-	-
		3676	1187	3.10	95	5	-	-
		3868	1245	3.11	95	5	-	-
		2762	1216	2.27	80	20	-	-
		3257	1118	2.91	80	20	-	-
		3172	1177	2.70	85	15	-	-
Henkel	60	247	1092	0.22	-	30	70	-
		224	1123	0.21	-	5	95	-
		168	1095	0.15	-	30	70	-
		306	1203	0.25	95	5	-	-
		211	1199	0.18	-	-	-	100
3M 3731	RT	2276	1160	1.96	20	20	60	-
		2338	1069	2.19	5	95	-	-
		2471	1165	2.12	-	-	-	100
		2166	1027	2.11	10	90	-	-
3M 3731	60	14	1095	0.013	-	-	-	100
		622	963	0.64	70	30	-	-
		564	1125	0.50	90	10	-	-
		262	1160	0.23	90	10	-	-
		223	1059	0.21	10	-	-	-
3M 3789	RT	3688	1021	3.61	30	70	-	-
		3981	1021	3.90	20	80	-	-
		3237	1129	2.87	20	80	-	-
		3474	979	3.55	50	50	-	-
		2940	1075	2.73	45	45	10	-
3M 3789	60	494	843	0.59	-	10	90	-
		480	774	0.62	80	20	-	-
		680	927	0.73	90	10	-	-
		519	955	0.54	10	90	-	-
		554	775	0.71	15	85	-	-

Table K.7: Test strength data of double lap shear tensile test with thermoplastic adhesives tested at RT and 60°C

Adhesive	Test temperature	Maximum force [N]	Bonding area [mm^2]	Shear strength [MPa]	Adhesive failure [%]	Resin-mesh debonding [%]	Cohesive failure [%]	Undetermined [%]
Epoxy	RT	18868	987	19.12	-	-	100	-
		18824	887	21.22	-	-	100	-
		16179	845	19.16	-	-	100	-
		16218	1063	15.26	-	-	100	-
		21251	1050	20.23	-	-	100	-
		15360	986	15.58	-	-	100	-
Epoxy	60	18969	907	20.91	-	-	100	-
		19296	930	20.75	-	-	100	-
		21125	1046	20.20	100	-	-	-
		20237	998	20.27	-	100	-	-
		18535	876	21.16	-	-	100	-
		23438	1141	20.54	-	-	-	100

Table K.8: Test strength data of double lap shear tensile test with epoxy adhesives tested at RT and 60°C

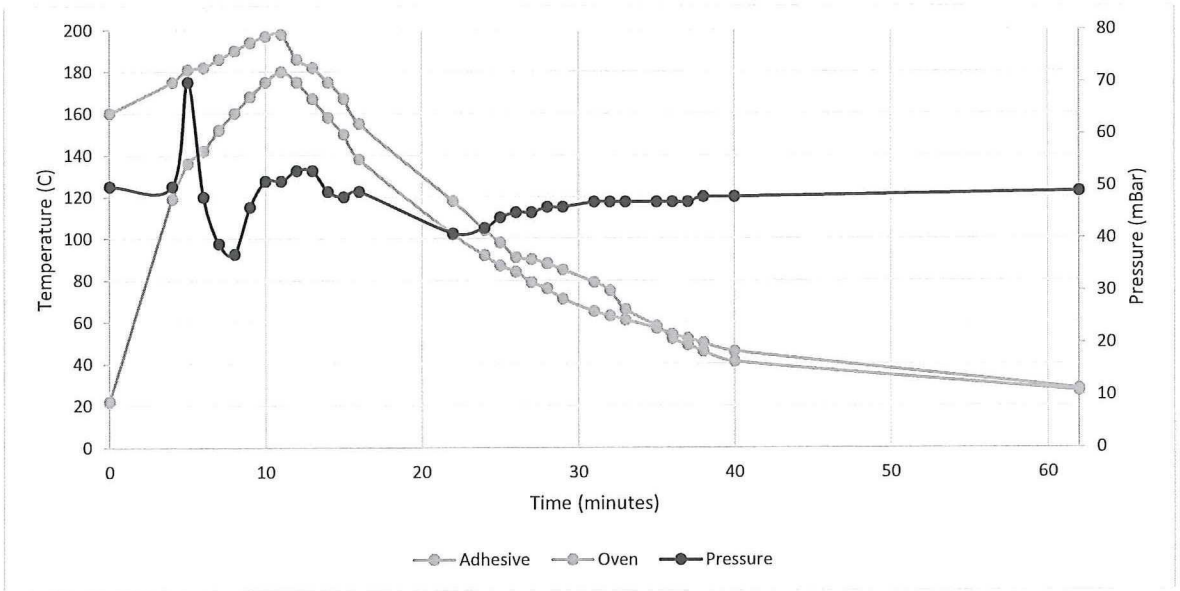

Figure K.11: Temperature profile of the single lap joint without mesh, heated in an oven

K.7 Single lap shear tests

A complete list of results of the single lap shear tests (from chapter 10) are shown in table K.9.

Group	Maximum force [N]	Bonding area [mm^2]	Adhesive layer thickness [mm]	Shear strength [MPa]	Adhesive failure [%]	Resin-mesh debonding [%]	Cohesive failure [%]
Benchmark	1414	331	0.11	4.28	20	80	-
	1400	331	0.12	4.23	20	80	-
	1329	579	0.10	2.30	20	80	-
	1225	332	0.11	3.68	40	60	-
	785	329	0.10	2.38	60	40	-
	1023	330	0.08	3.10	60	40	-
Removal	31	303	0.08	0.101	20	80	-
	21	308	0.09	0.069	-	100	-
	0	308	0.03	0	-	100	-
	0	312	0.12	0	-	100	-
	0	312	0.07	0	-	100	-
Without mesh	1954	339	0.07	5.76	30	-	70
	2604	336	0.09	7.74	30	-	70
	2067	339	0.03	6.10	30	-	70
	2074	340	0.01	6.10	20	-	80
	2397	338	0.00	7.09	20	-	80
	1700	339	0.01	5.01	30	-	70
Re-use	1357	334	0.17	4.07	40	60	-
	1349	328	0.19	4.12	30	70	-
	1355	328	0.15	4.14	20	80	-
	1308	331	0.11	3.95	30	70	-
	1262	333	0.13	3.79	30	70	-
	1134	338	0.16	3.36	50	50	-

Table K.9: Shear strength data of single lap shear tensile test adhered with 3M 3789, tested at 180°C (*Removal* group) and RT (other groups).